uOttawa

L'Université canadienne
Canada's university

FACULTÉ DES ÉTUDES SUPÉRIEURES ET POSTOCTORALES

uOttawa

L'Université canadienne
Canada's university

FACULTY OF GRADUATE AND POSDOCTORAL STUDIES

Irena Szymanska

AUTEUR DE LA THÈSE / AUTHOR OF THESIS

M.Sc. (Cellular and Molecular Medicine)

GRADE / DEGREE

Department of Cellular and Molecular Medicine

FACULTÉ, ÉCOLE, DÉPARTEMENT / FACULTY, SCHOOL, DEPARTMENT

Exploration of Lentiviral Vectors and TAT-Fusion Proteins for the Delivery of XIAP Protein to Neonatal Retinal Progenitor Cells

TITRE DE LA THÈSE / TITLE OF THESIS

Dr. C. Tsilfidis

DIRECTEUR (DIRECTRICE) DE LA THÈSE / THESIS SUPERVISOR

CO-DIRECTEUR (CO-DIRECTRICE) DE LA THÈSE / THESIS CO-SUPERVISOR

EXAMINATEURS (EXAMINATRICES) DE LA THÈSE / THESIS EXAMINERS

Dr. D. Lohnes

Dr. R. Korneluk

Gary W. Slater

Le Doyen de la Faculté des études supérieures et postdoctorales / Dean of the Faculty of Graduate and Postdoctoral Studies

Exploration of Lentiviral Vectors and TAT-Fusion Proteins for the Delivery of XIAP Protein to Neonatal Retinal Progenitor Cells

Irena Szymanska

This thesis is submitted as a partial fulfillment of the M.Sc. program in Cellular and Molecular Medicine

Submitted: July 2nd, 2008

University of Ottawa, Canada

Your file Votre référence
ISBN: 978-0-494-48628-3
Our file Notre référence
ISBN: 978-0-494-48628-3

ABSTRACT

Post-transplant apoptosis is a major obstacle to successful cell replacement therapy for retinitis pigmentosa. Over-expression of the X-linked inhibitor of apoptosis (XIAP) protein could increase transplant survival leaving a greater numbers of cells available to replenish photoreceptors lost during retinal degeneration. Sonic Hedge hog expanded C57BL/6 mouse neonatal retinal progenitor cells (Hh-RPCs) were infected with two lentiviral constructs, encoding XIAP/GFP or GFP only, as well as with the TAT-fusion protein, TAT-eGFP. The optimal delivery conditions and expression patterns were assessed. It was found that lentiviral infection, in conjunction with fluorescence activated cell sorting (FACS) allowed for the creation of a nearly pure line of Hh-RPCs which over-expressed XIAP protein for at least one month. Although the TAT-fusion protein efficiently transduced Hh-RPCs, its nuclear localization made it unsuitable for XIAP protein delivery. These results demonstrated two methods of transducing primary retinal progenitor cells and represent an important first step towards efficient cell replacement therapy in the retina.

TABLE OF CONTENTS

LIST OF TABLES

LIST OF FIGURES

LIST OF ABBREVIATIONS

AAV	Adeno-associated virus
Antp	Antennapedia
aRPCs	Adult retinal progenitor cells
ARVO	Association of research in vision and ophthalmology
BH	BCL-2 homology
BIR	Baculoviral IAP repeat
CTP	Cytoplasmic transduction peptide
DAPI	4'-6'-Diamidino-2-phenylindole dihydrochloride
DHA	Docosahexaenoic acid
DMEM	Dulbecco's Modified Eagle's Medium
DMSO	Dimethyl sulfoxide
EGF	Epidermal growth factor
eGFP	Enhanced green fluorescent protein
EMCV	*Encephalomyocarditis virus*
ERG	Electroretinogram
FACS	Fluorescence activated cell sorting
FBS	Fetal bovine serum
FGF2	Fibroblast growth factor 2
GCL	Ganglion cell layer
GFP	Green fluorescent protein
HA	Hemoagglutinin
Hh	Sonic hedge hog
Hh-RPCs	Hh agonist expanded retinal progenitor cells
HIV1	*Human immunodeficiency virus 1*
IAP	Inhibitor of apoptosis
INL	Inner nuclear layer
IPTG	Isopropyl β-D-1-thiogalactopyranoside
IRES	Internal ribosomal entry site
LTRs	Long terminal repeats
MNU	N-methyl-n-nitrosourea
MOI	Multiplicity of infection
MSCs	Mesenchymal stem cells
NLS	Nuclear localization signal
OCT	Optimal Cutting Temperature
ONL	Outer nuclear layer
PB	Polybrene
PBS	Phosphate buffered saline
PFA	Paraformaldehyde
PTD	Protein transduction domain
PVDF	Polyvinylidene difluoride
RECM	Retinal explant culture medium
RING	Really interesting new gene

RNAi	RNA interference
RP	Retinitis pigmentosa
RPCs	Retinal progenitor cells
RPE	Retinal pigment epithelium
SDS-PAGE	Sodium dodecyl sulfate-polyacrylamide gel electrophoresis
SFRCM	Serum free retinal cell culture media
SFRCM-Hh	Serum free retinal cell culture media supplemented with hedge hog agonist
TAT	Transactivator of transcription
TU	Transduction unit
VM	Ventral mesencephalic
XIAP	X-linked inhibitor of apoptosis protein

ACKNOWLEDGEMENTS

I would not be the person I am today without the experience of the past two years. First and foremost, I would like to thank my supervisor, Dr. Catherine Tsilfidis, for the unfailing support she provided in and outside the lab. Cathy trusted my judgment and abilities, and provided the ideal balance of guidance and independence.

This project would not have been possible without the expertise of Dr. Wai Gin Fong and Dr. Yaping Wang. Dr. Fong generated the fusion proteins and viral constructs, and was an endless well of knowledge and advice. Dr. Wang, of the Wallace lab, generously provided the progenitor cells and her continual assistance.

A special thank you to Adam Baker for teaching me lab techniques, for bestowing invaluable advice and assistance throughout the duration of the project, but most of all, for always listening and demonstrating infinite patience.

I would like to thank the members of my thesis committees (Dr. Valerie Wallace, Dr. Robert Korneluk and Dr. David Lohnes) for providing comments and feedback, which have given my project direction.

I also must mention the remaining members of the Tsilfidis lab, who were critical to the success of this project. It was a pleasure going to work everyday, and I would like to thank them for their support and faith in me.

I would like to thank my family for instilling in me the drive to succeed, and for keeping me grounded and on track. Finally, a special thank you to Greg and all my friends, who always believed in me and wholeheartedly supported my pursuits.

1. INTRODUCTION

Retinitis pigmentosa (RP), a major cause of irreversible blindness worldwide, is caused by degeneration of photoreceptor cells. Current therapies for RP aim to slow the progress of the disease. Cell replacement therapy could be employed to replenish photoreceptors allowing for a reversal of the damage caused by RP. Various sources of retinal precursor cells exist including embryonic stem cells and adult and neonatal progenitor cells. A line of hedgehog agonist-expanded retinal progenitor cells (Hh-RPCs), isolated from neonatal mouse retina, is an especially good candidate for cell replacement therapy for RP. These cells can be maintained in culture for up to 6 months and have the potential to differentiate into photoreceptors *in vitro* and *in vivo* (Wang and Wallace, unpublished). A major obstacle to successful cell replacement therapy is post-transplant apoptosis. It is thought that if retinal progenitor cells were made resistant to apoptosis they would better survive transplantation. By increasing transplant survival, a greater population of donor cells would be available to repopulate retinas damaged by various forms of retinal degeneration, such as RP. Retinal progenitor cells could be made resistant to apoptosis by over-expressing the X-linked inhibitor of apoptosis (XIAP) protein. XIAP protein has been shown to be a highly potent suppressor of programmed cell death (Holcik, Gibson et al. 2001).

The parameters of XIAP protein delivery to retinal progenitor cells have to be established before it can be ascertained whether the XIAP protein treatment protects against post-transplant apoptosis. Therefore, this project, by outlining transgene expression from a lentiviral vector and a TAT-fusion protein, serves as a very important first step towards testing the above hypothesis.

1.1 Apoptosis

Apoptosis, or programmed cell death, allows an organism to selectively eliminate cells that are damaged, are dangerous to the host or have completed their function (Kerr, Wyllie et al. 1972). The breakdown of the cell is mediated by caspases, a family of proteases dependent on a cysteine nucleophile to cleave motifs containing aspartic acid residues (Thornberry and Lazebnik 1998). Caspases are produced as inactive zymogens. Upstream caspases, also known as initiator caspases, are capable of autocatalytic activation. Downstream, or effector, caspases, such as caspases-3 and -7, require the activity of initiator caspases to become activated (Thornberry, Rano et al. 1997).

1.1.1 Regulation of Apoptosis

Apoptosis is a critical process during embryonic development and for the maintenance of homeostasis throughout life (Danial and Korsmeyer 2004); therefore, it is no surprise that it is highly regulated. Two largely independent pathways to programmed cell death have been identified (Strasser, Harris et al. 1995). Apoptosis can be triggered by the binding of ligands to a subgroup of the tumor necrosis factor receptor family of cell surface receptors, known as 'death-receptors', such as CD95/Fas/APO-1. This pathway is called the 'extrinsic pathway' and it leads to the activation of an initiator caspase, caspase-8 (Fig. 1) (Krammer 2000). In the second major pathway, the 'intrinsic pathway', a diverse range of stress conditions, such as cytokine deprivation and DNA damage, cause the expulsion of cytochrome-c from the mitochondria. This leads to the activation of the initiator caspase, caspase-9 (Fig. 1) (Nicholson 1999). The initiator caspases from both pathways converge on the activation of effector caspases-3 and -7. The activity of these two effector caspases leads to the morphological changes associated

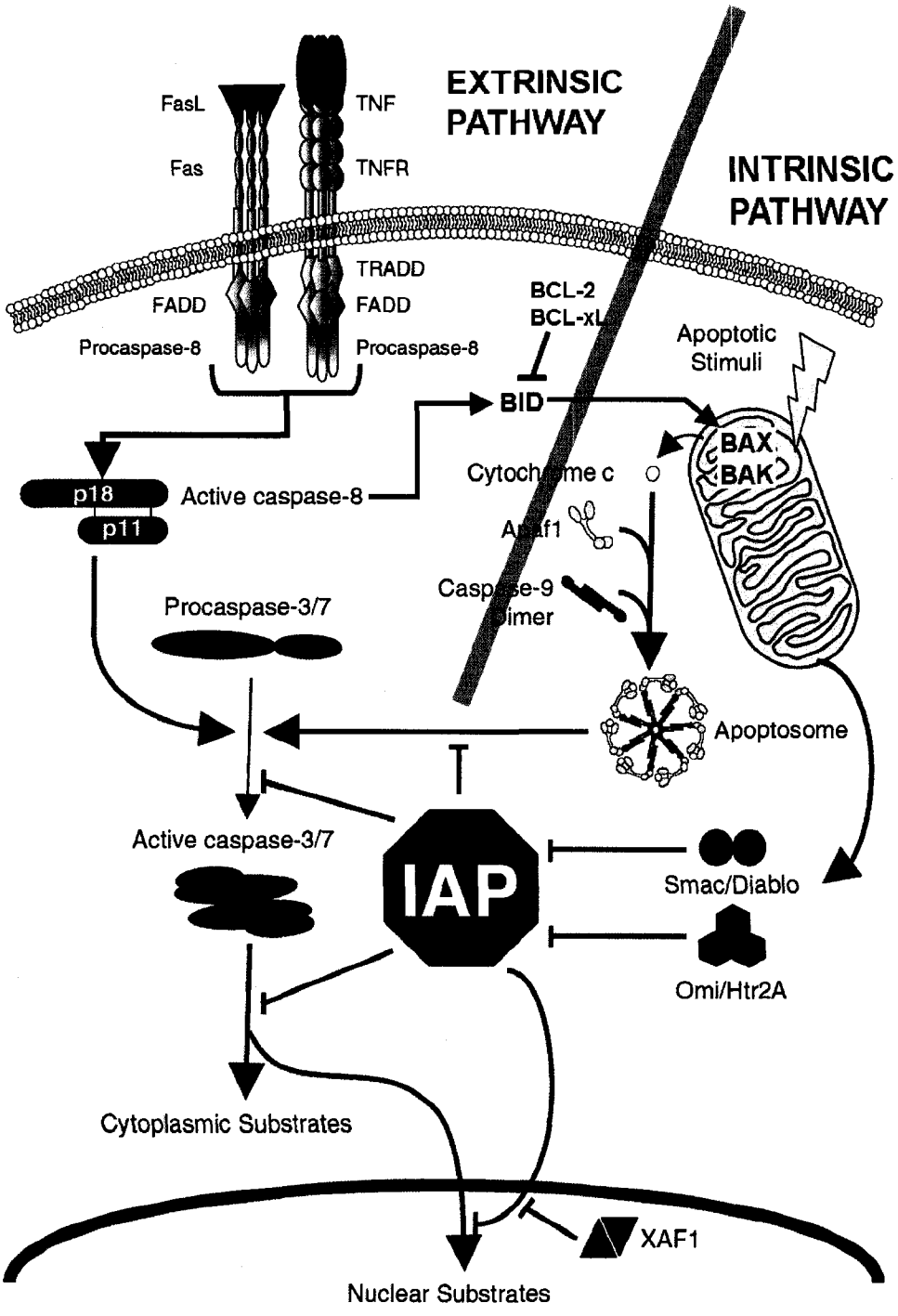

Figure 1: Role of the inhibitor of apoptosis (IAP) and the BCL-2 family of proteins in regulating both the extrinsic and intrinsic apoptotic pathways. Modified from Liston, Fong et al. 2003.

with apoptosis, including DNA degradation, chromatin condensation, and membrane blebbing (Fig. 1) (Nicholson 1999; Danial and Korsmeyer 2004).

Within each cell are pro- and anti-apoptotic proteins, the ratio of which determines the cell's susceptibility to apoptosis (Oltvai, Milliman et al. 1993). In mammals, a major group of both pro- and anti-apoptotic proteins belongs to the BCL-2 family. The BCL-2 proto-oncogene was discovered at chromosomal breakpoint t(14;18) which gave rise to human B-cell lymphomas (Bakhshi, Jensen et al. 1985; Cleary and Sklar 1985; Tsujimoto, Cossman et al. 1985). Members of the BCL-2 family of proteins consist of up to four conserved BCL-2 homology (BH) domains, designated BH1 through BH4, which correspond to α-helical segments (Adams and Cory 1998). The proteins of the BCL-2 family are also characterized by their capacity to form homo- and heterodimers (Gross, McDonnell et al. 1999) and their ability to become integral membrane proteins.

There are multidomain anti-apoptotic proteins which contain all 4 BH domains. Proteins in this group include BCL-2, BCL-X_L, MCL-1, A1 and BCL-$_W$. In these proteins the BH1, BH2 and BH3 domains are in close proximity and create a hydrophobic pocket which can accommodate the BH3 domain of a pro-apoptotic member (Chipuk and Green 2008). Multidomain pro-apoptotic members of the BCL-2 family include BAX and BAK and they possess BH domains 1 through 3. There is also a group of pro-apoptotic proteins which has homology only with the BH3 domain. This group is termed the "BH3-only" proteins and it includes proteins such as BAD and BID (Fig. 2) (Chipuk and Green 2008).

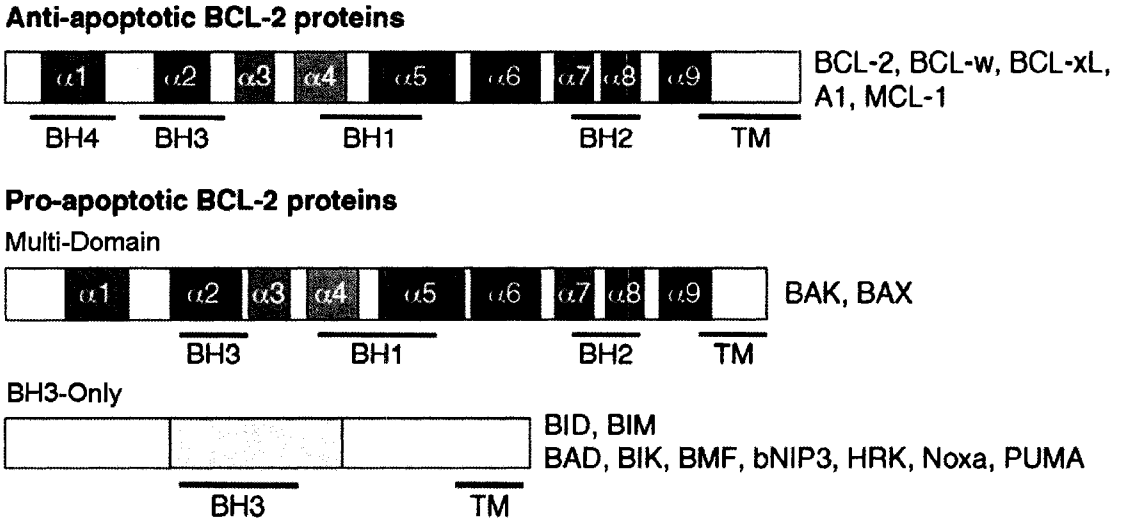

Figure 2: The BCL-2 family of pro- and anti-apoptotic proteins. This protein family is divided into three functional groups based on their composition of BCL-2 homology (BH) domains. The anti-apoptotic members include BCL-2, BCL-$_X$L, BCL-$_W$, A1 and MCL-1 and contain four BCL-2 homology domains (designated BH1–4). The pro-apoptotic multi-domains (BAX and BAK) contain BH1–3 domains. The BH3-only proteins are structurally diverse and contain only one conserved region, the BH3. The α-helices of each protein are designated and the regions contained within each BH domain are illustrated by bold lines under each protein. The hydrophobic carboxyl terminal transmembrane domain (TM) of each protein is not necessarily present in each member. Modified from Chipuk and Green 2008.

In a healthy cell, BAX and BAK exist as monomers in the cytosol or are loosely attached to the mitochondrial outer membrane. Upon receipt of a death signal along the intrinsic pathway, both proteins form homo-oligomerized multimers, which insert into the mitochondrial outer membrane and permeabilize it. Inter-membrane space proteins, such as cytochrome-c, are released. Cytochrome-c binds to Apaf-1 which then recruits caspase-9. The now active caspase-9 goes on to cleave and activate the effector caspases, caspase-3 and -7 (Fig. 1) (Danial and Korsmeyer 2004).

Engagement of a cell surface death receptor leads to the initiation of apoptosis along the extrinsic pathway. Initiator caspase-8 becomes activated and proceeds to cleave effector caspases-3 and -7, as well as the BH3-only pro-apoptotic protein BID. The cleaved BID targets the mitochondria where it activates BAX and BAK. Here the extrinsic and intrinsic pathways merge and BAX and BAK proceed to execute apoptosis as described above. The pro-apoptotic activity of BH3-only proteins is kept in check by transcriptional control or posttranslational modification (Danial and Korsmeyer 2004). The anti-apoptotic proteins, BCL-2 or BCL-X_L, function by binding and sequestering BH3-only proteins and preventing BAX and BAK activation (Fig. 1) (Cheng, Wei et al. 2001).

In summary, the activity of BCL-2 family pro- and anti-apoptotic proteins functions to determine whether caspases will be activated and apoptosis will be initiated. Once the caspases are activated, however, there exist other proteins which regulate their activity.

The inhibitor of apoptosis (IAP) family of proteins can inhibit apoptosis triggered by either the intrinsic or extrinsic pathways (Fig. 1). These proteins are highly conserved

and can be found in organisms ranging from mammals to insects. Members of this protein family are characterized by one or more 70-80 amino acid baculoviral IAP repeat (BIR) domains. The BIR domains are responsible for directly binding to, and inhibiting, caspases. IAP proteins also contain a RING (Really Interesting New Gene) zinc finger domain which may possess E3 ubiquitin ligase activity (Fig. 3). The activity of the IAPs is negatively regulated by proteins such as XAF1, Smac and Omi (Fig. 1) (Liston, Fong et al. 2003).

1.1.2 X-linked Inhibitor of Apoptosis Protein

The X-linked Inhibitor of Apoptosis (XIAP) protein is the most potent IAP and has been referred to as the prototype member of the IAP family (Holcik, Gibson et al. 2001). In humans, the XIAP gene is located on chromosome Xq25 (Rajcan-Separovic, Liston et al. 1996). XIAP protein contains 3 BIR domains in the N-terminal half of the protein, which are responsible for binding to and inhibition of caspases-3, -7 and -9 (Fig. 4). The BIR domains, although structurally similar, inhibit caspases via different mechanisms. The linker region between XIAP protein's BIR1 and BIR2 domains stretches across the active sites of caspases-3 and -7 and inhibits these caspases by precluding substrate entry. Inhibition of caspase-7 requires the linker region as well as the BIR2 domain (Liston, Fong et al. 2003). The linker region alone accounts entirely for the inhibition of caspase-3 and the BIR2 domain can be replaced with an irrelevant protein (Chai, Du et al. 2000; Huang, Park et al. 2001). The BIR3 domain binds to caspase-9 and inhibits its activity by preventing it from homodimerizing and by stabilizing the enzyme in its inactive form (Shiozaki, Chai et al. 2003).

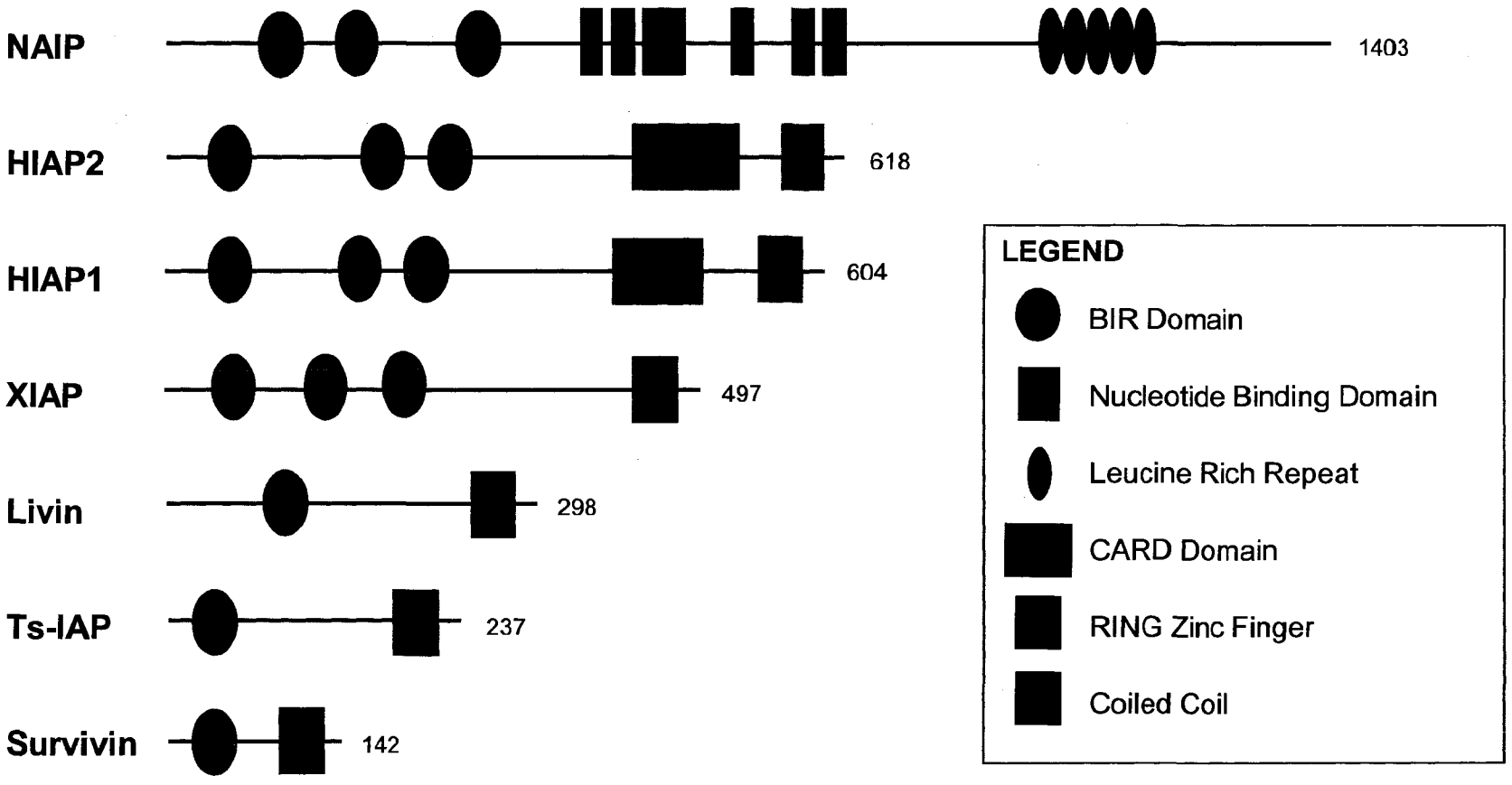

Figure 3: Schematic diagram of the IAP (inhibitor of apoptosis) family of known anti-apoptotic proteins. At least one IAP-defining BIR domain is present in all members, while five of the seven members including XIAP protein, also contain a RING zinc finger motif. Modified from Liston, Fong et al. 2003.

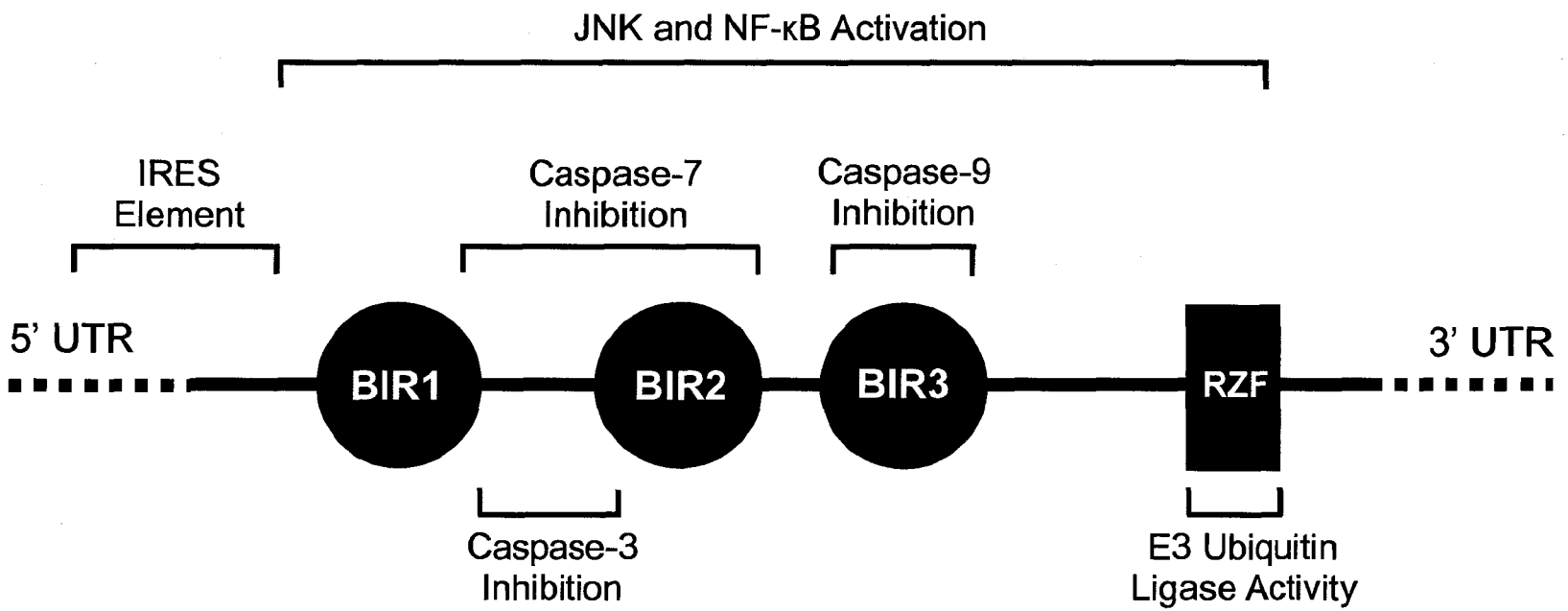

Figure 4: Functional map of XIAP protein activities and interactions. Some interactions have not been mapped to individual domains within the protein, and are indicated as requiring the entire protein. The 5' and 3' UTR regions are not shown to scale. BIR: baculoviral IAP repeat; IRES: internal ribosomal entry site; RZF: RING zinc finger; UTR: untranslated region. Modified from Liston, Fong et al. 2003.

In addition to direct binding to and inhibition of caspases, recent work has revealed other potential mechanisms of apoptosis inhibition by XIAP protein. XIAP protein can function as a cofactor in signaling pathways which inhibit apoptosis, including NF-κB, Smad and JNK (Lewis, Burstein et al. 2004). These signaling properties of XIAP protein are dependant on domains other than the BIR domains (Lewis, Burstein et al. 2004).

1.2 The Retina

1.2.1 Retinal Morphology

The retina is responsible for converting light input into electrical signals, which our brain then interprets as vision. On the very outside of the retina are the retinal pigment epithelium (RPE) and the vascular choroid, which provide nutritive support for the neural retina. The vertebrate neural retina contains five primary neural cell types, which are arranged into five layers (Fig. 5) (Ross, Romrell et al. 1995). The outermost neural layer, the outer nuclear layer (ONL), is composed of rod and cone photoreceptor cells, which are responsible for generating electrical signals in response to light. The photoreceptors synapse with bipolar cells in the inner nuclear layer (INL), which in turn synapse with the ganglion cells that lie at the inner surface of the retina in the ganglion cell layer (GCL). The ganglion cells give rise to optic nerve fibers which project to the visual cortex of the brain. The two layers where synapse occurs are the plexiform layers. The outer plexiform layer connects cells in the ONL and INL, and the inner plexiform layer connects cells in the INL and GCL (Nicholls, Martin et al. 2001). The other neuronal cell types in the retina are the horizontal and amacrine cells, which predominantly make lateral connections and serve to modify the responses of the bipolar

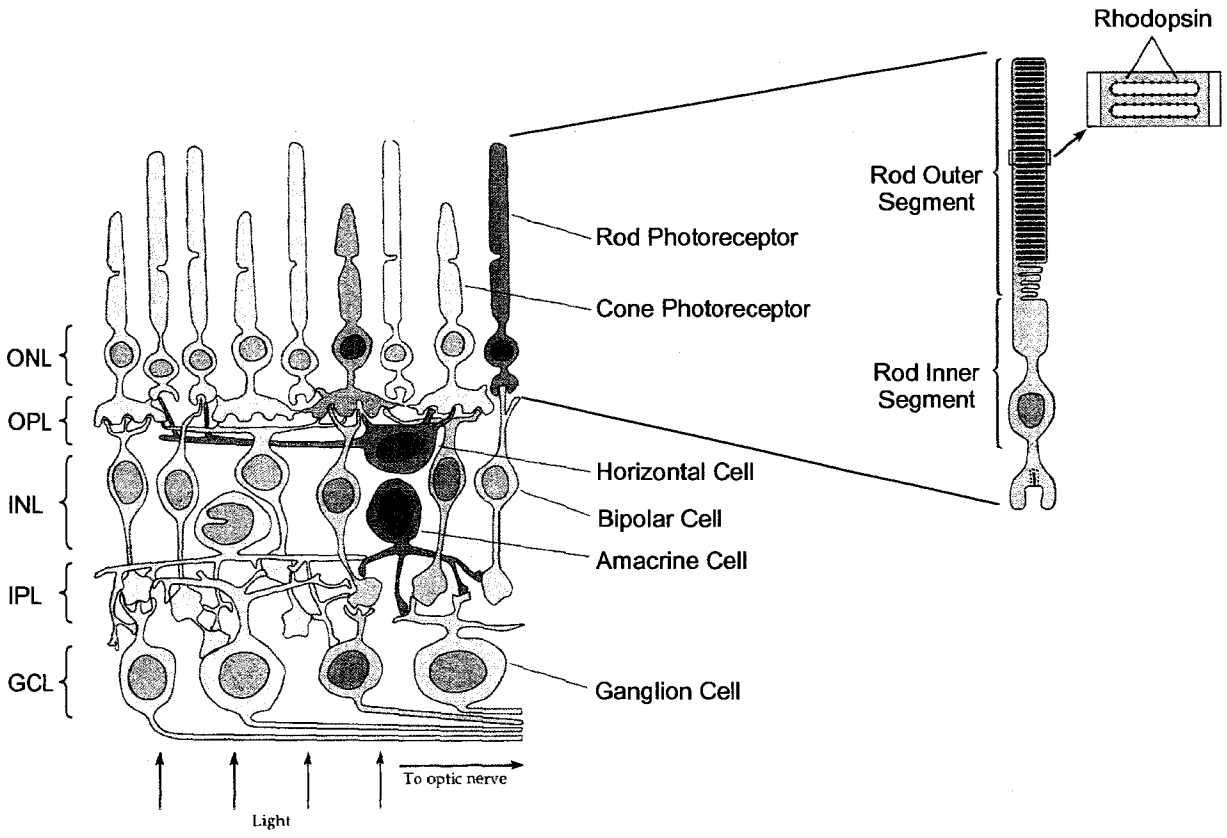

Figure 5: Schematic diagram of the mammalian retina showing retinal layers and individual cell types. ONL: outer nuclear layer; OPL: outer plexiform layer; INL: inner nuclear layer; IPL: inner plexiform layer; GCL: ganglion cell layer. Modified from Nicholls, Martin et al. 2001.

and ganglion cells. In addition to these neurons, the retina contains Müller cells, which are the glial cells of the retina (Ross, Romrell et al. 1995). Müller cells form the architectural support of the retina and can often span its entire width. They also form the outer and inner limiting membranes of the retina (Kolb, Fernandez et al. 2008).

1.2.2 Photoreceptors

The retina contains two kinds of photoreceptors, rods and cones. Rods constitute 95 to 99% of human photoreceptors and are responsible for vision in dim light conditions. The remaining photoreceptors are the cones, which are responsible for detailed visual acuity and colour detection. Cones are highly concentrated in a region of the central retina known as the macula (Kolb, Fernandez et al. 2008).

Each photoreceptor cell contains an inner segment and an outer segment. The inner segments contain the nucleus, which lies in the ONL. They also contain the other organelles, which lie just distal to the ONL. The outer segments contain photopigments, which detect light. The rod outer segments contain stacks of approximately 1000 discs, formed by invaginations of the plasma membrane. The photopigment rhodopsin constitutes up to 85% of the total protein in the rod outer segments (Nicholls, Martin et al. 2001; Kolb, Fernandez et al. 2008). The outer segment discs are constantly being renewed. New discs are added at the base of the outer segment while old discs are displaced to the top of the outer segment, pinched off and phagocytosed by RPE cells (Kolb, Fernandez et al. 2008).

1.3 Retinitis Pigmentosa

Retinitis pigmentosa (RP) refers to a group of heterogeneous disorders that are characterized by apoptotic loss of photoreceptor cells in the retina (Berson 1993).

Melanin released from the RPE accounts for the pigment deposits observed in the peripheral retina of individuals with RP, a hallmark of the disease (Krill 1972). Symptoms are variable; they generally present at 30 years of age and include progressive night blindness, reduction or loss of visual acuity, and constriction of the visual field leading to complete vision loss by the age of 60 (Hamel 2006).

RP is the most common cause of inherited blindness in the developed world affecting approximately one in 3500 individuals (Hamel 2006). To date, 40 genes have been linked to RP (Daiger 2008) with autosomal dominant, autosomal recessive and X-linked modes of inheritance. Rhodopsin mutations are the most common, but other genes linked to RP include proteins of rod visual transduction (α and β subunits of rod phosphodiesterase, α and β subunits of the rod cGMP gated channel, arrestin), cytoskeletal proteins (peripherin/RDS, ROM1, fascin 2), trafficking proteins (RPGR, RP1, PR2), proteins involved in photoreceptor differentiation (NRL, CRX), as well as genes expressed by photoreceptor supporting tissue, the retinal pigment epithelium, which are involved in retinol (vitamin A) metabolism (Hamel 2006).

The disease-causing mutations are generally only expressed in rod photoreceptors, leading these cells to be primarily affected. Rod degeneration accounts for the initial night blindness and the loss of the peripheral visual field. As the disease progresses, cone photoreceptors also die bringing about the loss of day vision and the central visual field, leading to complete vision loss (Phelan and Bok 2000).

Despite the heterogeneity of causative genes and modes of inheritance, the final common outcome of all forms of RP analyzed in animal models and patients so far is apoptosis of photoreceptor cells (Marigo 2007). What is less clear is the mechanism by

which the mutations lead to apoptosis. Some potential mechanisms have been suggested and include disruption of photoreceptor outer segment morphogenesis, metabolic overload, dysfunction of RPE cells and chronic activation of the phototransduction cascade (Pierce 2001). This lack of understanding of the underlying mechanisms, as well as the heterogeneous genetic basis of RP, make the development of specific therapies for the treatment of RP a challenge.

1.3.1 Current Therapies for RP

The therapies currently in use for the treatment of RP are aimed at slowing down the degeneration process and treating complications associated with RP. Some studies in animals suggest that some types of RP may be partly light-dependent (Wang, Lam et al. 1997), therefore RP patients are recommended to wear dark glasses outdoors or yellow-orange glasses to minimize photophobia (Hamel 2006). The main course of treatment for RP is vitamin therapy. Vitamin A may protect photoreceptors by anti-oxidant effects. Anti-oxidants have been shown to prolong rod and cone survival in animal studies (Komeima, Rogers et al. 2007), and long-term vitamin A supplementation in humans was shown to slightly decrease the loss of retinal function, as shown by electroretinograms (ERGs) (Berson, Rosner et al. 1993). In another study, patients were given docosahexaenoic acid (DHA) in addition to vitamin A and it was shown that the initial course of disease was slowed down, but the effect did not last beyond 2 years (Berson, Rosner et al. 2004).

Research into novel therapies for RP is extensive. It has been suggested that, as the mechanisms of photoreceptor death are elucidated, an approach via pharmacological treatment targeting specific pathways could become possible (Hamel 2006). Another

approach is hyperbaric oxygen therapy, which was shown to increase visual acuity, visual field and ERG response in one human study (Vingolo, Rocco et al. 2008). The use of growth factors is another avenue of treatment for RP. For example, ciliary neurotrophic factor, glial-derived neurotrophic factor, cardiotrophin-1, brain-derived neurotrophic factor and fibroblast growth factor, were shown to have neuroprotective effects in animal models. In another study, a rod-derived cone viability factor significantly delayed cone death in a mouse model of RP (Leveillard, Mohand-Said et al. 2004). Growth factors, however, pose several problems when used to treat RP; they have a short half-life, they need to be injected directly into the eye, and side effects, such as neovascularization and cataract formation, are often observed (Hamel 2006).

A highly promising approach to treating RP is gene therapy, where a vector is used to administer the correct version of a mutated gene. In one mouse study, a dominant mutated rhodopsin gene was silenced with RNA interference (RNAi) and wild type rhodopsin was expressed from an adeno-associated virus (AAV) vector (O'Reilly, Palfi et al. 2007). In a study targeting a different ocular disease, AAV was used to subretinally deliver RPE65 cDNA into dogs with Leber's Congenital Amaurosis. Vision was restored in these dogs and the effect appeared to be stable even after five years (Acland, Aguirre et al. 2001; Acland, Aguirre et al. 2005).

Based on the heterogeneous genetic basis of RP and the lack of knowledge of specific mechanisms, designing gene therapy approaches for the disease is a challenge. The most desirable treatment for RP is one that is applicable to all forms of the disease, regardless of the mutation, and targets a feature common to all, such as the apoptotic death that all photoreceptors succumb to.

1.3.2 XIAP Gene Therapy

XIAP protein has been used to protect the retina is several models of retinal degeneration. In one study, N-methyl-n-nitrosourea (MNU), a potent DNA methylating agent, was used to induce rapid and severe retinal degeneration via apoptosis in rats. Eyes which had received a subretinal injection of AAV vector encoding the XIAP gene showed structural and functional protection of the retina, as shown with histology and ERG, respectively. In eyes where the control vector encoding green fluorescent protein (GFP) was injected, all photoreceptors had died by 72 hours (Petrin, Baker et al. 2003). In another study, rat eyes received injections of either AAV-XIAP or AAV-GFP. Six weeks after injection ischemic apoptosis was induced by raising ocular pressure. Four weeks following ischemia, XIAP-treated eyes showed structural and functional protection (Renwick, Narang et al. 2006). Finally, XIAP was delivered with AAV to two different transgenic rat models of RP. XIAP treatment preserved the structure of retinas in both the P23H and S334ter rats, and retinal function in P23H rats for up to 28 weeks (Leonard, Petrin et al. 2007).

1.3.3 Limitations of Current Therapies

The various avenues of treatment for RP currently being employed or explored only focus on slowing the progress of the disease. No therapies to date can reverse the damage or restore vision once it has been lost. Cell replacement therapy could replenish photoreceptors in patients with RP and would allow for the move from a preventative treatment to one which could reverse the effects of the disease.

1.4 Cell Replacement Therapy

1.4.1 Current Use and Research

Cell replacement therapy is already an established treatment for various disorders. A simple example is the transfusion of blood to treat patients with anemia or blood cancers (Tortora and Grabowski 2003). A second example is the development of skin grafts. Skin grafts were first introduced in 1871 to cover skin wounds, such as those resulting from burns. Initially the protocol was to graft the patient's own skin from a healthy donor site. Today it is possible to harvest a healthy portion of skin and to expand it in culture, decreasing the amount of donor skin required (Horch, Kopp et al. 2005). More recently, the Edmonton protocol was developed. It involves transplantation of pancreatic islets under a glucocorticoid-free immunosuppression regimen. It has proven to be a viable route to achieving insulin independence in patients with type I diabetes (Shapiro, Lakey et al. 2000).

Extensive research is being conducted to discover whether other disorders can be targeted with cell replacement therapy and to explore new cell sources. Some examples include transplantation of embryonic stem cells to treat traumatic brain injury (Maegele and Schaefer 2008); the use of reprogrammed fibroblasts to treat Parkinson's disease (Wernig, Zhao et al. 2008); transplantation of embryonic and adult stem cells for Huntington's disease (Clelland, Barker et al. 2008); the use of embryonic, adult and mesenchymal stem cells, Schwann and olfactory ensheathing cells to treat spinal cord injury (Eftekharpour, Karimi-Abdolrezaee et al. 2008); and the use of autologous skeletal myoblasts (Sherman 2007), bone-marrow and cardiac-derived stem cells to treat heart disease (Leri, Kajstura et al. 2008).

In addition, research is underway to explore cell replacement therapy as a potential means of treating RP. In one study, a rat model was used to show that RPE grafts could rescue photoreceptors in certain forms of RP, which are caused by a lack of phagocytosis of the outer segments by mutated RPE cells (Hamel 2006). More useful for the treatment of RP is therapy aimed at replenishing photoreceptors, which are directly affected in most forms of RP. MacLaren and his colleagues isolated retinal progenitors from suspensions of postnatal day 1 (P1) mice and transplanted these by subretinal injection into neonatal and adult mice. They found that the transplanted cells successfully migrated into the ONL, integrated into the host retinas, differentiated into photoreceptors and made appropriate synaptic connections with the surrounding tissue. When the same cells were injected into mouse models of inherited retinal degeneration, it was found that the vision of the test animals was improved (MacLaren, Pearson et al. 2006).

1.4.2 Sources of Retinal Precursor Cells

There are various sources of retinal precursor cells which could be used to treat retinal degenerative disorders, such as RP. One source is embryonic stem cells (Zhao, Liu et al. 2002; Ikeda, Osakada et al. 2005; Lamba, Karl et al. 2006). However, the use of embryonic tissues is controversial and there is still incomplete knowledge of the genetic control programs driving embryonic stem cell fate and plasticity. Adult retinal progenitor cells (aRPCs) can be harvested from RPE cells within the ciliary body of the eye (Ahmad, Tang et al. 2000; Tropepe, Coles et al. 2000; Coles, Angenieux et al. 2004). These cells are of a neural lineage and in culture form free-floating aggregates, or neurospheres. aRPCs can be maintained in an undifferentiated state when cultured

without serum in the presence of fibroblast growth factor 2 (FGF2) and epidermal growth factor (EGF). It was also reported that under differentiating conditions, these cells can be induced to form various cell types including photoreceptors, bipolar neurons, astrocytes and Müller glia (Ahmad, Tang et al. 2000; Tropepe, Coles et al. 2000; Coles, Angenieux et al. 2004). However, various lines of evidence suggest that aRPCs have very limited proliferative capabilities (Tropepe, Coles et al. 2000; Seaberg and van der Kooy 2003; Giordano, De Marzo et al. 2007; Xu, Sta Iglesia et al. 2007) and that they primarily differentiate into glial cell types (Ahmad, Tang et al. 2000; Akagi, Mandai et al. 2004; Coles, Angenieux et al. 2004; Xu, Sta Iglesia et al. 2007), making the ciliary body-derived aRPCs unsuitable for photoreceptor cell replacement therapy.

Yet another source of retinal progenitors is neonatal retinal tissue. In the MacLaren study mentioned above, the source of retinal precursor cells was neonatal mouse retinas harvested at P1, the ontogenetic period which coincides with peak rod photoreceptor development (MacLaren, Pearson et al. 2006). Thus far, this cell source has shown to be the most successful for use in transplantation and as a potential therapy for RP. The cells in this study, however, were transplanted directly after harvesting, and were not kept or expanded in culture (MacLaren, Pearson et al. 2006). If this approach was translated to the clinic, harvesting of cells from donor eyes at the time of surgery would be required. It would be far easier, as far as donor tissue availability and timing are concerned, to possess a source of cells which can be harvested once, maintained and expanded in culture for long periods of time and used as needed.

1.4.3 Hh-RPCs

A method has been developed for the isolation and long-term propagation of retinal progenitor cells (RPCs) from the neonatal mouse retina (Wang and Wallace, unpublished).

Activation of sonic hedgehog (Hh) signaling is critical for progenitor and stem cell maintenance in the central nervous system and it was found to promote cell division in retinal precursor cells (Jensen and Wallace 1997; Wang, Dakubo et al. 2005). Hh was used, in combination with mitogens employed previously for retinal progenitor cell culture (Ahmad, Tang et al. 2000; Tropepe, Coles et al. 2000; Coles, Angenieux et al. 2004), to promote long-term propagation of RPCs outside of the retinal environment. The use of an Hh-agonist, along with EGF and FGF2, reliably allowed for the establishment of adherent cell lines from dissociated P1 mouse retinas. These Hh-agonist expanded RPCs (Hh-RPCs) expressed neural progenitor markers *Nestin and* Chx10 (Fig. 6.A) (Wang and Wallace, unpublished). *Nestin* is a neurofilament protein that is expressed largely by neuroepithelial stem cells, while *Chx10* is a homeobox gene that is expressed in uncommitted retinal progenitors (Ahmad, Tang et al. 2000; Tropepe, Coles et al. 2000).

It was shown that the Hh-RPCs could be maintained in culture for over 60 passages or 6 months and could recover following cryopreservation. After 8 days of co-culture with P1 mouse retinal explants or 14 days after transplantation *in vivo* into 3 day old mouse eyes, Hh-RPCs exhibited a high degree of integration throughout the INL and ONL of the retina (Fig. 6.B). The transplanted Hh-RPCs were found to robustly differentiate into photoreceptors (Wang and Wallace, unpublished). Being a stable, long-

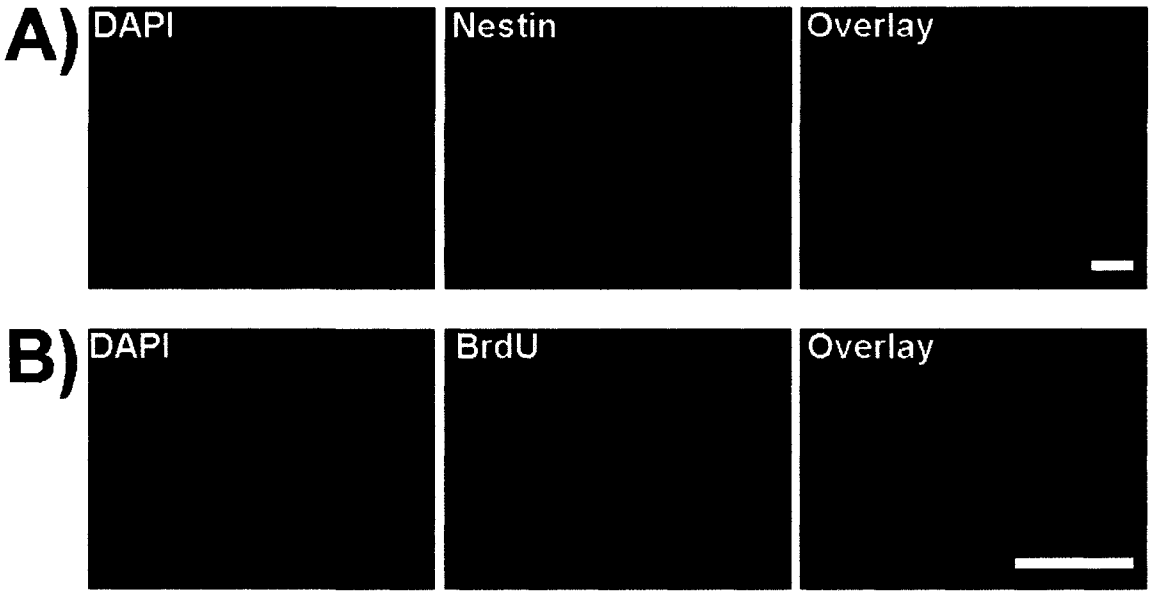

Figure 6: Properties of C57BL/6 mouse Hh-RPCs.

A) Fluorescence images of Nestin expression by Hh-RPCs. Hh-RPCs were cultured for 28 days, labeled for Nestin (red) and counterstained with DAPI (blue). Courtesy of Dr. Yaping Wang. **Bar = 10μm**

B) Fluorescence images of Hh-RPCs integrating in mouse retinal explant. Hh-RPCs were labeled with BrdU and then co-cultured with P0 mouse retinal explant for 8 days. Explant sections were labeled with anti-BrdU antibody (red) to detect integrating Hh-RPCs. Explants were counterstained with DAPI (blue). Courtesy of Dr. Yaping Wang. **Bar = 100μm**

term source of retinal progenitor cells with the ability to differentiate into photoreceptors, the Hh-RPCs are ideal candidates for applications in cell replacement therapy of the retina.

1.5 Post-Transplant Apoptosis

For cell replacement therapy of RP using Hh-RPCs to be useful, the grafted tissue must survive and integrate into its host environment in significant numbers. One major obstacle to achieving this is apoptotic loss of donor tissue following transplantation. Various research groups exploring diverse model systems and tissue sources have shown that large numbers of cells are lost via programmed cell death within a short period of their delivery to the host tissue. For example, Bakshi *et al.* showed that 24 hours after transplanting neonatal mouse neural progenitor cells into rat brain, only 2-4.5% of the grafted tissue had survived. It was subsequently discovered that as much as 42% of the cells had died via apoptosis (Bakshi, Keck et al. 2005). Similarly, transplantation of fetal ventral mesencephalic (VM) neurons into the central nervous system was forwarded as a means of structural brain repair for patients with Parkinson's disease. However, it was found that up to 99% of grafted tissue dies within one week of transplantation, limiting the utility of the treatment. Apoptotic death was found to be largely responsible for the grafted tissue loss (Boonman and Isacson 1999). In a study conducted in rats, Schwann cells were transplanted into injured and healthy spinal cords. Of the two million transplanted cells, only a few individual survivors were detected two weeks after the transplant, and the massive tissue loss was again attributed to apoptosis (Hill, Moon et al. 2006). Finally, it was found that during the Edmonton Protocol, over 60% of transplanted islets died via apoptosis (Biarnes, Montolio et al. 2002).

1.5.1 Increasing Transplant Survival

Based on extensive experimental evidence, examples of which were just presented, post-transplant apoptosis has been identified as a key player in limiting the efficacy of cell replacement therapy. In light of this, several lines of research are emerging which target apoptosis in hopes of increasing transplant survival. For example, donor islets were induced to over-express XIAP protein from a viral vector. When these islets were used for transplantation according to the Edmonton protocol, it was found that 70% less islet mass was required to confer insulin independence in mouse models with Type 1 Diabetes (Emamaullee, Rajotte et al. 2005). In another study, rat cardiomyocytes over-expressing BCL-2 from an adenoviral vector were delivered to an infarcted rat heart which was explanted and cultured into the abdomen of recipients in a "working heart" model. Up to 4 weeks after the procedure, more cells were detected in the recipient hearts if they had been pre-treated with BCL-2 (Kutschka, Kofidis et al. 2006). In a similar study, mesenchymal stem cells (MSCs) derived from adult rat bone marrow were transfected with the BCL-2 gene and delivered to infarcted rat hearts via intracardiac injection. Transplant survival with BCL-2-MSCs increased 2.2-fold, 1.9-fold, and 1.2-fold at 4 days, 3 weeks, and 6 weeks, respectively, compared with controls (Li, Ma et al. 2007). Studies such as these provide promising evidence that the efficacy of cell replacement therapy can be increased by preventing post-transplant apoptosis. Along the same lines, it may be possible to increase the numbers of Hh-RPCs integrating into degenerating retinas by making them over-express a potent inhibitor of apoptosis, such as XIAP protein.

1.6 Vectors

Several vectors were available for the delivery of XIAP protein to Hh-RPCs when this study was undertaken, each with its advantages and disadvantages.

1.6.1 AAV

AAV is a parvovirus and one of the smallest animal-infecting DNA viruses. AAV is a defective parvovirus meaning that it requires co-infection with a helper virus, such as adenovirus or herpes virus simplex, for productive infection. In the absence of a helper virus, AAV integrates its DNA into the host genome. This property, along with AAV not being linked to any known disease, makes AAV an attractive vector for *in vivo* and *in vitro* gene delivery (Grieger and Samulski 2005). AAV vectors are being extensively used in research studies. Recent publications include the use of AAV to deliver genes to the mouse cochlea to prevent hereditary prelingual deafness (Iizuka, Kanzaki et al. 2008) and delivery of the myotubularin gene to mouse skeletal muscle (Buj-Bello, Fougerousse et al. 2008). In addition, clinical trials employing AAV as vectors for gene therapy are underway. In one study, AAV was used to deliver the RPE65 gene to three patients with Leber's Congenital Amaurosis (Maguire, Simonelli et al. 2008); another study presented the results of a phase I clinical trial using AAV gene therapy to treat Parkinson's disease (Eberling, Jagust et al. 2008).

Despite the widespread application of AAV vectors, their use has certain drawbacks. The wild type AAV genome is approximately 4.7kb, and a vector based on AAV can accommodate a maximum insert of only 4.5kb (Grieger and Samulski 2005). This puts a limit on which genes can be delivered using AAV. Many strains, or serotypes, of AAV have been discovered. The best characterized are serotypes 1 through

11, which range in sequence homology from 55 to 85%. Based on differences in viral capsid proteins as well as genes required for viral DNA integration, each AAV serotype selectively targets and infects only certain cell types (Grieger and Samulski 2005), and the optimal serotype for every application has to be determined. Instead of screening serotypes, AAV capsid proteins can be modified to include molecules that serve as specific targets for desired cell types, however this approach is also time and labour intensive (Stachler and Bartlett 2006).

When considering AAV as a potential vector for delivery of genes to retinal precursor cells, the main obstacle is that evidence from literature suggests AAV vectors do not efficiently transduce stem and progenitor cells (Hughes, Moussavi-Harami et al. 2002; Smith-Arica, Thomson et al. 2003; Surace, Auricchio et al. 2003; Srivastava 2005). In previous work, I tested AAV serotypes 1, 7, and 8 on mouse and rat aRPCs. I found that of the serotypes tested, serotype-1 was most successful at delivering genes to aRPCs. However, it showed very minimal (<1%) infection rates even at multiplicities of infection (MOIs) as high as 1000x. I also tested AAV serotype-1 on C57BL/6 mouse Hh-RPCs. Again, it had very low (<1%) infection efficiency at MOIs as high as 1000x (Szymanska 2006). These findings led to the exclusion of AAV from the current study.

1.6.2 Lentivirus

Lentiviruses are enveloped viruses carrying two copies of coding RNA. They belong to the retrovirus family, and their natural life cycle includes integration of the viral genome into that of the host. They are unique due to their very long incubation times, ranging from months to years. These properties of lentiviruses, when harnessed in vector form, allow for long-term expression of transgenes (Federico 2003). In addition

to infecting dividing cells, lentiviral vectors have the advantage of being able to transduce non-dividing cells. Lentiviruses can chaperone their provirus into the nucleus instead of having to wait until breakdown of the nuclear envelope during S phase. The use of *human immunodeficiency virus 1* (HIV1)-based lentivectors is especially advantageous because the virus has been so well studied and there is a wealth of information concerning its replication cycle and structure. This has allowed for the exploitation of certain features, like its long terminal repeats (LTRs), which are required for integration and expression of the virus, and exclusion of other genes, such as *gag* and *pol*, to ensure safety when handling the vectors (Lu, Humeau et al. 2004). Another advantage of lentiviral vectors is their ability to accommodate large inserts. The size of the wild type HIV1 genome, provirus, is approximately 9kb. Vectors based on HIV1 with proviral length in excess of 18kb have been successfully produced (Kumar, Keller et al. 2001).

A major disadvantage of using lentiviral-based vectors is the fact that they integrate randomly into the host genome. Schroder and his colleagues demonstrated integration of wild-type HIV-1 into actively transcribing genes and regional integration hotspots in which a small 2.4-kb area accounted for 1% of the integration sites (Schroder, Shinn et al. 2002). Despite such findings, which suggest a slight preference for integration sites, in the majority of cases HIV1 DNA insertion into host chromosomes is random, which can lead to insertional mutation (Park 2007).

Lentiviral infections are carried out in the presence of polybrene. Polybrene, or hexadimethrine bromide, is a cationic polymer which has been shown to increase infection efficiency of retroviruses in cell culture. It is thought to do so by complexing with viral particles to form aggregates which sediment allowing the virus to reach cells

quicker than it would by simple diffusion (Landazuri and Le Doux 2004), and by neutralizing charges on cell and viral surfaces allowing for more efficient cell to virus binding (Davis, Rosinski et al. 2004). One can actually increase infection efficiency by increasing polybrene concentrations but only to a point. Polybrene is known to be a cytotoxic agent (Ransdell, Haller et al. 1965; Ribelin 1984).

Based on their many advantages and studies indicating that they have been successfully used to transduce stem cells in the past (Gropp and Reubinoff 2006; Capowski, Schneider et al. 2007; Cherqui, Kingdon et al. 2007; Hong, Hwang et al. 2007; Zhao and Lever 2007; Ricks, Kutner et al. 2008), lentiviral vectors were chosen to be explored in this study as a means of delivering the XIAP gene to Hh-RPCs.

1.6.3 TAT PTD

Protein transduction domains (PTDs) are amino acid sequences that, when linked to other proteins, DNA, RNA or drugs, mediate delivery of the complexes across cell membranes. To date, 3 PTDs have been studied. The first resides in the Antennapedia (Antp) protein from *Drosophila* (Derossi, Joliot et al. 1994). The HSV VP22 protein from herpes virus simplex also contains a PTD (Elliott and O'Hare 1997). The third and best studied PTD comes from the HIV1 transactivator of transcription (TAT) protein. The TAT PTD is 11 amino acids long with the sequence: YGRKKRRQRRR (Frankel and Pabo 1988; Green and Loewenstein 1988). TAT-mediated uptake is thought to occur by macropinocytosis, a form of fluid phase endocytosis. It is known that the highly charged Arginine residues in the TAT PTD are required to trigger uptake; however the molecules which serve as receptors on target cells have not been positively identified. It

is thought that the TAT PTD could bind to ubiquitous glycan chains on cell surfaces or to heparan sulfate proteoglycans (Gump and Dowdy 2007).

TAT fusion proteins show concentration-dependent delivery to the cytoplasmic and nuclear compartments with practically 100% efficiency (Wadia and Dowdy 2002). The fusion protein can be detected within the target cells in as little as 5 minutes (Schwarze, Ho et al. 1999). Another advantage of using the TAT PTD is that it has been used previously, in conjunction with XIAP protein, to protect against apoptosis. Constructs consisting of various domains of XIAP protein linked to the TAT PTD were injected intravenously into rats. Following cerebral ischemia, induced with distal occlusion of the middle cerebral artery, rats which had received TAT-XIAP showed smaller infarct volumes and performed better in a water maze test (Guegan, Braudeau et al. 2006).

One disadvantage of using a TAT-fusion protein is that, while initial uptake is very efficient, the over-expression of the target protein is transient. The delivered TAT-fusion protein is degraded within the host cells and expression drops off. The exact time course of expression varies depending on each cell type. Before TAT-fusion protein-transduced Hh-RPCs can be used in any experiments, the exact expression pattern of the particular fusion protein has to be mapped out. For example, to use the TAT PTD to deliver XIAP protein in hopes of protecting cells against post-transplant apoptosis, it would be necessary to know when expression of the fusion protein peaks so as to time the transplants with the period where greatest protection against apoptosis can be provided.

1.7 FACS

Vector transduction is not always 100% efficient. If the delivered transgene is fluorescent, or possesses a fluorescent tag, the amount of transgenic cells can be enriched with fluorescence activated cell sorting (FACS).

During FACS, cells are dissociated to generate a single-cell suspension. Individual cells traveling single file in a fine stream of media, typically phosphate-buffered saline (PBS), pass through a laser beam. The laser rapidly measures the fluorescence of each cell. Next, a vibrating nozzle generates tiny droplets, which are given either a positive or negative charge at the moment of formation. The charge assigned to each droplet depends on whether it contains a fluorescent cell. The droplets containing fluorescent cells are deflected by a strong electric field into an appropriate container. Any large clumps of cells, detected by their increased light scattering, are left uncharged and are discarded. This technology can detect 1 fluorescent cell in a pool of 1000 unlabeled cells and allows for the sorting of thousands of cells each minute (Alberts, Johnson et al. 2002).

The procedure has certain drawbacks. Firstly, the equipment required for FACS is very expensive and requires extensive training to operate (Alberts, Johnson et al. 2002). Secondly, while FACS can greatly increase the proportion of fluorescence-positive cells in a population, 100% purity is not always achieved (Hempel, Sugino et al. 2007).

1.8 XIAP Protein in Differentiation

Recently, it has been shown that endogenous caspase-3 activity is required for the differentiation of skeletal muscle (Fernando, Kelly et al. 2002), neurons (Fernando,

Brunette et al. 2005) and osteoclasts (Szymczyk, Freeman et al. 2006). The same could potentially also be true of photoreceptors. Caspase-3 is a target of XIAP protein, therefore the concern exists that if retinal progenitor cells were made to over-express XIAP protein, their ability to differentiate into photoreceptors could be inhibited.

In 2004, a study by Zeiss *at al.* looked at retinal development in caspase-3 knockout mice. They found that caspase-3 deficient animals show ocular abnormalities such as: marginal microphthalmia, peripapillary retinal dysplasia, delayed regression of vitreal vasculature, and retarded apoptotic kinetics of the INL. However, cross-sections of retinas from postnatal days 0, 5 and 16 showed comparable morphology between wild type and caspase-3 knockout mice. Nuclei in the ONL of caspase-3 knockout mice appeared normal and photoreceptor discs were observed indicating that photoreceptors do form in these mice (Zeiss, Neal et al. 2004). These findings suggest that caspase-3 is not required for photoreceptor differentiation. It therefore follows that XIAP protein over-expressing retinal progenitor cells should retain the ability to differentiate into photoreceptors.

1.9 Thesis Experiments & Hypothesis

Based on previous studies that show apoptosis to be largely responsible for death of donor tissue during transplantation and the fact that XIAP protein over-expression has been shown to improve transplant survival, it is thought that retinal progenitor cells induced to over-express XIAP protein will better survive transplantation. By increasing transplant survival, a greater population of donor cells will be available to repopulate retinas damaged by various forms of retinal degeneration, such as RP.

An initial set of experiments sought to map out optimal conditions for delivery and expression patterns of XIAP protein in C57BL/6 mouse Hh-RPCs following lentiviral and TAT fusion delivery. It was found that infection conditions for the lentiviral vectors, which optimally balance moderate infection efficiency with moderate cytotoxicity, are achieved in the presence of 7.5μg/mL of polybrene. FACS of lentivirally-transduced cells produced a virtually homogenous population in which steady levels of XIAP protein expression could be observed for up to 36 days after infection. TAT fusion protein experiments were carried out with a reporter construct containing TAT PTD linked to enhanced GFP (eGFP). The results indicated that maximal uptake of TAT-eGFP by Hh-RPCs occurred within 24 hours and that the protein persisted for up to 5 days. The TAT PTD, however, appeared to direct fusion proteins to the nucleus of target cells. This fact precludes the TAT PTD from being used for XIAP protein delivery. Modified PTDs, which direct their target to the cytoplasm, will have to be explored before PTDs can be applied towards the ultimate aim of this project.

While transduction of Hh-RPCs with a TAT-fusion protein proved problematic, this study describes in detail the conditions for lentiviral delivery of XIAP. Preliminary results also suggest that these cells retain the ability to differentiate into photoreceptors. Once the robustness of their differentiation potential is assessed these cells can be analyzed for resistance to apoptosis, increased transplant survival and vision improvement in animal models of retinal degeneration. This study represents a very important first step towards developing cell replacement therapy as a potential treatment for RP.

2. MATERIALS AND METHODS

2.1 Animals

All animals used in this study were C57BL/6 mice, obtained from Charles River Laboratories (Wilmington, MA). The mice were bred to generate pups for sampling of tissues. The date of birth of pups was designated as postnatal day 0 (P0). P0 and P1 mice were used to generate Hh-RPCs and for *in vitro* retinal explant studies. The animals were cared for in accordance with the Association of Research in Vision and Ophthalmology (ARVO) Statement for the Use of Animals in Ophthalmic and Vision Research and the guidelines of the University of Ottawa Animal Care Committee. Animals were housed under standard laboratory conditions (22 ± 2°C; 60 ± 10% relative humidity; 12:12 hr light/dark cycle; food and water available ad libitum).

2.2 Generation of Lentiviral Vectors

The two lentiviral vectors used in this study were generated by Dr. Wai Gin Fong (Postdoctoral Fellow, Tsilfidis lab, OHRI). The first lentivector encodes GFP only and is referred to as HIV1-GFP. The second vector, which encodes the XIAP gene and co-expresses GFP, is referred to as HIV1-XIAP/GFP.

The HIV1-GFP vector is based on an un-modified pWPXLd plasmid (Tronolab). The plasmid contains LTRs from HIV1 and encodes GFP under the control of the human EF1-α promoter (Fig. 7). The HIV1-XIAP/GFP lentivector is also based on the pWPXLd plasmid, which has had a hemoagglutinin (HA) tagged XIAP gene cloned in. The vector contains LTRs from HIV1 and HA-XIAP expression is driven by the human EF1-α promoter. It co-expresses GFP, which is driven by the *Encephalomyocarditis virus* (EMCV) internal ribosomal entry site (IRES) (Fig. 8).

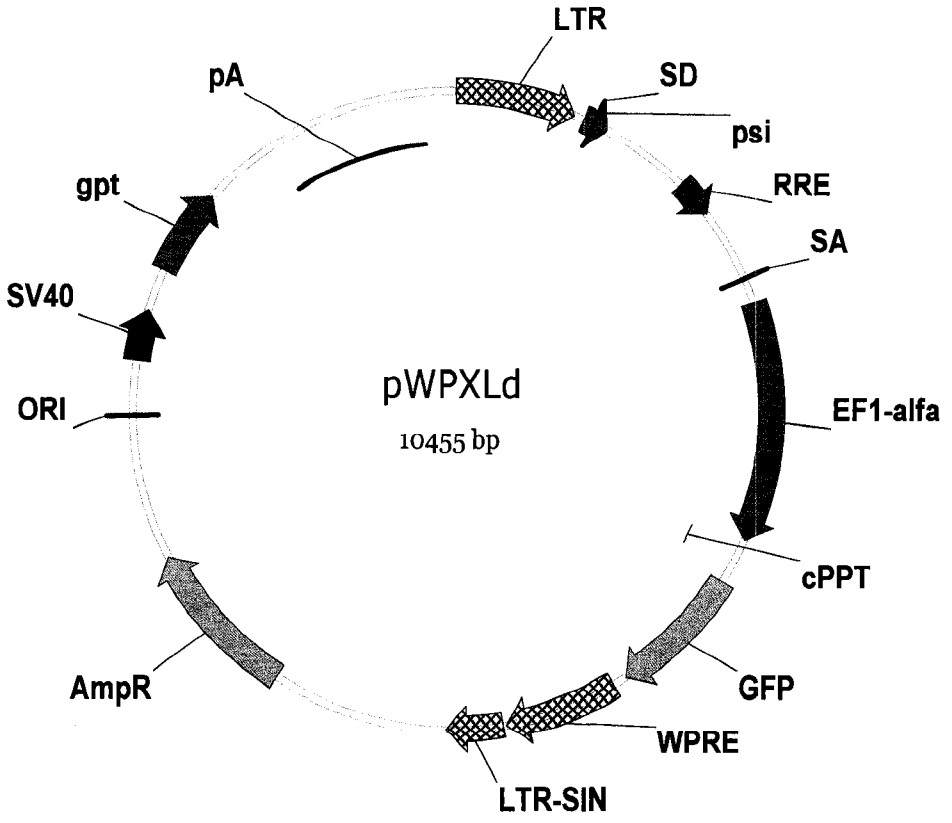

Figure 7: Map of the unmodified pWPXLd plasmid, which is the basis of the HIV1-GFP lentiviral vector. The long terminal repeats (LTRs) are from the *Human Immunodeficiency Virus 1* (HIV1) and green fluorescent protein (GFP) expression is driven by the human EF1-α promoter. Courtesy of Dr. Wai Gin Fong.

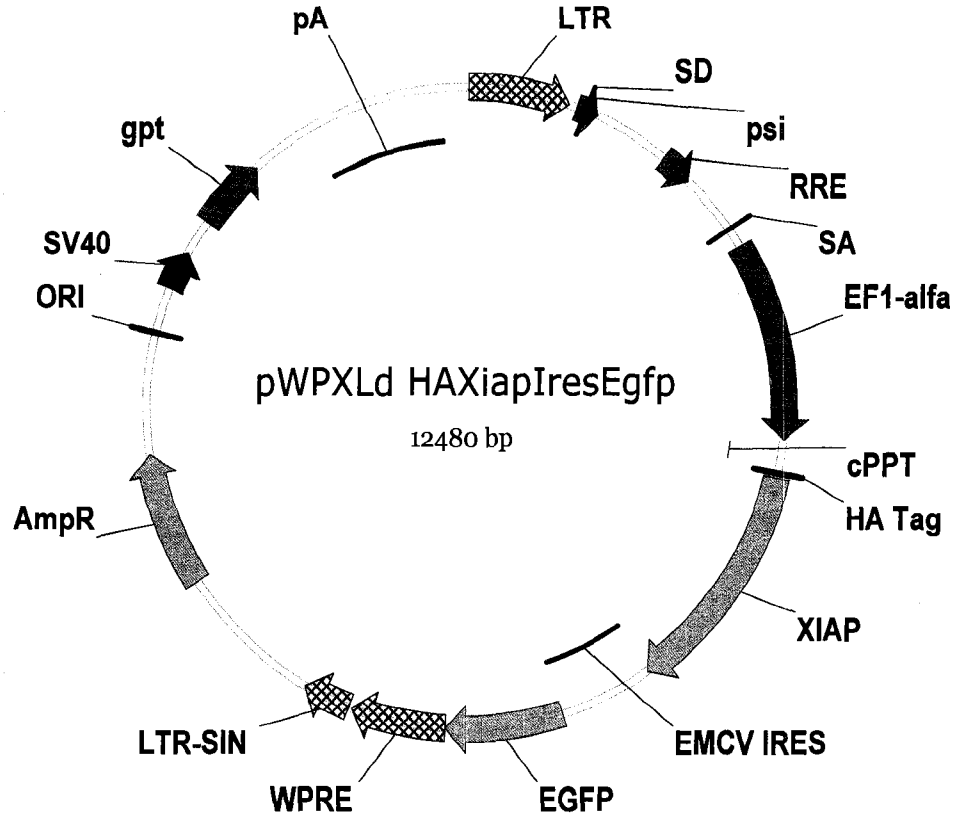

Figure 8: Map of the modified pWPXLd plasmid, which is the basis of the HIV1-XIAP/GFP lentiviral vector. The plasmid has had a copy of hemoagglutinin (HA) tagged XIAP gene cloned in. The expression of HA-XIAP is driven by the human EF1-α promoter. The long terminal repeats (LTRs) are from the *Human Immunodeficiency Virus 1* (HIV1). Green fluorescent protein (GFP) is co-expressed by this vector and its expression is driven by the *Encephalomyocarditis virus* (EMCV) internal ribosomal entry site (IRES). Courtesy of Dr. Wai Gin Fong.

To generate the lentivirus, 293T cells were plated in a 10cm culture dish at a density sufficient to achieve 70% confluency the next day. The 293T cells were cultured in Dulbecco's Modified Eagle's Medium (DMEM; HyClone) supplemented with 5% heat inactivated fetal bovine serum (FBS; Sigma), 2mM L-glutamine (Gibco), 100 units/mL penicillin-0.1mg/mL streptomycin (Gibco) and 1mM sodium pyruvate (Sigma). The cells were incubated at 37°C, 5% CO_2 and 100% relative humidity. One day after plating, lipofectamine transfection was carried out. Twenty micrograms of transfer vector (pWPXLd for HIV1-GFP virus or pWPXLdHAXiapIresGfp for HIV1-XIAP/GFP) was added to 1.5mL of serum free DMEM, along with 15μg of packaging plasmid (psPAX2 or pCMV delta R8.2; Tronolab) and 15μg VSV envelope plasmid (pMD2G; Tronolab). Sixty micrograms of Lipofectamine 2000 (Invitrogen) was added to another 1.5mL of serum-free DMEM. This mixture was incubated at room temperature for 5 minutes. The lipofectamine and DNA-containing media were combined, inverted 10 times and incubated at room temperature for 30 minutes. This mixture was added to the 293T cells in a drop-wise manner. One day after the transfection, the 293T media was changed. Every day for the next 3 days, the virus containing 293T media was collected. The media was centrifuged in a swinging bucket rotor for 5 minutes at room temperature. It was then filtered through a 0.45μm pore syringe-tip filter (Fisher), and stored at 4°C until concentration. Any cells collected with the 293T media remained in the pellet following centrifugation. These were resuspended and returned to the culture dish, which was overlaid with fresh media. To concentrate and purify the virus, 7mL of the viral supernatant was pipetted into Ultra-clear 14x89mm ultracentrifuge tubes (Beckman-Coulter) and was underlaid with 2mL of 20% sucrose in PBS at pH 7.5. The tubes were

centrifuged for two hours at 28000rpm in a Beckmann XL-90 centrifuge using a SW41ti rotor. The supernatant was discarded and the pellet was re-suspended in 500μL of 20% sucrose. At this point, each preparation of vector was complete, it was given a name for tracking purposes (Lent # HIV1-GFP or Lent # HIV1-XIAP/GFP) and the titre was determined.

To determine lentiviral titre, 293A cells were seeded at sufficient density to reach confluency within 48 hours (5×10^4 cells per well of 24-well plate). The 293A cells were cultured under the same conditions as the 293T cells. Serial dilutions (10^{-2} to 10^{-6}) of the viral vector were prepared in regular culture media and 250μL of each was added per well 24 hours after seeding. Infections were carried out for one hour at 37°C in the presence of 10.0μg/mL polybrene. The media was then topped up to 500μL and cells were cultured for an additional 23 hours. Cells were then fixed, immunolabeled and examined with fluorescence microscopy (Nikon Eclipse TE2000-E; Nikon; Melville, New York). The number of infected (GFP-expressing or GFP and HA-expressing) cells was counted in five randomly selected fields of view, and once dilution factor and area ratios were taken into account, an approximate titre was expressed as the number of transduction units (TU)/mL. See Appendix 1 for sample calculations.

2.3 Generation of TAT-Fusion Proteins

The TAT fusion protein used in this study was generated by Dr. Wai Gin Fong. BL-21 (DE3) competent *Escherichia coli* (*E. coli*) cells were transfected with a modified pET-28a plasmid (Novagen). The plasmid encodes T7 and 6xHis tags and had the TAT PTD cloned in along with enhanced green fluorescent protein (eGFP) (Fig. 9) under the control of the bacterial T7 promoter. The fusion protein resulting from transcription and

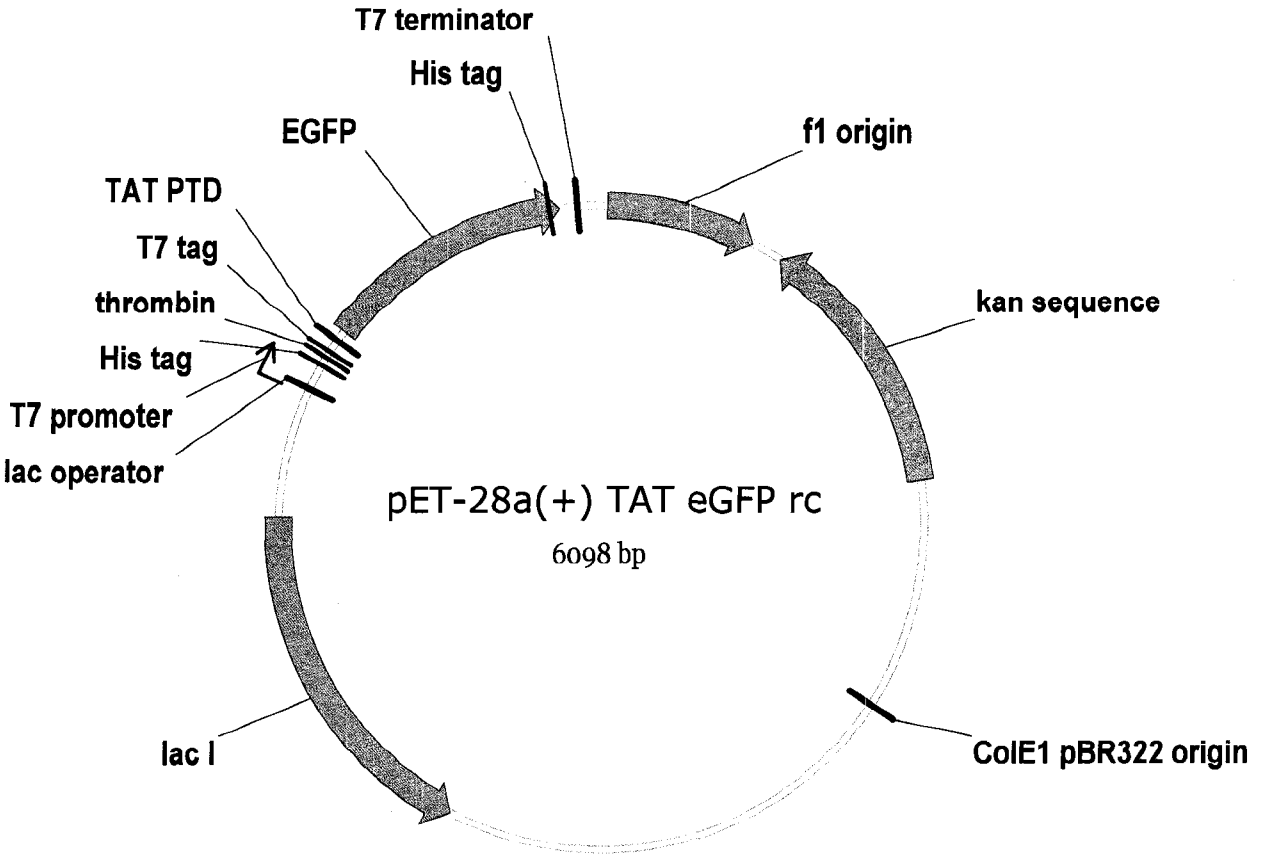

Figure 9: Map of the modified pET-28a (+) plasmid, which is the basis of the TAT-eGFP fusion protein. It encodes eGFP along with the TAT PTD and a 6x His tag driven by the T7 bacterial promoter. Courtesy of Dr. Wai Gin Fong.

translation of this modified plasmid is referred to as TAT-eGFP. The final protein contains the T7 tag, which allows for immunohistological localization, and the 6xHis tag, which allows for chromatographic purification.

Plasmid-containing *E. coli* cells were seeded into Luria Broth and incubated at room temperature on a shaker for 24 hours. The cells were induced with 0.5mM isopropyl β-D-1-thiogalactopyranoside (IPTG) and cultured for an additional 24 hours at room temperature with shaking. Cell lysis and protein purification using nickel-charged resin (Ni-NTA Agarose; Quiagen) was performed under denaturing conditions with 8M urea as described by Becker-Hapak *et al.* (Becker-Hapak, McAllister et al. 2001). See Appendix 2 for complete protocol of TAT-fusion protein purification. To solubilize the denatured protein a volume of TAT-eGFP in 8M urea buffer was placed in dialysis tubing with a 10kDa molecular weight cut off. The dialysis tubing was immersed in a volume of PBS, one hundred times the amount of TAT-eGFP solution, and allowed to equilibrate at 4°C overnight. The PBS solution was changed and allowed to equilibrate again at 4°C overnight. Having been reduced a hundred fold twice, the urea concentration in the final TAT-eGFP preparation is 0.8mM. The protein in the preparation was quantified using the DC protein assay (Biorad) and TAT-eGFP purity was assessed by 12% sodium dodecyl sulfate-polyacrylamide gel electrophoresis (SDS-PAGE) followed by Coomassie staining.

To stain the SDS-PAGE gels, they were immersed in Coomassie stain solution: 50% methanol, 10% glacial acetic acid, 40% de-ionized water and 0.05% Coomassie Blue (ICN Biomedical). The gels in solution were brought to a boil in a microwave and then incubated for 5 minutes. The stain solution was poured out, and the gels were rinsed

twice with de-stain solution: 10% methanol, 10% glacial acetic acid in de-ionized water. The gels were then covered in 200mL of de-stain solution and microwaved twice for 45 seconds. The corner of a knotted Kimwipe was immersed into the de-stain solution and the gels were incubated on a rocker for 20 minutes. As the stain leached out of the gels, it was absorbed by the Kimwipe allowing for the resolution of protein bands.

2.4 Retinal Cell Culture

2.4.1 Generation of Retinal Explants

Whole eyes from P0 or P1 C57BL/6 mice were harvested and dissected in CO_2-Independent DMEM (Gibco). Retinal explants were generated from the eyes by removing the RPE, sclera and lens and transferring the neural retina onto a 13mm polycarbonate membrane (0.8μm pore size; Nucleopore) with the photoreceptor-side down. The membranes were transferred to a 24-well plate containing 0.5mL of retinal explant culture medium (RECM): 1:1 DMEM (Gibco): F12 (Sigma), 10µg/mL insulin (Sigma), 100µg/mL transferrin (Sigma), 100 mg/mL bovine serum albumin (BSA Fraction V; Sigma), 60ng/mL progesterone (Sigma), 16µg/mL putrescine (Sigma), 40ng/mL sodium selenite (Sigma), 25µg/mL Gentamicin (Gibco) and supplemented with Hh agonist (Frank-Kamenetsky, Zhang et al. 2002); gift from Curis) depending on the experiment. The explants were cultured at 37°C with 8% CO_2 and 100% relative humidity. See Appendix 2 for the complete protocol.

2.4.2 Generation of Hh-RPCs

The majority of the Hh-RPCs used in this study were obtained from Dr. V. Wallace. The protocol to generate Hh-RPC monolayers was established by Dr. Y. Wang of the Wallace Lab and is as follows: retinal explants were generated and cultured with

20nM Hh agonist from P0 or P1 C57BL/6 mice as described above. After two days of culture, the retinal explants were digested in 1mL of trypsin solution (0.75μg/mL; Sigma) at 37°C for 10 minutes. The digestion was stopped by the addition of 1mL trypsin inhibitor (Sigma) diluted at 1mg/mL in serum-free retinal cell culture media (SFRCM; as described by Tropepe et al. (Tropepe, Coles et al. 2000)); 1:1 DMEM (Gibco): F12 (Gibco), 6ng/mL progesterone (Sigma), 5ng/mL sodium selenite (Sigma), 100μg/mL transferrin (Sigma), 9.5μg/mL putrescine, 250μg/mL insulin (Sigma), 25ng/mL human EGF (Sigma), 10ng/mL human FGF2 (Sigma), 2μg/mlL Heparin (Sigma). The cells were triturated to generate a single-cell suspension and then spun down at 1500rpm for 5 minutes. The pellet was re-suspended in SFRCM and cultured in 24-well plates at a density of 5-10 x 10^4 cells/well. The cells were cultured in 0.5mL SFRCM supplemented with 5nM Hh agonist (SFRCM-Hh), which was refreshed every second day. The cells were cultured at 5% CO_2 and 100% relative humidity. After approximately two weeks, a monolayer formed and the cultures could be passaged every second day. To passage the cells, they were mechanically triturated to obtain a single-cell suspension which was diluted 1:2 in fresh SFRCM-Hh.

2.5 Lentiviral Infection of Hh-RPCs

2.5.1 Lentiviral Infection Optimization

Infections with HIV1-GFP and HIV1-XIAP/GFP lentivectors were carried out at various concentrations of polybrene. Twenty-four hours after seeding cells into a 24-well plate, cells from one well were resuspended and counted using a hemocytometer to determine the amount of viral preparation to add to achieve a 2x MOI for HIV1-GFP and a 1.5x MOI for HIV1-XIAP/GFP. Virus was added to cells in 250μL of SFRCM-Hh

with 5.0, 7.5 or 10.0μg/mL of polybrene. Two controls were run for each experiment, one containing 10.0μg/mL polybrene and no virus, and a second control without any polybrene or virus. One hour after addition of virus, an additional 250μL of SFRCM-Hh was added to each treatment. Cells were cultured for an additional 23 or 47 hours at which point immunohistochemistry was performed to localize infected cells and determine infection efficiency. The percentage of GFP-positive cells out of total counted 4'-6'-Diamidino-2-phenylindole dihydrochloride (DAPI)-stained nuclei was determined for five randomly-selected fields of view per treatment. The mean value represented the infection efficiency. All experiments were carried out in triplicate and the mean values were used for statistical analysis.

2.5.2 Live Counts

To determine the total number of cells, as well as the amount of dead cells following lentiviral infection, infections were carried out as described above for a total of 24 or 48 hours. At the end of each time point, all the cells in each treatment, including any dead ones, which had lifted off the bottom of the plate, were resuspended using mechanical trituration and collected by centrifugation at 1500rpm for 5 minutes. The pellet was resuspended in 100μL of SFRCM and 100μL of 0.4% Trypan Blue Solution (Sigma). Using a hemocytometer, the number of dead (blue) and live (clear) cells was counted for each treatment. All counts were performed four times and the mean values were used to determine the percentage of dead cells and the total cell number ratio as follows:

Equation 1 $$\% \text{ Dead Cells} = \frac{\text{Number of Dead (Blue) Cells}}{\text{Number Cells Total}_{(\text{Blue + Clear})}} \times 100\%$$

Equation 2 Total Cell Ratio = $\frac{\text{Mean Counted Total Cell Number in Particular Treatment}}{\text{Mean Counted Total Cell Number in 0.0}\mu\text{g/mL Polybrene Control}}$

Based on Equation 2, the total number of cells in the no virus and 0.0μg/mL polybrene control always becomes 1.000. All experiments were carried out in triplicate and the mean values were used for statistical analysis.

2.5.3 Shorthand Notation

Treatment groups which received virus are specified by the MOI and polybrene concentration used, e.g. 2x MOI 10.0PB. The polybrene concentration is abbreviated to xPB, where x indicates the amount in μg/mL. Treatment groups labeled as Ctrl followed by a polybrene concentration, e.g. Ctrl 10.0PB, are controls which did not receive any virus.

2.5.4 Long-Term Transgene Expression from Lentiviral Vectors

To monitor long-term expression of transgenes following lentiviral infection of Hh-RPCs, the cells were infected with lentivirus when their density was approximately 50% confluent. The infections were carried out under optimized conditions, with 7.5μg/mL of polybrene at 2x MOI and 1.5x MOI for the HIV1-GFP and HIV1-XIAP/GFP lentivectors, respectively. Once the cells reached 100% confluency, they were passaged at 1:2 into two new dishes and cultured until 100% confluent again. At this point, the cells were examined using a fluorescent microscope (Nikon Eclipse TE2000-E; Nikon; Melville, New York) to monitor GFP expression. Protein was extracted from the Hh-RPCs in one dish to be later analyzed by Western blot. The cells in the second dish were passaged as above and the cycle of photomicrography, protein extraction and passaging was repeated every time the Hh-RPCs became confluent.

2.6 FACS

Hh-RPCs were seeded into 6-well plates 24 hours prior to infection with HIV1-GFP and HIV1-XIAP/GFP lentivectors under optimized conditions. Cells were cultured for 8 days after infection and expanded by passaging every second day. On the day of the sort, cells were resuspended with mechanical trituration and pooled. The total cell number was determined by counting with a hemocytometer. The cells were centrifuged at 1500rpm for 5 minutes and the pellet was resuspended in sufficient SFRCM to achieve a cell density of 5 x 10^6 cells/mL. Immediately before sorting, the cells were passed through a 50μm CellTrics wire mesh filter (Partec). The cells were then sorted based on GFP expression using a DakoCytomation MoFlo (Fort Collins, Colorado). The GFP was excited with a 488nm Argon ion laser from Spectra-Physics (Irvine, California). GFP emission was collected using a 530/40nm bandpass filter. The flow rate was approximately 8500 events per second. Flow data was analyzed with DakoCytomation Summit version 4.0 software.

Upon completion of the sort, GFP-positive cells were contained within a mixed solution of SFRCM and PBS. The cells were spun down at 1500rmp for 5 minutes, the pellet was resuspended in 500μL of SFRCM-Hh which was transferred to 1 well of a 24-well plate. Once the well reached 100% confluency, it was split into 2 wells of a 24-well plate and the contents of these wells, once confluent, were transferred to 1 well of a 12-well plate. This 1 well was split into 2 and allowed to grow to confluency. These cells were finally transferred to 1 well of a 6-well plate. Once this well was 100% confluent, the cells were judged to be recovered from the FACS treatment, the whole process taking approximately 7 days. At this point, the sorted HIV1-GFP and HIV1-XIAP/GFP

infected cells were passaged and used as needed. A protein sample was extracted from cells in the HIV1-XIAP/GFP infected group for use in Western blot analysis to show enrichment of XIAP protein over-expressing cells.

2.6.1 Cryopreservation of FACS Hh-RPCs

To preserve cells which had been sorted following HIV1-GFP and HIV1-XIAP/GFP lentiviral infection, 8 confluent 35mm dishes were grown for each treatment. The cells from each group were pooled and centrifuged at 1500rpm for 5 minutes. The cell pellet was resuspended in a total of 4mL of SFRCM containing 10% dimethyl sulfoxide (DMSO), 20% heat-inactivated FBS and 5nM Hh agonist. The cell suspensions were transferred to 1mL cryovials (Corning) which were placed in a Cryo 1°C Freezing Container (Nalgene) in the -80°C freezer to allow for slow freezing overnight. The next day the cryovials were transferred to liquid nitrogen for long-term storage.

2.6.2 Transgene Expression by FACS Treated Hh-RPCs

To assess the long-term expression of lentiviral vector-delivered XIAP protein in a homogenous population of infected cells, 1 well of a 6-well plate of HIV1-XIAP/GFP infected Hh-RPCs was put aside 14 days after FACS treatment. This well was split into two new wells and was confluent 2 days later. Protein was extracted from cells in one of the confluent wells, and the second well was split into two again. The cycle of protein extraction and splitting was carried out every second day until protein samples had been collected for up to 28 days after the sort. Eight days elapsed between lentiviral infection and FACS treatment of Hh-RPCs. The last time point at which protein was collected in this experiment, 28 days, corresponds to a total of 36 days after initial infection.

2.7 Photoreceptor Differentiation of Hh-RPCs

To verify whether XIAP protein over-expressing Hh-RPCs can differentiate into photoreceptors, the cells were co-cultured with retinal explants (Wang and Wallace, unpublished). P1 C57BL/6 mouse retinal explants were generated as described in section 2.4.1. The explants were placed in 0.5mL RECM, without any Hh agonist, in 24-well plates. HIV1-XIAP/GFP and HIV1-GFP-infected Hh-RPCs were used for the co-culture, the GFP-only expressing Hh-RPCs were used as controls. The cells had been infected under optimized conditions, at 2x MOI and 1.5x MOI for the HIV1-GFP and HIV1-XIAP/GFP lentivectors, respectively, 15 days prior. The cells had also been sorted using FACS, 8 days after infection and 7 days before the photoreceptor differentiation experiment. To prepare the Hh-RPCs for the assay, the cells were resuspended by mechanical trituration and counted using a hemocytometer. The cells were then centrifuged at 1500rpm for 5 minutes and the pellet was resuspended in a volume of SFRCM to achieve a cell density of 1.0×10^8 cells/mL. One microliter of the cell suspension (total of 1.0×10^5 cells) was added per explant. The explants were cultured at 37°C in 8% CO_2 and 100% relative humidity. The explant media was refreshed every fourth day. After 8 days in culture, the explants were fixed, cryoembedded, sectioned and immunohistochemistry was performed to detect photoreceptor differentiation. The tissue sections were examined using fluorescence microscopy (Zeiss Axioskop; Zeiss; Oberkochen, Germany).

At the same time as the photoreceptor differentiation assay was started, protein was extracted from a sample of the HIV1-XIAP/GFP lentivector-infected Hh-RPCs used

for the co-culture with explants. The protein was analyzed with Western blot to show over-expression of XIAP protein by the cells.

2.8 TAT-eGFP Assays in Hh-RPCs

Hh-RPCs to be treated had been seeded into 12-well plates 24 hours prior to the start of the assay. The cells were washed once with PBS and then covered with 1mL of fresh SFRCM-Hh. TAT-eGFP protein preparation in PBS was spun down at 5000rpm for 5 minutes prior to use to sediment any large protein aggregates and then was added directly to SFRCM-Hh at volumes calculated to achieve final concentrations of 100.0μg/mL, 50.0μg/mL and 10.0μg/mL. Control wells received only PBS. Hh-RPCs were incubated with TAT-eGFP for 1, 24 and 48 hours as well as 3 and 5 days. Twenty-four hours after the start of the assay, the Hh-RPCs reached 100% confluency, and had to be passaged. They were suspended using mechanical trituration and then split 1:2 in fresh SFRCM-Hh. The treated cells were passaged every second day after this for the duration of the assay. At the end of each time point, the Hh-RPCs were fixed and immunohistochemistry was performed to detect GFP expression. In all experiments, the number of GFP-positive cells was counted for each treatment in five randomly-selected fields of view. The mean was used to determine the percentage of GFP-positive cells out of total counted DAPI-stained nuclei. All experiments were carried out in triplicate and the mean values were used for statistical analysis.

TAT-eGFP assays were also carried out on Hh-RPCs in 6-well plates. The assay was conducted as above, except that only 100.0μg/mL and 50.0μg/mL TAT-eGFP treatments were performed for 1, 24 and 48 hours as well as 3 and 5 days. At the end of these time points, protein was extracted from the cells to be run on Western blots.

2.9 Tissue Processing and Immunohistochemistry

2.9.1 Lentiviral Titration

293A cells were washed with PBS and fixed with 4% paraformaldehyde (PFA). Cells infected with both constructs were labeled with rabbit anti-GFP primary antibody (1:500; Invitrogen) and Alexafluor 488-conjugated goat anti-rabbit IgG secondary antibody (1:500; Invitrogen). In addition, cells infected with the HIV1-XIAP/GFP lentivector were also labeled with mouse anti-HA primary antibody (1:200; Roche) and Cy3-conjugated goat anti-mouse IgG secondary antibody (1:500; Jackson ImmunoResearch Laboratories). All cells were also labeled with DAPI (1:10,000; Sigma). See Appendix 2 for standard immunohistochemistry protocols.

2.9.2 Lentiviral Infection of Hh-RPCs

Hh-RPCs were washed with PBS and fixed with 4% PFA. Staining for GFP and DAPI was carried out on cells infected with HIV1-GFP. Cells infected with HIV1-XIAP/GFP were additionally labeled for the HA tag. All immunohistochemistry was carried out as described above in section 2.9.1. Direct immunohistochemistry was also carried out on HIV1-XIAP/GFP infected Hh-RPCs; the cells were labeled with fluorescein-conjugated rat anti-HA antibody (1:10; Roche), and counterstained with DAPI (1:10,000; Sigma). See Appendix 2 for standard immunohistochemistry protocols.

2.9.3 Photoreceptor Differentiation of Hh-RPCs

At the end of the 8 day co-culture with Hh-RPCs, the retinal explants were washed with PBS and fixed with 4% PFA for 1 hour. They were then placed in 30% sucrose solution at 4°C for 24 to 48 hours. The retinal explants were then transferred, along with the membrane on which they were cultured, into a plastic base mold

containing a 1:1 mixture of 30% sucrose and Optimal Cutting Temperature (OCT) compound. The mold was placed onto a Petri dish floating on liquid nitrogen and, once frozen, transferred to a -80°C freezer until ready to section. Cryosections of 10μm thickness were prepared with a Thermo Electron Corporation cryostat, air dried for 2 hours and stored at -20°C with desiccant.

To immunolabel the sections, they were removed from storage and allowed to come to room temperature. Chosen slides were post fixed with 4% PFA for 5 minutes and then labeled to detect co-cultured Hh-RPCs and photoreceptors. GFP labeling was carried out with rabbit anti-GFP primary antibody (1:500; Invitrogen) and Alexafluor 488-conjugated goat anti-rabbit IgG secondary antibody (1:500; Invitrogen). Rhodopsin was detected with mouse anti-rhodopsin primary antibody (1:6; from B630 cell supernatant) and Cy3-conjugated goat anti-mouse IgG secondary antibody (1:500; Roche). All sections were counterstained with DAPI (1:10,000; Sigma). See Appendix 2 for standard immunohistochemistry protocols.

2.9.4 TAT-eGFP Assays in Hh-RPCs

Prior to fixing Hh-RPCs treated with TAT-eGFP, extensive washing had to be carried out to remove any residual TAT-eGFP protein which had not been taken up by the cells. The Hh-RPCs were washed 3 times quickly with PBS, twice with SFRCM 5 minutes, followed by GFP and DAPI labeling, carried out as described in section 2.9.1.

2.10 Protein Extraction Western Blot Analysis

Western blots were generated with protein extracted from Hh-RPCs treated with lentivirus or TAT-eGFP. Prior to protein extractions, lentivector-infected Hh-RPCs were washed once with PBS. Cells treated with TAT-eGFP were washed 3 times quickly with

PBS, twice with SFRCM for 5 minutes and once again with PBS to remove any residual TAT-eGFP protein which had not been taken up by the cells. All protein was extracted using 350μL CelLyticM Reagent (Sigma) containing Protease Inhibitor Cocktail (Roche). Samples were incubated with the reagent for 15 minutes on a shaker at room temperature and then centrifuged at 18000rpm for 15 minutes. Total protein concentration of the collected supernatant was determined using the DC protein assay (Biorad) and the extracts were stored at -80°C. Fifteen or 20μg of protein from each sample was electrophoresed on either a 10 or 12% SDS-PAGE gel, along with Precision Plus Protein Dual Color Standards marker (Biorad). The protein was transferred onto a polyvinylidene difluoride (PVDF) membrane (Immobilon P; Millipore). To detect exogenous XIAP protein, the blots were probed with a primary antibody against the HA tag (Rat anti-HA at 1:1500; Roche), and a horseradish peroxidase-conjugated goat anti-rat IgG secondary antibody (1:2500; GE Healthcare). To detect GFP, blots were probed with anti-GFP primary antibody (Rabbit anti-GFP at 1:2000; Invitrogen), and a horseradish-peroxidase-conjugated donkey anti-rabbit IgG secondary antibody (1:4000; GE Healthcare). In addition, probing for XIAP protein was carried out using an anti-GST-XIAP primary antibody (Rabbit anti-GST-XIAP at 1:2500; provided by Dr. Robert Korneluk, CHEO) and a horseradish-peroxidase-conjugated donkey anti-rabbit IgG secondary antibody (1;5000; GE Healthcare).

Protein was detected on the blot using SuperSignal West Pico Chemiluminescent Substrate detection kit (Pierce). Following chemiluminescent detection, all blots were stripped using Re-Blot Plus Strong Solution (Chemicon) and then re-probed using rabbit anti-β-actin loading control primary antibody (1:10,000; Abcam), and a horseradish-

peroxidase-conjugated donkey anti-rabbit IgG secondary antibody (1:10,000; GE Healthcare). Protein was detected as above.

2.11 Statistical Analysis

To assess whether the increase in infection efficiency varied significantly with polybrene concentration at a particular time point during infection of Hh-RPCs with HIV1-GFP and HIV1-XIAP/GFP, the mean values were compared using Single Factor ANOVA. Single Factor ANOVA was also used to determine whether the percentage of GFP-positive cells was dependent on the concentration of TAT-eGFP added to Hh-RPCs.

For lentiviral infection optimization experiments, two-tailed Student's T-tests were used to compare the infection efficiency for both lentivectors between the 24 and 48 hour time points. To analyze live count data, percentage of cell death and total cell ratio following infection, two-tailed Student's T-tests were used to compare the values in the 0.0μg/mL polybrene no virus control (Ctrl 0.0PB) to all other treatments. Finally, this same test was used to compare the percentage of dead cells and the total cell number within each treatment, between the two time points (24 and 48 hours). All statistical analysis was performed using Microsoft Excel (Microsoft).

3. RESULTS

3.1 Titration of Lentiviral Vectors

Immunohistochemistry demonstrated that the HIV1-GFP vector expressed GFP and that the HIV1-XIAP/GFP vector co-expressed GFP with XIAP protein in 293A cells (Fig. 10). Table 1 is a summary of titres for the viral preparations which were used and they ranged from 4.65 x 10^6 to 5.34 x 10^7 TU/mL. Note that the lentiviral vector titres are low and the HIV1-XIAP/GFP vector titers are generally lower than the GFP-only constructs.

3.2 Lentiviral Infection of Hh-RPCs

3.2.1 HIV1-GFP Infection of Hh-RPCs

Phase contrast microscopy revealed no gross morphological alterations in Hh-RPCs following infection with the HIV1-GFP lentivector (Fig. 11). Fluorescence images of live cells as well as immunohistochemistry on fixed cells confirmed that Hh-RPCs expressed GFP following infection and the number of infected cells increased with increasing polybrene concentration (Fig. 11 and 12). A maximum infection efficiency of 32.87% was observed in the 2xMOI 10.0PB treatment, 24 hours after infection (Fig. 13). When looking at each time point separately, there is a statistically-significant increase in infection efficiency with increasing polybrene concentration ($P<0.05$). T-tests were used to compare infection efficiencies within the same polybrene concentration, between the 24 and 48 hour time points. No significant difference was observed.

Counts of dead and live cells following infection with HIV1-GFP lentivector show that, compared to the 0.0μg/mL polybrene no virus control (Ctrl 0.0PB), there was a significant amount of cell death only in the 2x MOI 10.0PB treatment 24 hours after

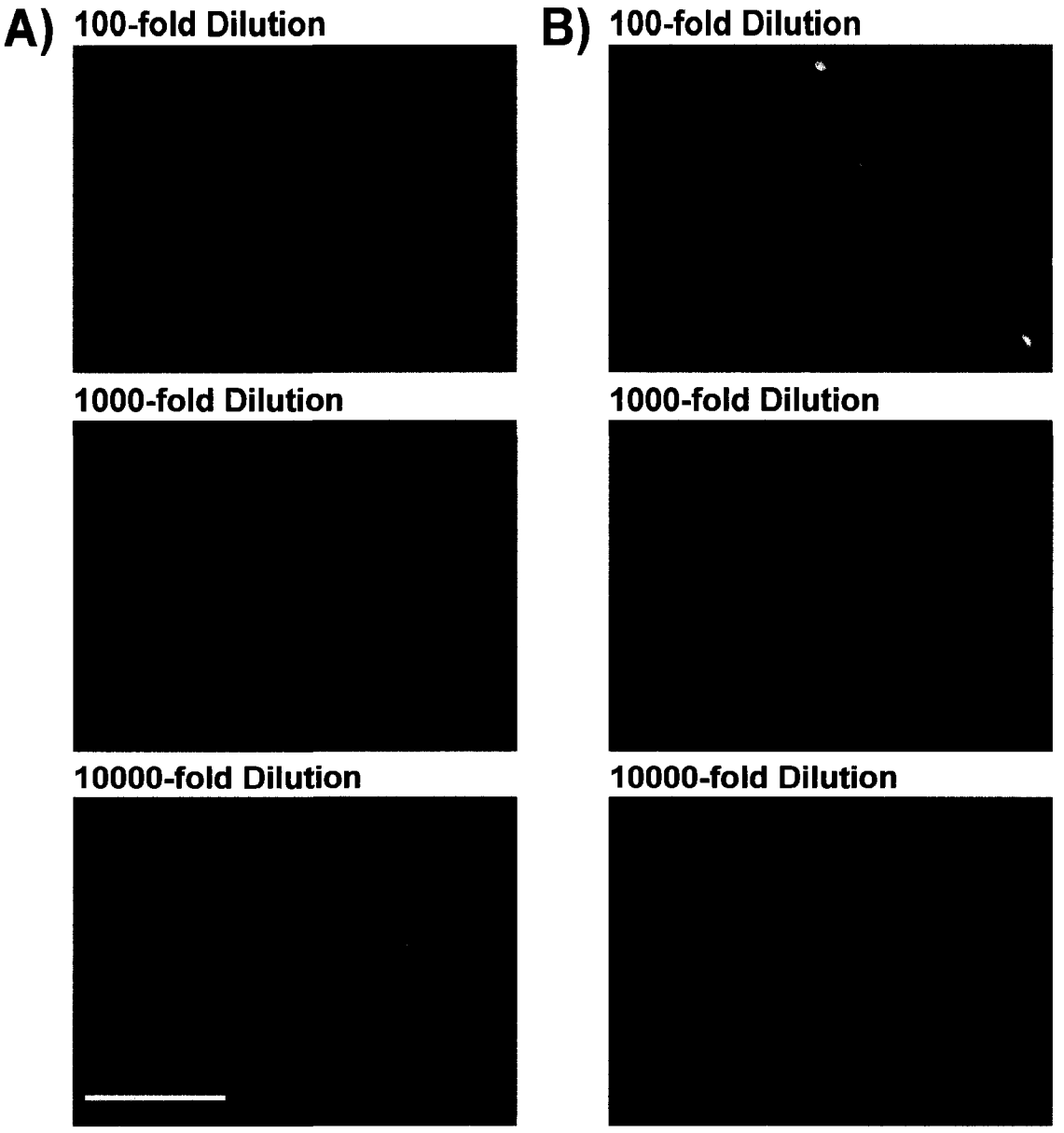

Figure 10: Fluorescence images following immunohistological analysis of 293A cells treated for 24 hours with serial dilutions of lentivector in the presence of 10.0μg/mL polybrene. Twenty four hours after infection cells were fixed with 4% paraformaldehyde and immunolabeled. Titre was determined by counting immunopositive cells. **Bar = 200μm**

A) Cells treated with HIV1-GFP lentivector, labeled for GFP (green) and counterstained with DAPI (blue).

B) Cells treated with HIV1-XIAP/GFP, labeled for GFP (green), HA tag (red) and counterstained with DAPI (blue).

Table 1: Summary of calculated titres for preparations of HIV1-GFP and HIV1-XIAP/GFP lentivectors. To calculate titre, number of GFP-positive (and HA-positive cells in the case of HIV1-XIAP/GFP infection) cells in five fields of view was counted for each serial dilution. The dilution and area observed:total area of well ratio were then accounted for.

Abbreviated Viral Prep Name	Date of Titration	Approximate Titre (Transduction Units/mL)
HIV1-GFP Lentivctors		
Lent 1 HIV1-GFP	25-10-2007	7.72×10^6
Lent 2 HIV1-GFP	05-11-2007	0*
Lent 3 HIV1-GFP	19-11-2007	1.64×10^7
Lent 4 HIV1-GFP	16-12-2007	2.00×10^7
Lent 6 HIV1-GFP	04-02-2008	2.34×10^7
Lent 7 HIV1-GFP	29-02-2008	1.74×10^7
Lent 9 HIV1-GFP	20-03-2008	4.65×10^6
Lent 11 HIV1-GFP	10-04-2008	5.84×10^7
HIV1-XIAP/GFP Lentivectors		
Lent 5 HIV1-XIAP/GFP	24-01-2008	9.01×10^6
Lent 8 HIV1-XIAP/GFP	29-02-2008	8.38×10^6
Lent 10 HIV1-XIAP/GFP	20-03-2008	1.19×10^7
Lent 12 HIV1-XIAP/GFP	01-05-2008	9.34×10^6

* Virus was lost during purification step.

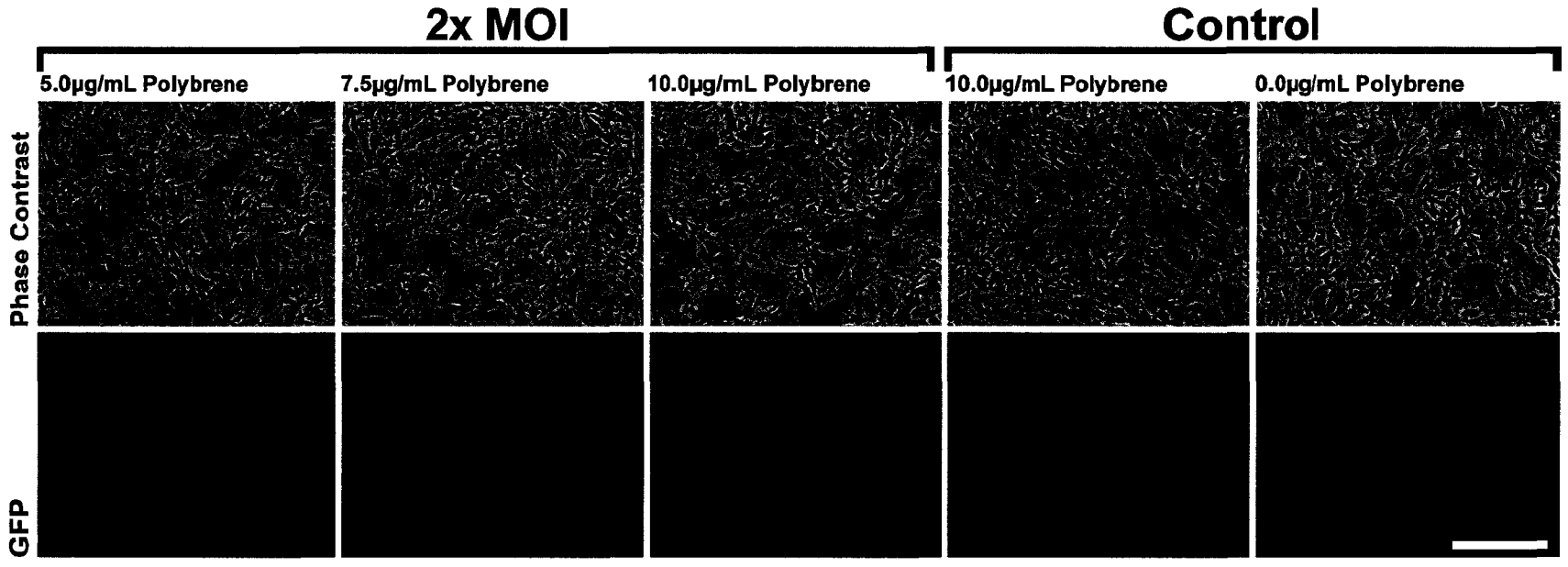

Figure 11: Phase contrast and fluorescence images of C57BL/6 mouse Hh-RPCs 24 hours after infection with HIV1-GFP lentivector at 2x MOI and various concentrations of polybrene. **Bar = 200µm**

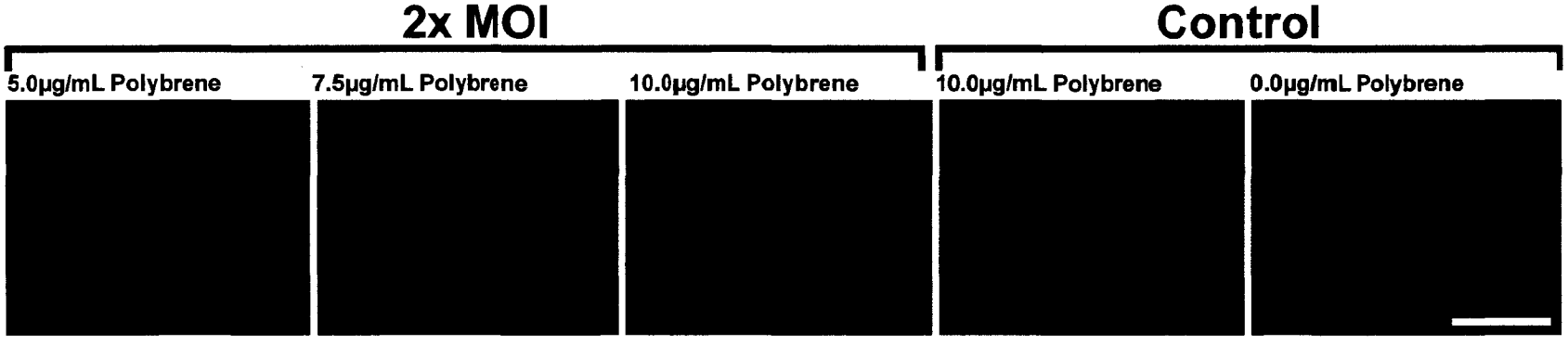

Figure 12: Fluorescence images following immunohistological analysis of C57BL/6 mouse Hh-RPCs 24 hours after infection with the HIV1-GFP lentivector at 2x MOI and various concentrations of polybrene. At the end of the viral incubation, the cells were fixed with 4% paraformaldehyde, labeled with anti-GFP antibody (green) and counterstained with DAPI (blue). The number of GFP-positive cells was counted and expressed as a percentage of total counted nuclei to determine infection efficiency. **Bar = 100µm**

Infection Efficiency of C57BL/6 Mouse Hh-RPCs with HIV1-GFP Lentivector at 2x MOI

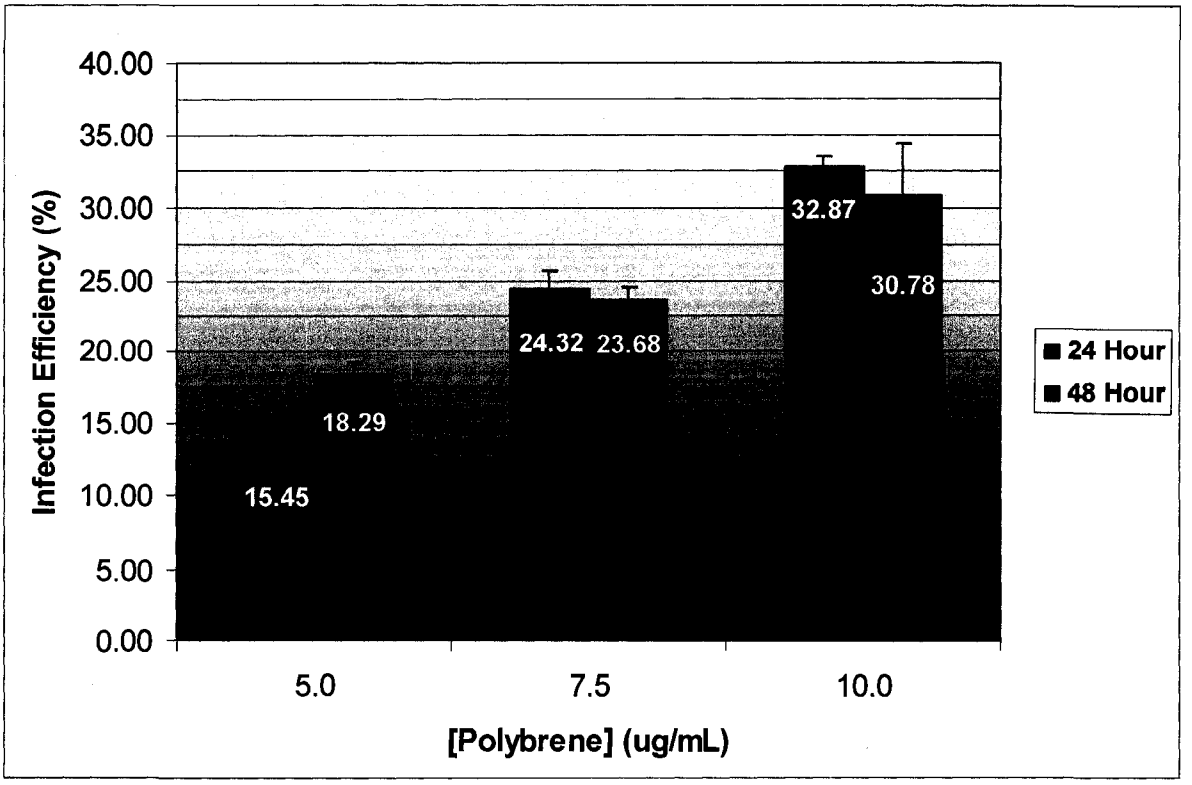

Figure 13: Infection efficiency at various polybrene concentrations for the infection of C57BL/6 mouse Hh-RPCs with HIV1-GFP at 2x MOI. Infection efficiency is expressed as % immunopositive cells out of total number of counted nuclei. Values represent the mean for three independent experiments; error bars indicate standard deviation. At both the 24 and 48 hour time points, there was significant increase in infection efficiency with respect to the polybrene concentration as determined by Single Factor ANOVA ($P<0.05$, $n=3$).

infection (Fig. 14.A). Following 48 hours of infection, there was a significant amount of death in this same treatment as well as the 2x MOI 7.5PB group (Fig. 15.A). At both time points, the percentage of dead cells in the Ctrl 10.0PB group was comparable to the Ctrl 0.0PB treatment. When the percentage of cell death within each treatment group was compared at the 24 and 48 hour time points, it was found that there was a significant increase in the 2x MOI 7.5PB and 2x MOI 10.0PB groups (Fig. 16).

When comparing the total cell number in all treatments to the Ctrl 0.0PB group, after 24 hours of infection there was a statistically significant decrease in the group treated with 2x MOI 10.0PB (Fig. 14.B). Following 48 hours of infection, there was a statistically significant decrease in cell number in all groups which received virus(Fig. 15.B).

3.2.2 HIV1-XIAP/GFP Infection of Hh-RPCs

Following infection with the HIV1-XIAP/GFP lentivector, Hh-RPCs appear normal in phase contrast images (Fig. 17). Fluorescence images of live Hh-RPCs as well as immunohistochemistry on fixed cells against GFP confirmed the expression of GFP following infection and that the number of infected cells increased with increasing polybrene concentration (Fig. 17 and 18). Immunohistochemistry against the HA-epitope tag also showed that these cells were expressing exogenous XIAP protein following infection with this lentivector (Fig. 19). The infection efficiency was determined for both infection time points, 24 and 48 hours, as with the HIV1-GFP vector (Fig. 20). At an MOI of 1.5x, a maximum infection efficiency of 26.48% was observed 24 hours after infection. When looking at each time point separately, there is a statistically-significant increase in infection efficiency with increasing polybrene concentration ($P<0.05$). T-tests

A) Percentage of Dead Cells following 24 Hour Infection of C57BL/6 Mouse Hh-RPCs with HIV1-GFP Lentivector at 2x MOI

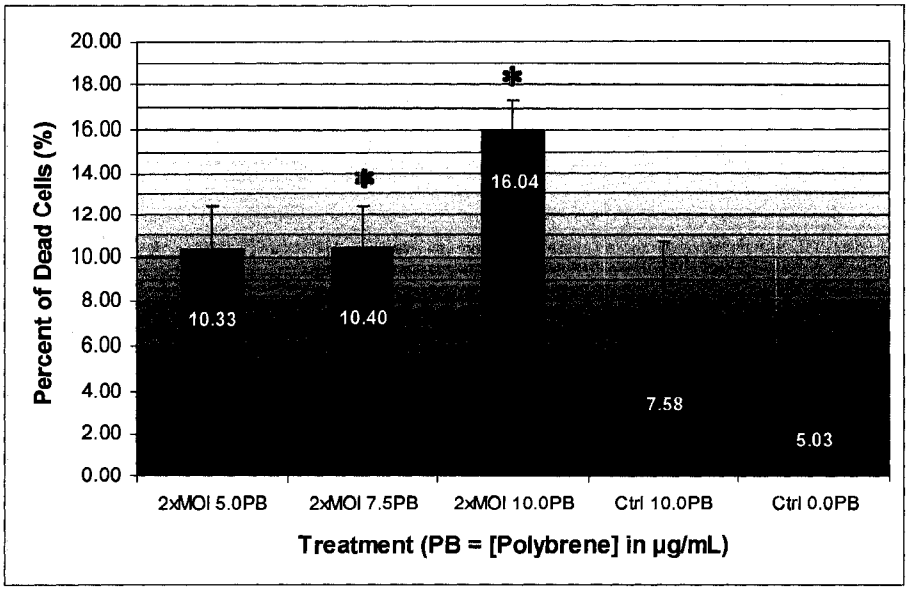

B) Ratio of Total Cell Number in Particular Treatment to Total Cell Number in 0.0µg/mL Polybrene Control following 24 Hour Infection of C57BL/6 Mouse Hh-RPCs with HIV1-GFP Lentivector at 2x MOI

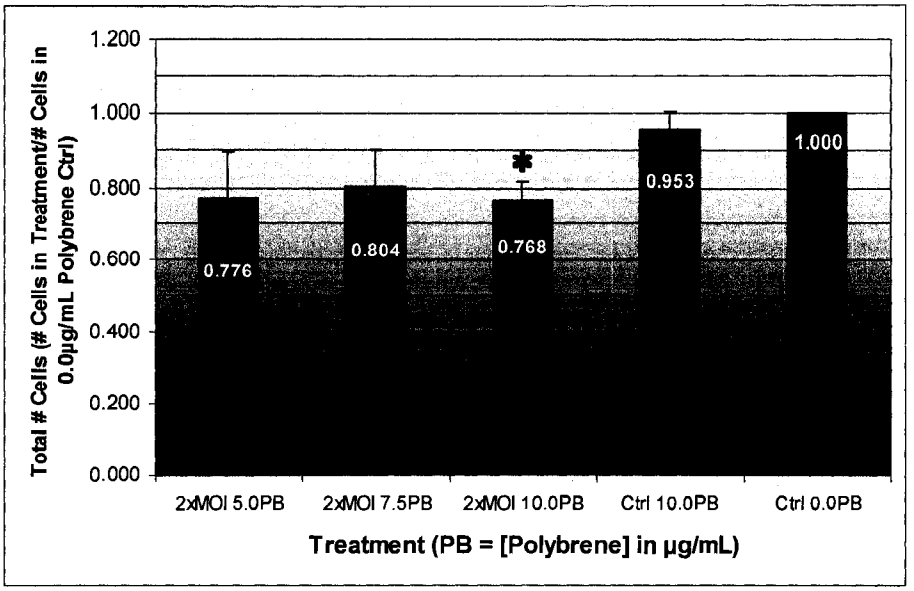

Figure 14: Results of live counts for 24 hour HIV1-GFP infection in C57BL/6 mouse Hh-RPCs at 2x MOI.

A) Percentage of dead cells (% Trypan Blue-stained cells out of total counted cells) for each treatment following 24 hours of infection.

B) Total number of cells (expressed as the number of cells in a particular treatment/number of cells in the 0.0µg/mL Polybrene Control) for each treatment following 24 hours of infection. Values represent the mean for three independent trials; error bars indicate standard deviation.

* Significant difference when compared to Ctrl 0.0PB. ($P<0.05$, $n = 3$, T-test).

A) Percentage of Dead Cells following 48 Hour Infection of C57BL/6 Mouse Hh-RPCs with HIV1-GFP Lentivector at 2x MOI

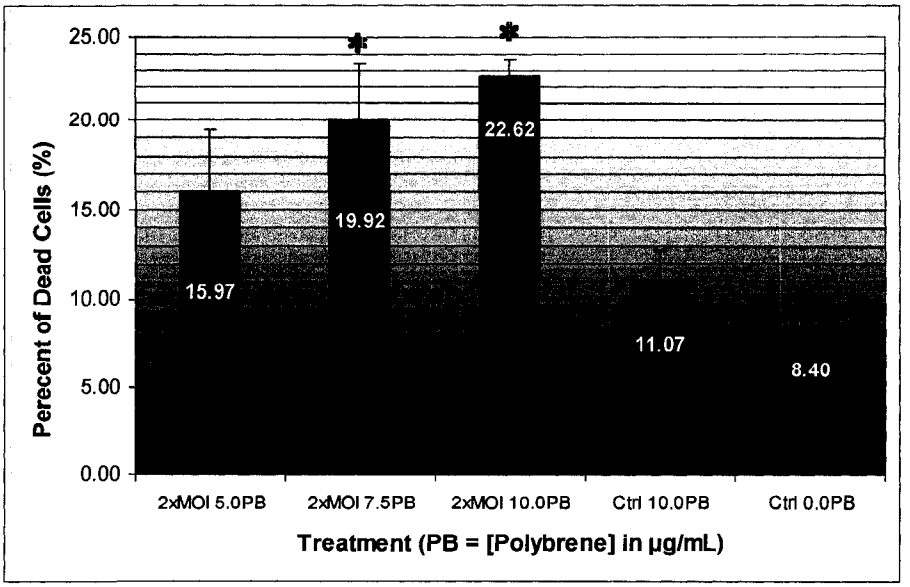

B) Ratio of Total Cell Number in Particular Treatment to Total Cell Number in 0.0µg/mL Polybrene Control following 48 Hour Infection of C57BL/6 Mouse Hh-RPCs with HIV1-GFP Lentivector at 2x MOI

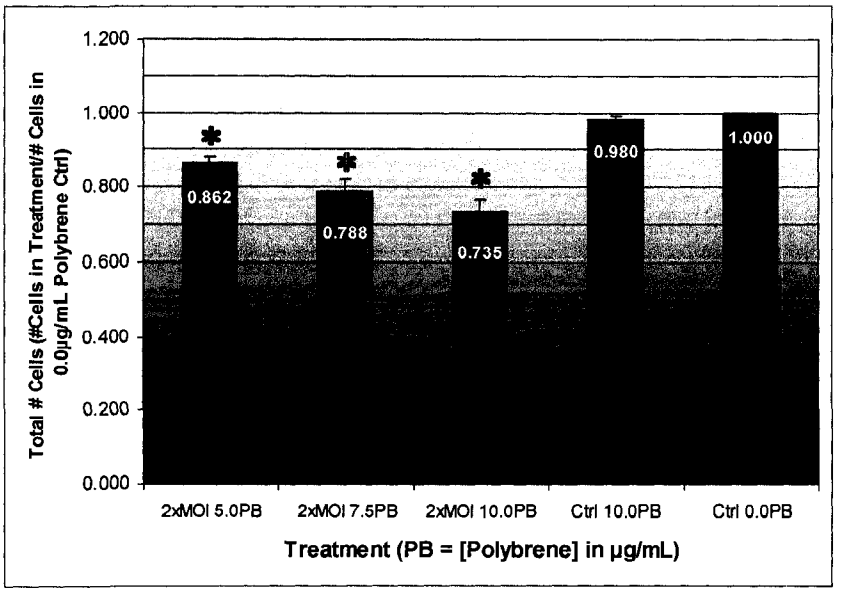

Figure 15: Results of live counts for 48 hour HIV1-GFP infection in C57BL/6 mouse Hh-RPCs at 2x MOI.

A) Percentage of dead cells (% Trypan Blue-stained cells out of total counted cells) for each treatment following 48 hours of infection.

B) Total number of cells (expressed as the number of cells in a particular treatment/number of cells in the 0.0µg/mL Polybrene Control) for each treatment following 48 hours of infection. Values represent the mean for three independent trials; error bars indicate standard deviation.

* Significant difference when compared to Ctrl 0.0PB. ($P<0.05$, $n = 3$, T-test).

Percentage of Dead Cells following 24 and 48 Hour Infection of C57BL/6 Mouse Hh-RPCs with HIV1-GFP Lentivector at 2x MOI

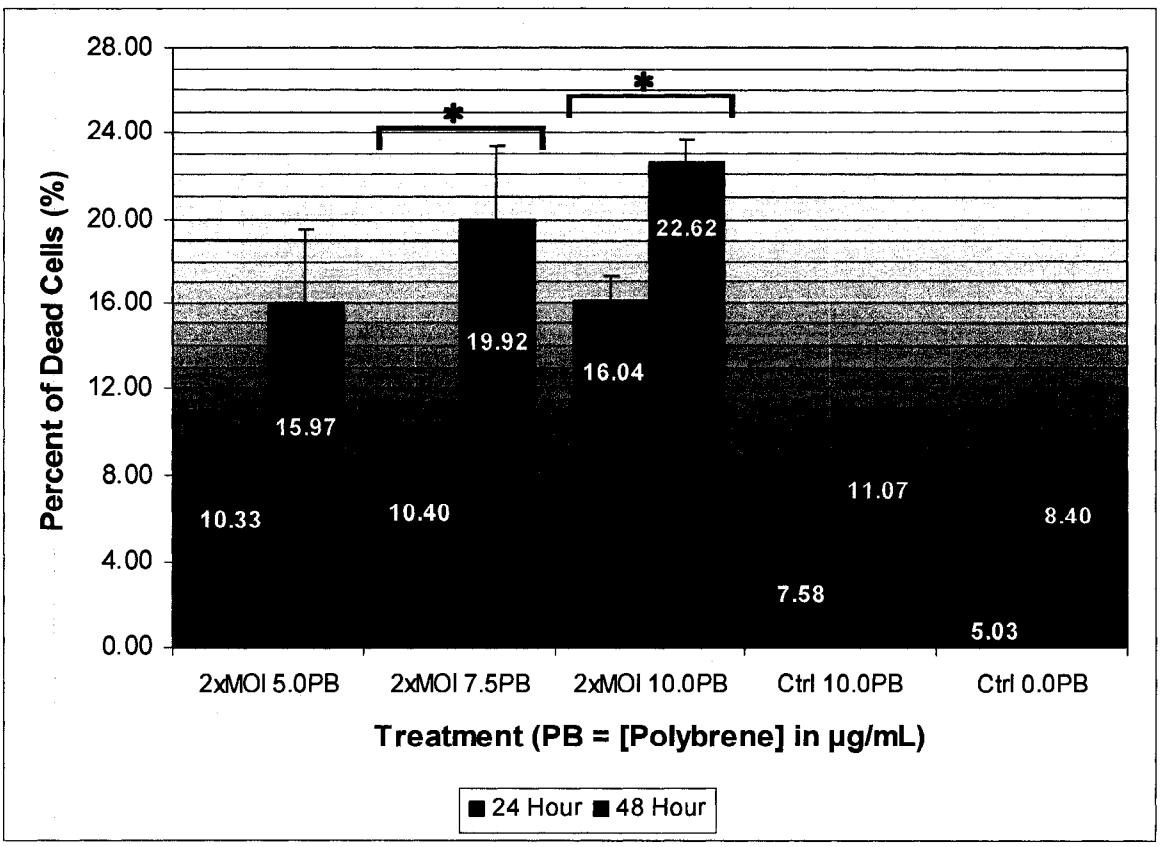

Figure 16: Comparison of percentage of cell death in all treatment groups following 24 and 48 hour infection of C57BL/6 mouse Hh-RPCs with HIV1-GFP lentivector at 2x MOI. Percentage of dead cells is expressed as % Trypan Blue-stained cells out of total counted cells. Values represent the mean for three independent trials; error bars indicate standard deviation.

- * Significant increase in percentage of dead cells between the 24 and 48 hour time points. ($P<0.05$, $n = 3$, T-test).

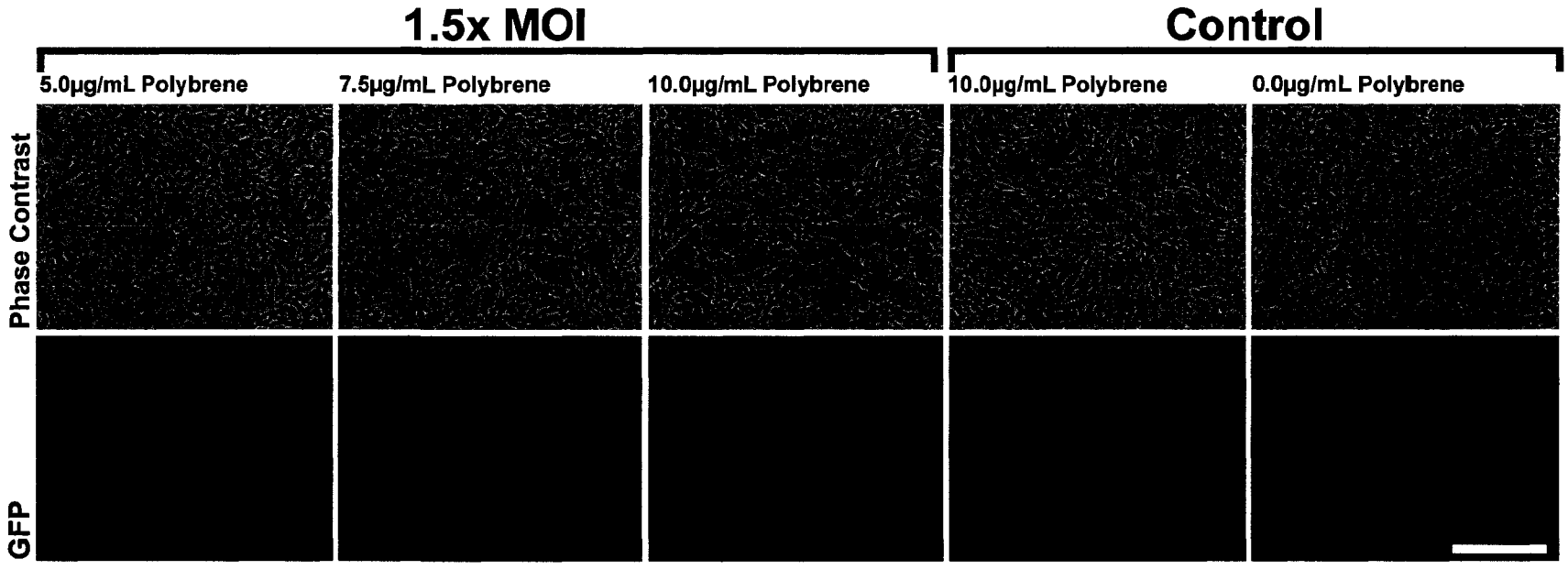

Figure 17: Phase contrast and fluorescence images of C57BL/6 mouse Hh-RPCs 24 hours after infection with HIV1-XIAP/GFP lentivector at 1.5x MOI and various concentrations of polybrene. **Bar = 200µm**

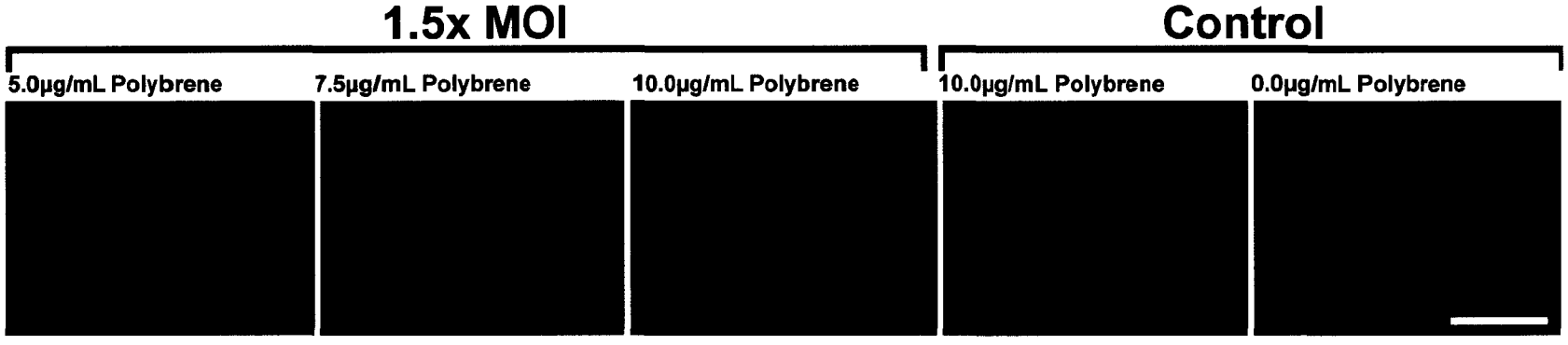

Figure 18: Fluorescence images following anti-GFP labeling of C57BL/6 mouse Hh-RPCs 24 hours after infection with the HIV1-XIAP/GFP lentivector at 1.5x MOI and various concentrations of polybrene. At the end of the 24 hour time point, the cells were fixed with 4% paraformaldehyde, labeled with anti-GFP antibody (green) and counterstained with DAPI (blue). The number of GFP-positive cells was counted and expressed as a percentage of total counted nuclei to determine infection efficiency. **Bar = 100µm**

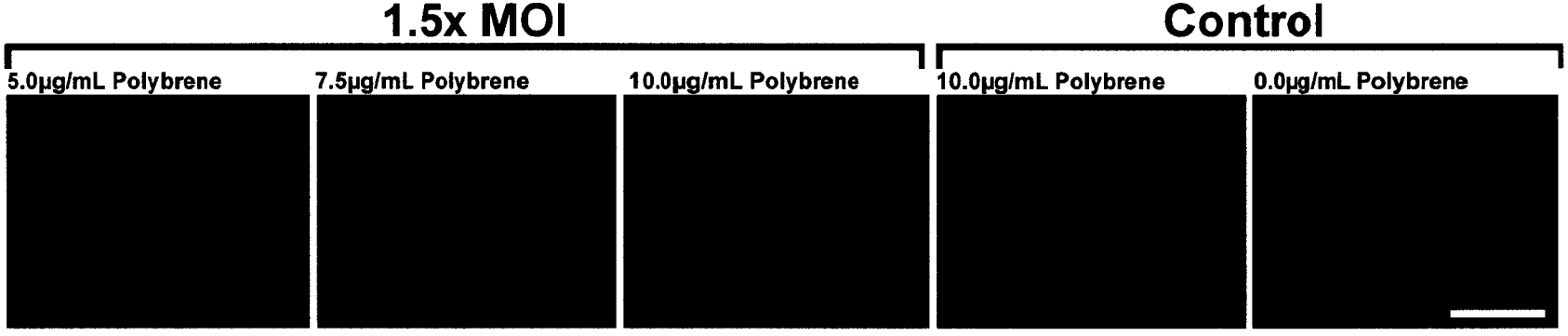

Figure 19: Fluorescence images following anti-HA labeling of C57BL/6 mouse Hh-RPCs 24 hours after infection with the HIV1-XIAP/GFP lentivector at 1.5x MOI and various concentrations of polybrene. Cells were fixed with 4% paraformaldehyde, labeled with FITC-conjugated anti-HA antibody (green) and counterstained with DAPI (blue). **Bar = 100µm**

Infection Efficiency of C57BL/6 Mouse Hh-RPCs with HIV1-XIAP/GFP Lentivector at 1.5x MOI

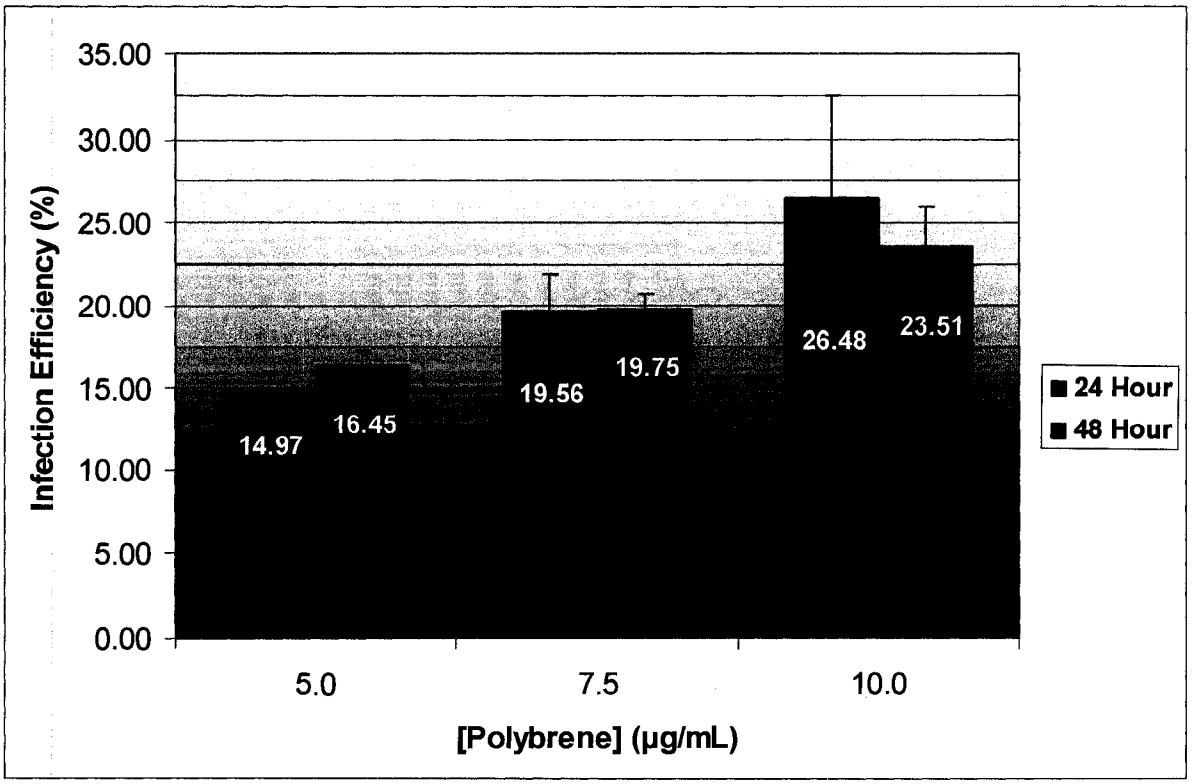

Figure 20: Infection efficiency at various polybrene concentrations for the infection of C57BL/6 mouse Hh-RPCs with HIV1-XIAP/GFP at 1.5x MOI. Infection efficiency is expressed as % immunopositive cells out of total number of counted nuclei. Values represent the mean for three independent experiments; error bars indicate standard deviation. At both the 24 and 48 hour time points, there was significant increase in infection efficiency with respect to the polybrene concentration as determined by Single Factor ANOVA ($P<0.05$, $n=3$).

were used to compare infection efficiencies within the same polybrene concentration, between the two time points. No significant difference was observed.

Twenty four hours after infection with HIV1-XIAP/GFP, there was a significant amount of cell death in the 1.5x MOI 10.0PB group as compared to the Ctrl 0.0PB (Fig. 21.A). After 48 hours of infection, significant amounts of cell death were observed in the 1.5x MOI 7.5PB and 1.5x MOI 10.0PB groups (Fig. 22.A). At both time points, the percentage of dead cells in the control receiving 10.0μg/mL polybrene (Ctrl 10.0PB) was comparable to the 0.0μg/mL polybrene no virus control (Ctrl 0.0PB). When the percentage of dead cells death within each treatment group was compared at the 24 and 48 hour time points, no significant increase in percentage of dead cells was observed in any of the treatments (Fig. 23).

There was a statistically significant decrease in the total cell number ratio observed for all treatments (1.5x MOI 5.0PB, 1.5x MOI 7.5PB, 1.5x MOI 10.0PB and Ctrl 10.0PB) when compared to the Ctrl 0.0PB group, after 24 hours of infection (Fig. 21.B). Following 48 hours of infection, a statistically significant decrease in cell number ratio was observed only in the groups which received virus (Fig. 22.B).

3.2.3 Summary

Overall, while higher polybrene concentration improved infection efficiency, there was also increased death of cells due to cytotoxicity. In addition, the presence of the virus affected cell number and viability. This was true for both the HIV1-GFP and HIV1-XIAP/GFP vectors.

A) Percentage of Dead Cells following 24 Hour Infection of C57BL/6 Mouse Hh-RPCs with HIV1-XIAP/GFP Lentivector at 1.5x MOI

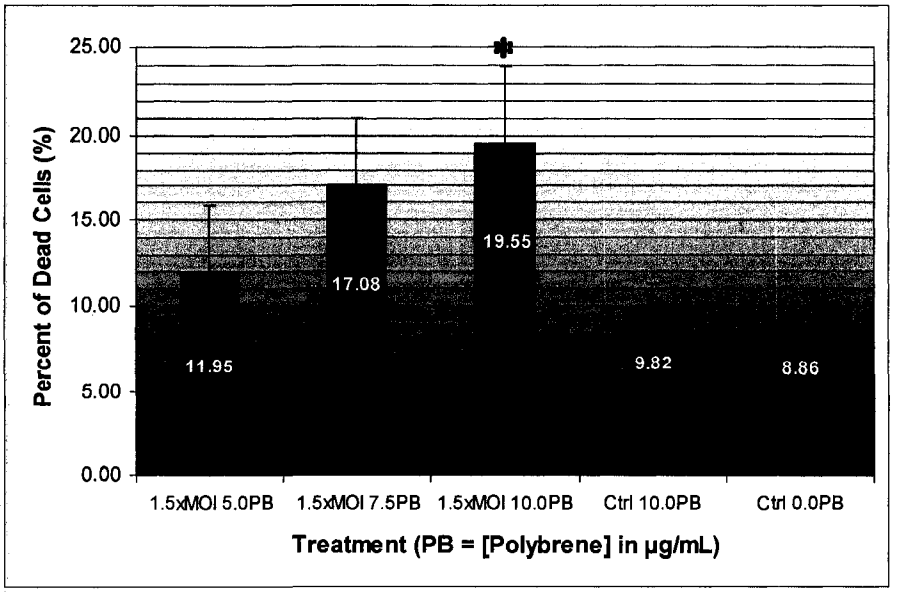

B) Ratio of Total Cell Number in Particular Treatment to Total Cell Number in 0.0µg/mL Polybrene Control following 24 Hour Infection of C57BL/6 Mouse Hh-RPCs with HIV1-XIAP/GFP Lentivector at 1.5x MOI

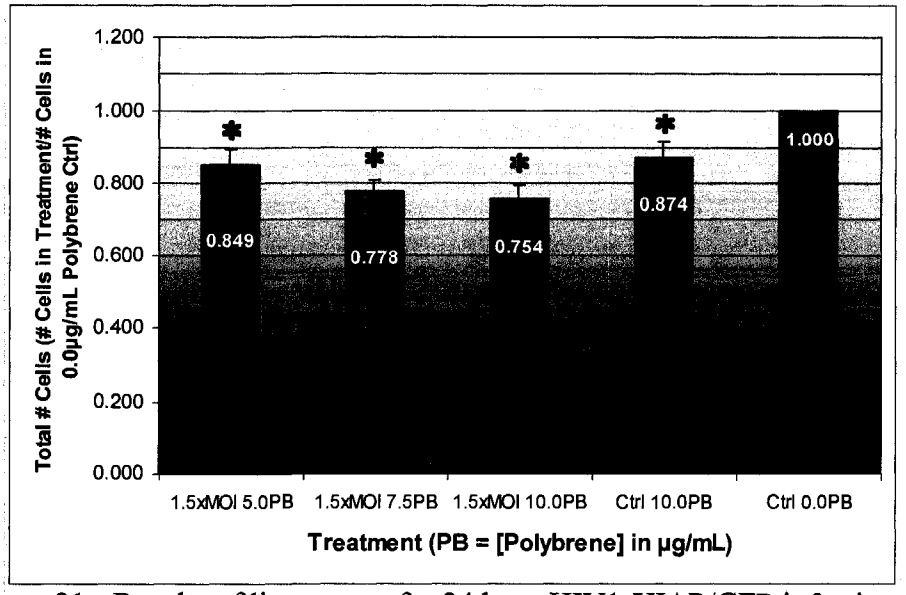

Figure 21: Results of live counts for 24 hour HIV1-XIAP/GFP infection in C57BL/6 mouse Hh-RPCs at 1.5x MOI.

A) Percentage of dead cells (% Trypan Blue-stained cells out of total counted cells) for each treatment following 24 hours of infection.

B) Total number of cells (expressed as the number of cells in a particular treatment/number of cells in the 0.0µg/mL Polybrene Control) for each treatment following 24 hours of infection. Values represent the mean for three independent trials; error bars indicate standard deviation.

* Significant difference when compared to Ctrl 0.0PB. ($P<0.05$, $n = 3$, T-test).

A) Percentage of Dead Cells following 48 Hour Infection of C57BL/6 Mouse Hh-RPCs with HIV1-XIAP/GFP Lentivector at 1.5x MOI

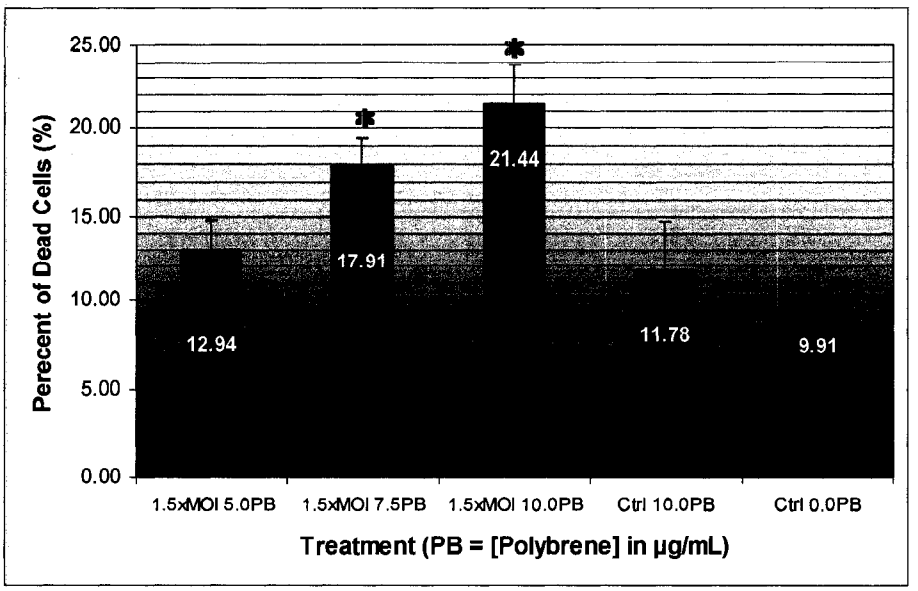

B) Ratio of Total Cell Number in Particular Treatment to Total Cell Number in 0.0µg/mL Polybrene Control following 48 Hour Infection of C57BL/6 Mouse Hh-RPCs with HIV1-XIAP/GFP Lentivector at 1.5x MOI

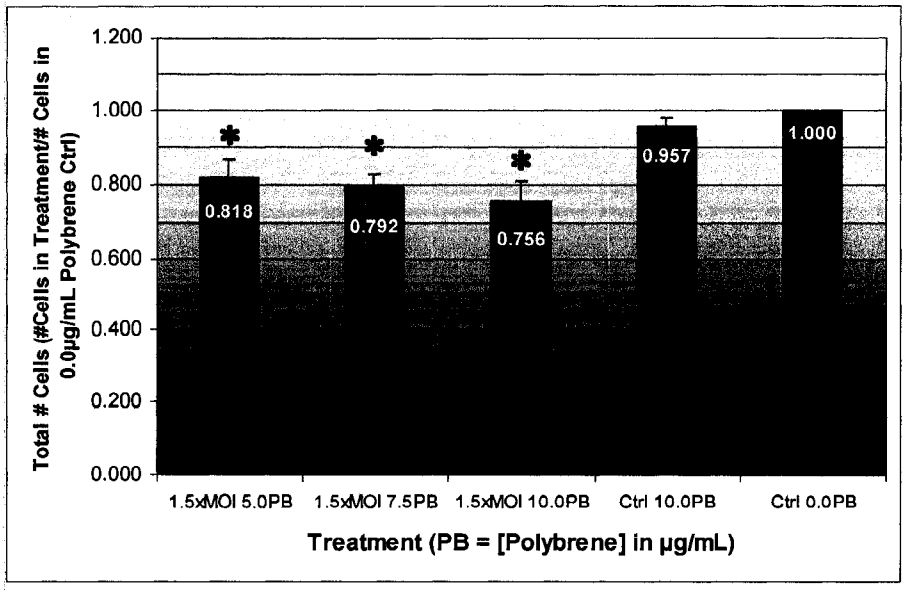

Figure 22: Results of live counts for 48 hour HIV1-XIAP/GFP infection in C57BL/6 mouse Hh-RPCs at 1.5x MOI.

A) Percentage of dead cells (% Trypan Blue-stained cells out of total counted cells) for each treatment following 48 hours of infection.

B) Total number of cells (expressed as the number of cells in a particular treatment/number of cells in the 0.0µg/mL Polybrene Control) for each treatment following 48 hours of infection. Values represent the mean for three independent trials; error bars indicate standard deviation.

* Significant difference when compared to Ctrl 0.0PB. ($P<0.05$, $n = 3$, T-test).

Percentage of Dead Cells following 24 and 48 Hour Infection of C57BL/6 Mouse Hh-RPCs with HIV1-XIAP/GFP Lentivector at 1.5x MOI

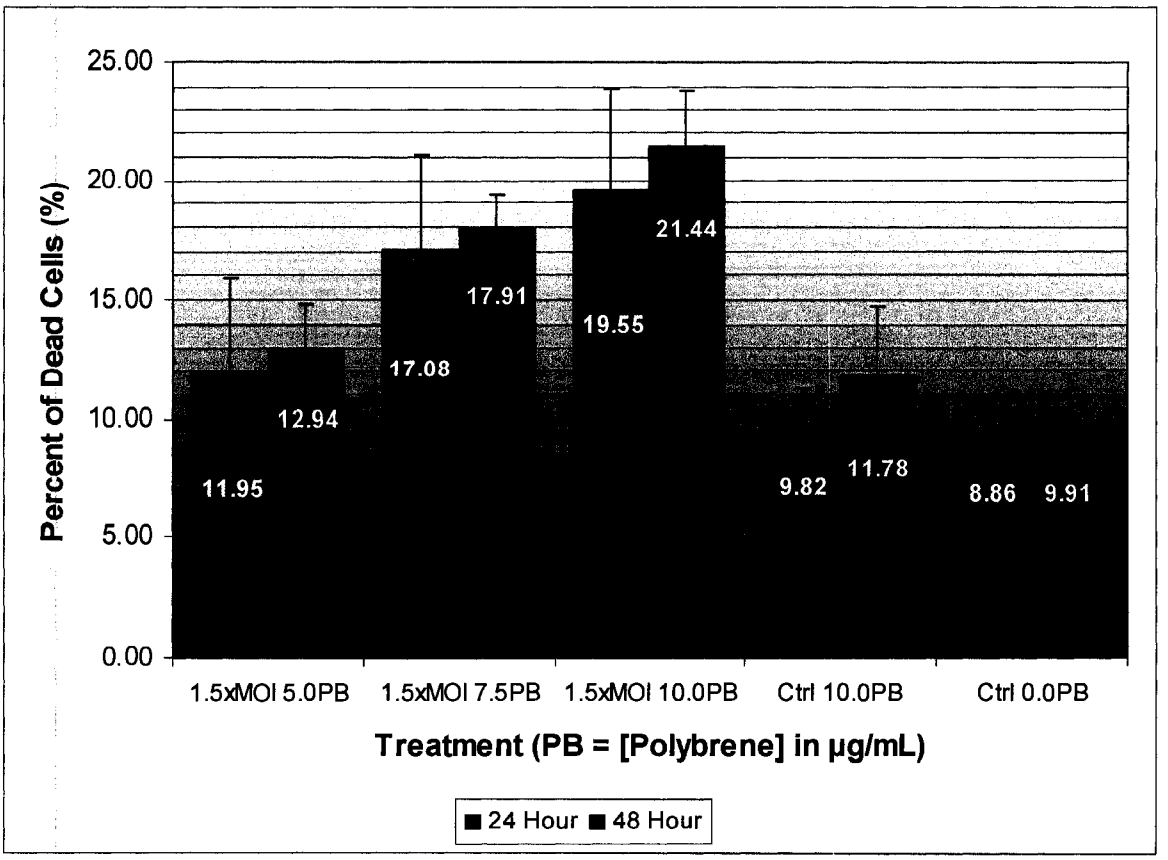

Figure 23: Comparison of percentage of cell death in all treatment groups following 24 and 48 hour infection of C57BL/6 mouse Hh-RPCs with HIV1-XIAP/GFP lentivector at 1.5x MOI. Percentage of dead cells is expressed as % Trypan Blue-stained cells out of total counted cells. Values represent the mean for three independent trials; error bars indicate standard deviation.

3.3 Long-Term Transgene Expression from Lentiviral Vectors

Fluorescent photomicrography demonstrated the expression of GFP from both lentivectors in C57BL/6 mouse Hh-RPCs for at least 13 days after infection (Fig. 24 and 25). The amount of GFP-positive cells appears to slightly decrease over time. Western blot analysis of protein samples collected periodically from HIV1-XIAP/GFP infected cells confirmed that exogenous XIAP protein was expressed for at least 13 days after infection with this construct (Fig. 26). The level of XIAP protein expression appeared to decrease throughout the time span examined.

3.4 FACS

3.4.1 FACS of Hh-RPCs

Figures 27 and 28 show scatter plots of a representative fractions of cells sorted following infection with HIV1-GFP and HIV1-XIAP/GFP lentivectors in two separate experiments. The average amount of GFP-positive cells in the HIV1-GFP infected group was 20.2%. In the HIV1-XIAP/GFP infected group, the average amount of GFP-positive cells according to the FACS data was only 9.64%. Of the cells sorted (approximately 20 million each time) an average of 7.34 and 3.03%, for the HIV1-GFP and HIV1-XIAP/GFP infected cells, respectively, was recovered and returned to culture (Table 2).

Phase contrast and fluorescence images of Hh-RPCs before and after sorting in the HIV1-GFP and HIV1-XIAP/GFP infected groups can be seen in Figures 29 and 30, respectively. From these images it was apparent that the cell population was not 100% pure but the proportional increase of GFP-expressing cells within the population could be clearly observed. In addition, no gross morphological changes were evident.

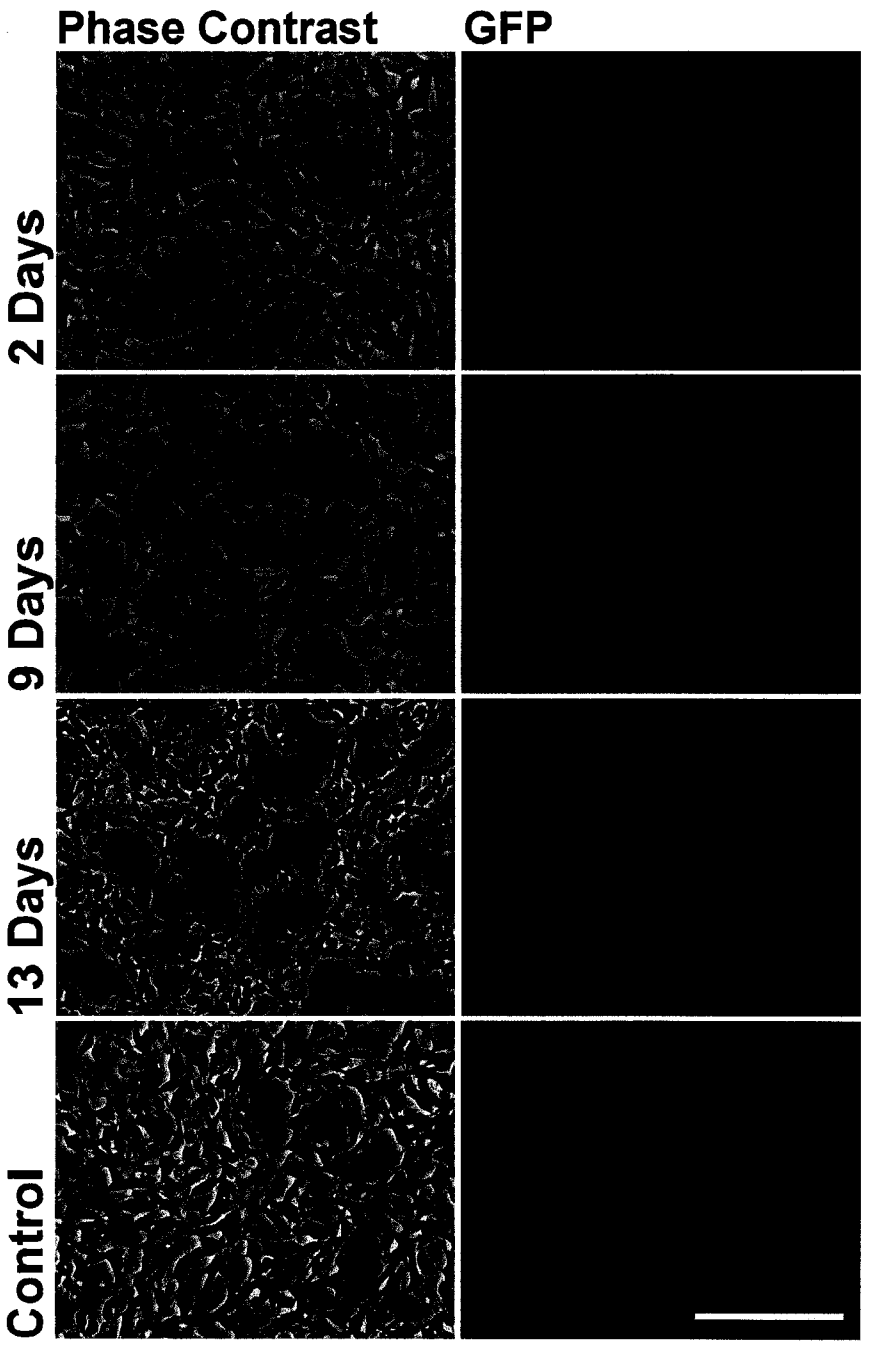

Figure 24: Phase contrast and fluorescence images of C57BL/6 mouse Hh-RPCs between 2 and 13 days after infection with HIV1-GFP lentivector. **Bar = 150μm**

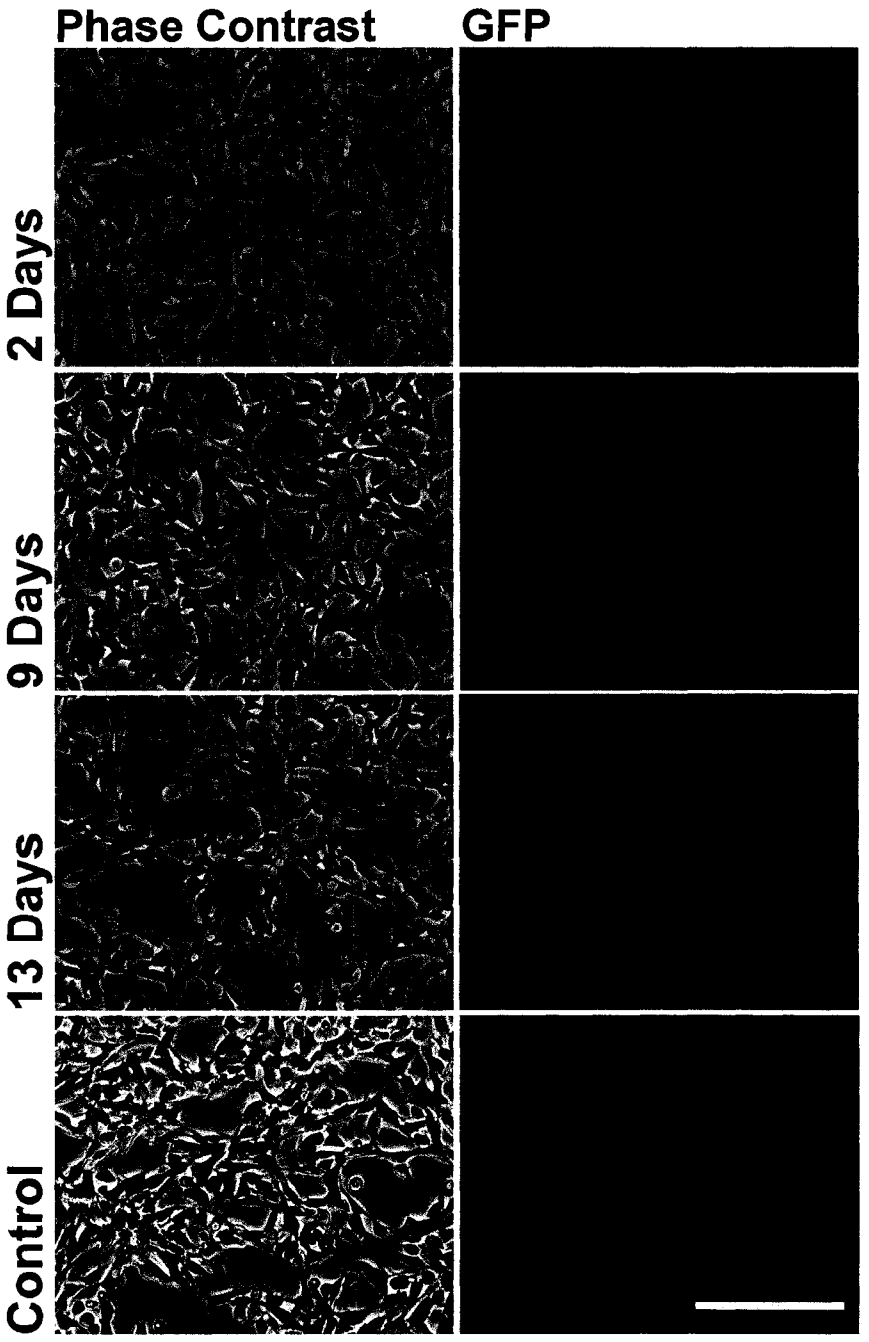

Figure 25: Phase contrast and fluorescence images of C57BL/6 mouse Hh-RPCs between 2 and 13 days after infection with HIV1-XIAP/GFP lentivector. **Bar = 150µm**

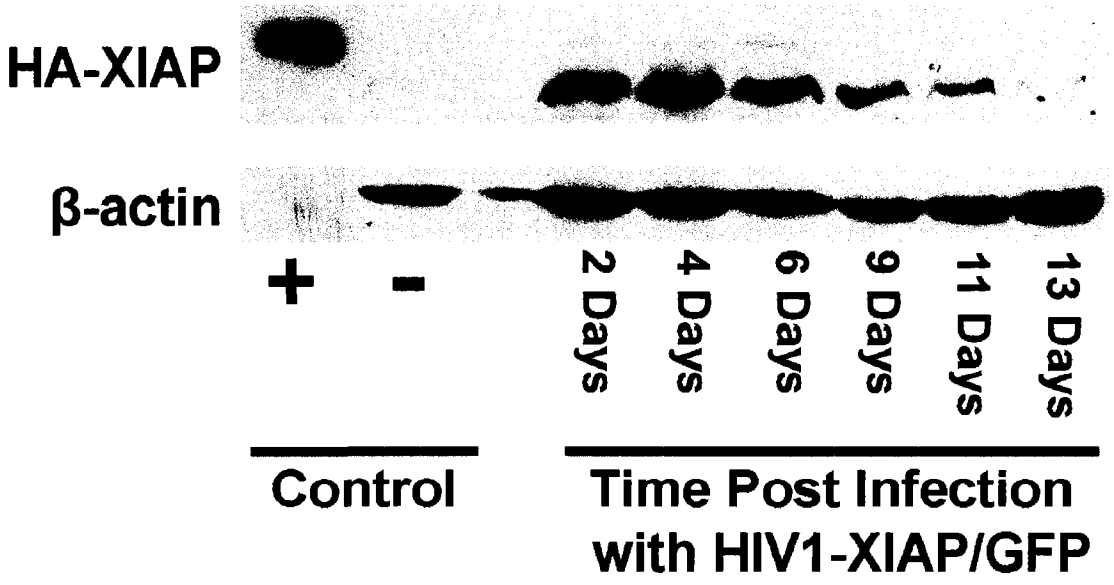

Figure 26: Western blot analysis of protein samples extracted from C57BL/6 mouse Hh-RPCs between 2 and 13 days after infection with HIV1-XIAP/GFP. 15μg of each protein sample was run on 10% SDS-PAGE and transferred onto PVDF membrane. Exogenous XIAP protein was detected with an anti-HA antibody. As a positive control, a sample of pure TAT-HA-XIAP was used. For a negative control a sample of protein extracted from uninfected cells was loaded. To demonstrate equal loading, the blot was stripped and re-probed with anti-β-actin antibody. HA-XIAP runs at approximately 55kDa. TAT-HA-XIAP runs at approximately 60kDa. β-actin runs at approximately 42kDa.

Sort #1

HIV1-GFP

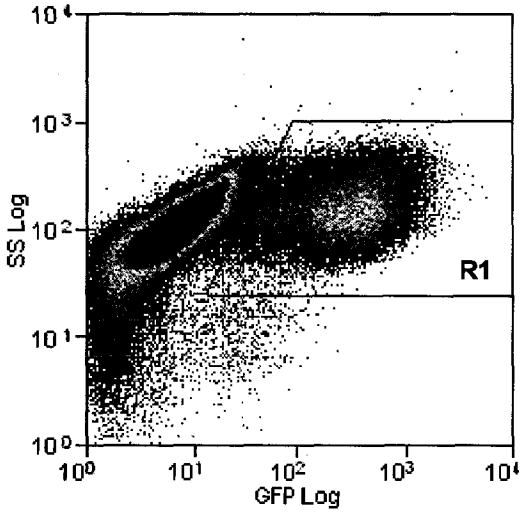

Region	Count	% Hist
Total	200000	100.00
R1	44000	22.00

HIV1-XIAP/GFP

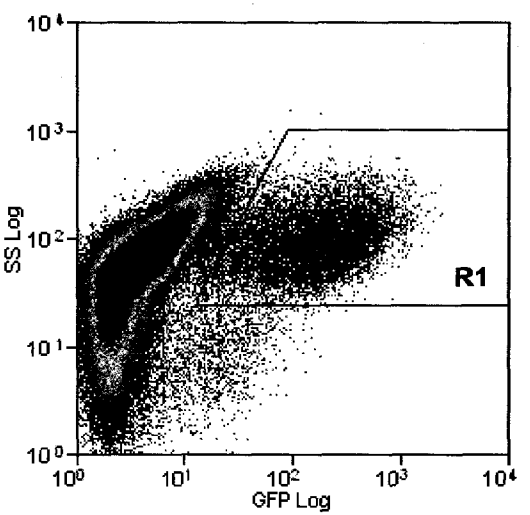

Region	Count	% Hist
Total	200000	100.00
R1	13414	6.71

Control

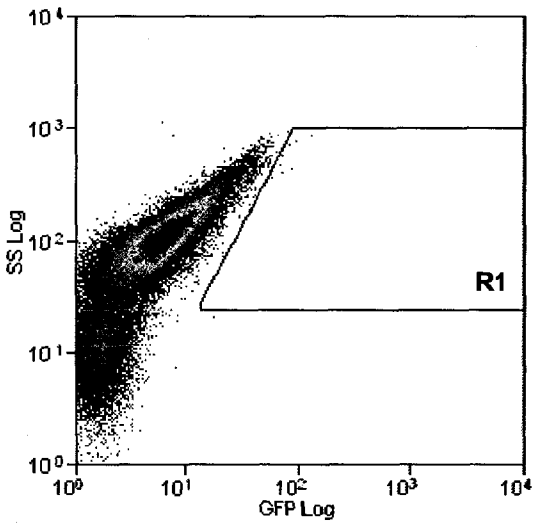

Region	Count	% Hist
Total	50850	100.00
R1	11	0.02

Fig. 27: Scatter diagrams of representative samples from the first sort of C57BL/6 mouse Hh-RPCs, based on expression of GFP following infection with either HIV1-GFP or HIV1-XIAP/GFP lentivectors. A sample of uninfected C57BL/6 mouse Hh-RPCs was used as a control.

Sort #2

HIV1-GFP

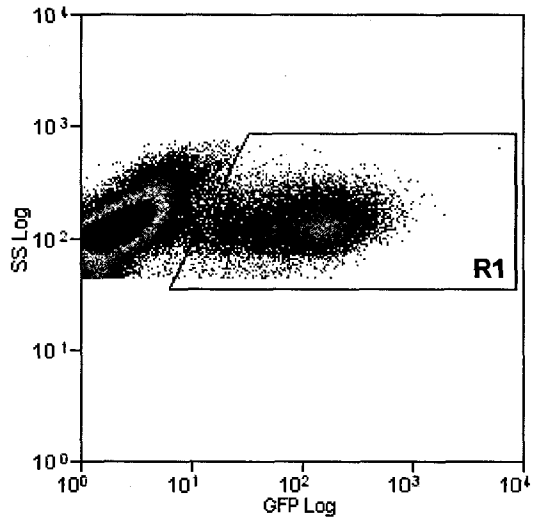

Region	Count	% Hist
Total	86228	100.00
R1	15867	18.40

HIV1-XIAP/GFP

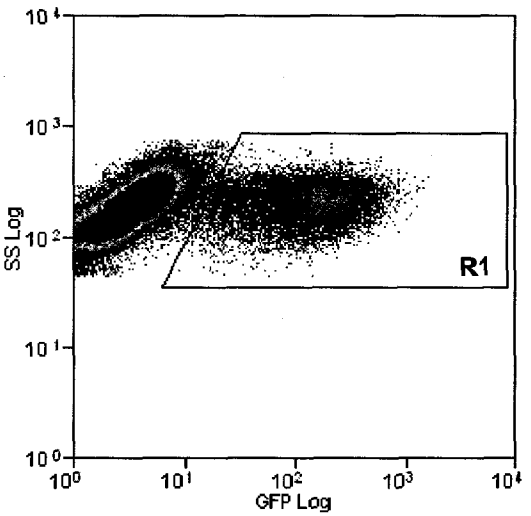

Region	Count	% Hist
Total	150180	100.00
R1	14358	9.56

Control

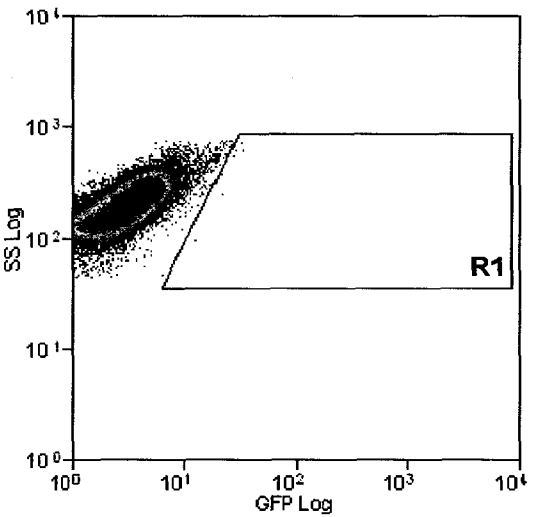

Region	Count	% Hist
Total	57270	100
R1	15	0.03

Fig. 28: Scatter diagrams of representative samples from the second sort of C57BL/6 mouse Hh-RPCs, based on expression of GFP following infection with either HIV1-GFP or HIV1-XIAP/GFP lentivectors. A sample of uninfected C57BL/6 mouse Hh-RPCs was used as a control.

Table 2: Collection data for FACS of C57BL/6 mouse HH-RPCs based on GFP expression from infection with HIV1-GFP or HIV1-XIAP/GFP lentivectors.

Experimental Group	Trial	# Cells Sorted	% GFP Positive Cells	Total Cells Collected
HIV1-GFP	1	1.29×10^7	5.60	7.25×10^5
	2	1.13×10^7	9.08	1.03×10^6
	AVG	1.21×10^7	7.34	8.78×10^5
HIV1-XIAP/GFP	1	2.09×10^7	3.12	6.54×10^5
	2	1.26×10^7	2.94	3.71×10^5
	AVG	1.68×10^7	3.03	5.12×10^5

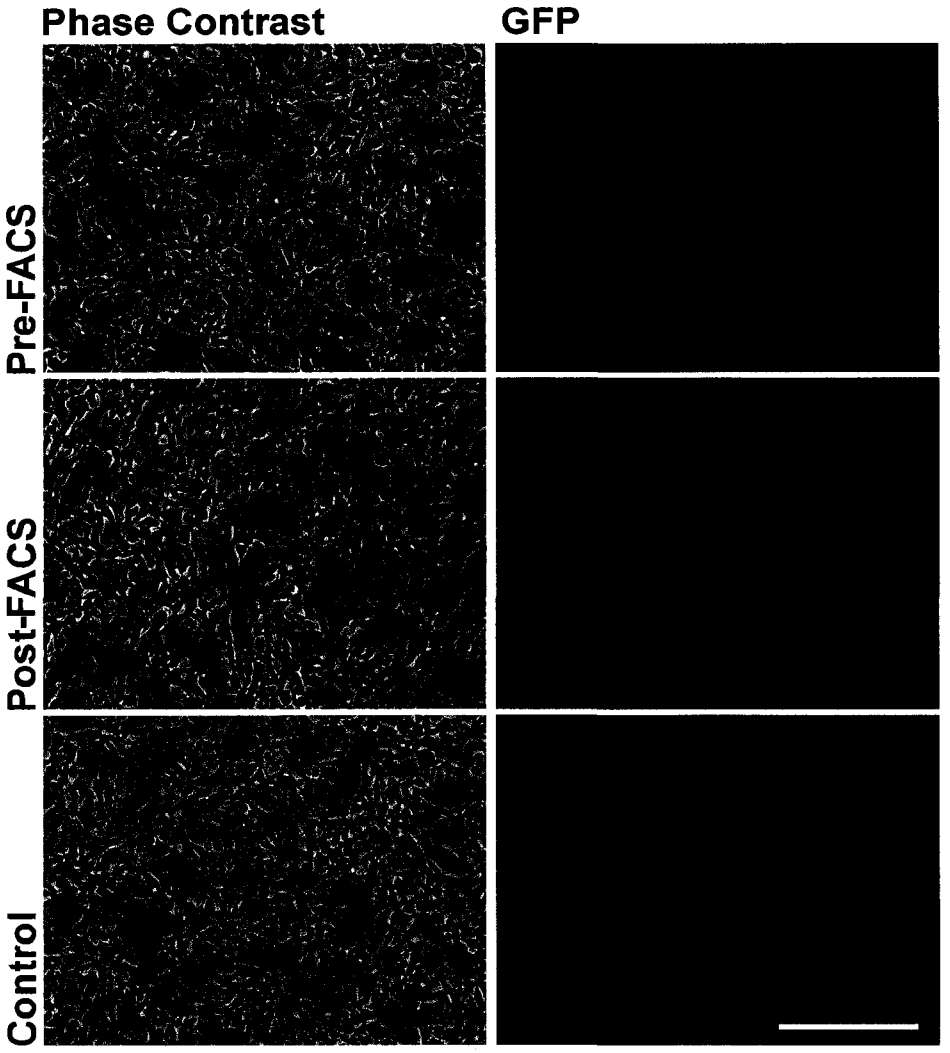

Figure 29: Phase contrast and fluorescence images of C57BL/6 mouse Hh-RPCs before and after FACS based on GFP expression following infection with the HIV1-GFP lentivector. **Bar = 200μm**

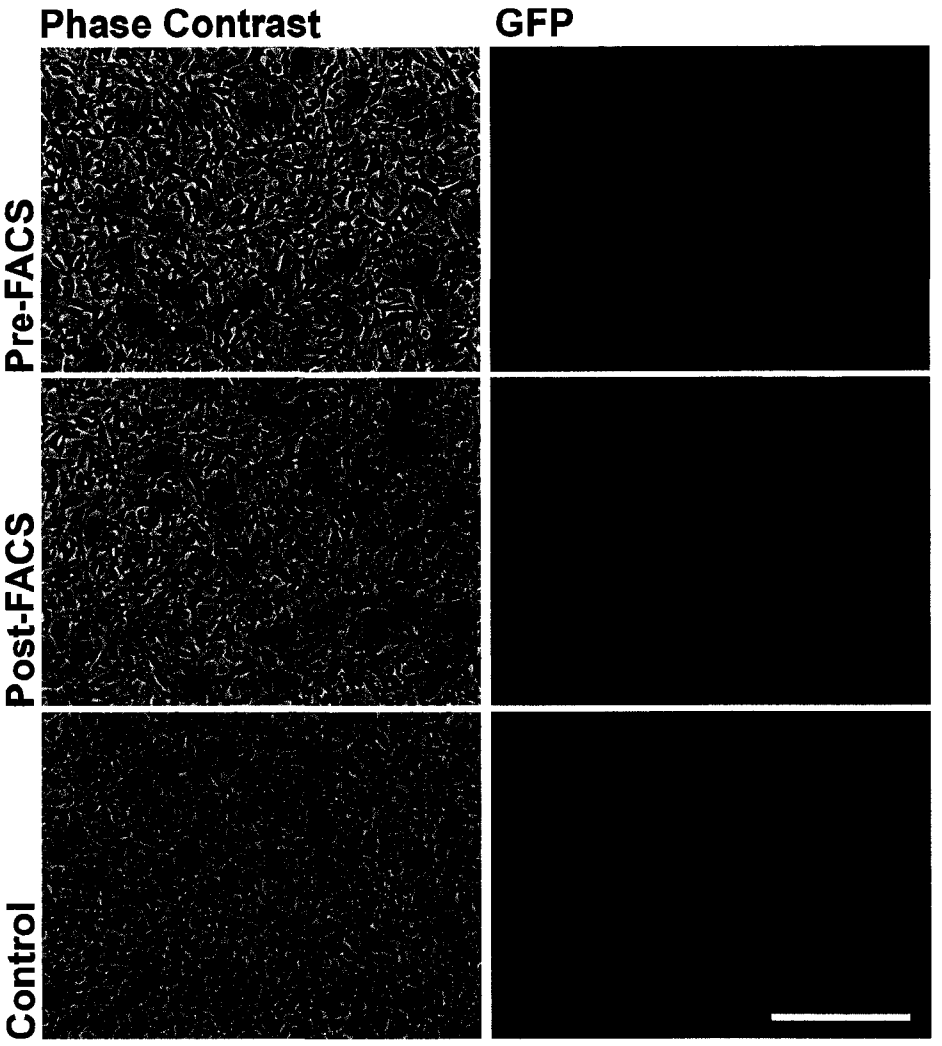

Figure 30: Phase contrast and fluorescence images of C57BL/6 mouse Hh-RPCs before and after FACS based on GFP expression following infection with the HIV1-XIAP/GFP lentivector. **Bar = 200μm**

To demonstrate the enrichment of XIAP protein over-expressing cells within the cell population, samples of protein extracted from cells before and after the sort were analyzed by Western blot (Fig. 31). Prior to the sort, the expression of XIAP protein was so diffuse that the HA signal was almost undetectable, but the amount of XIAP protein increased considerably following FACS.

3.4.2 Transgene Expression in FACS Treated Hh-RPCs

Protein samples extracted between 16 and 28 days after FACS treatment of HIV1-XIAP/GFP infected Hh-RPCs were analyzed using Western blot. Duplicate blots were run, one was probed with an anti-HA antibody (Fig. 32.A) and the other with an anti-GST-XIAP antibody (Fig. 32.B). Anti-HA probing demonstrated that exogenous XIAP protein was expressed at steady levels in the infected cells during the surveyed time period. Anti-GST-XIAP probing showed the total XIAP protein expression, that from the lentivirus as well as the endogenous protein. The total amount of XIAP protein expression did not appear to change throughout the experiment indicating that endogenous levels of XIAP protein were steady. In addition, probing for total XIAP protein expression demonstrated a marked over-expression of XIAP protein in samples from cells infected with the HIV1-XIAP/GFP lentivector.

3.5 Photoreceptor Differentiation of Hh-RPCs

After 8 days of co-culture with C57BL/6 mouse retinal explants, the number of HIV1-GFP and HIV1-XIAP/GFP lentivector-infected Hh-RPCs which had integrated into the explants was low. In each experimental group, GFP-expressing Hh-RPCs which appeared to co-localize with rhodopsin staining could be detected (Fig. 33 and 34). Morphologically only the cells infected with HIV1-XIAP/GFP resembled photoreceptors

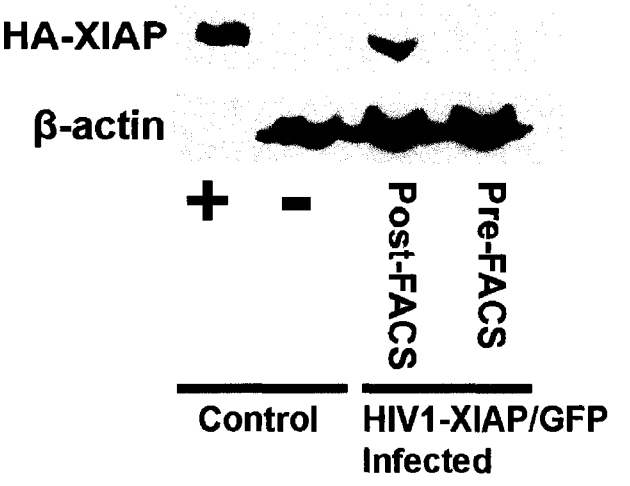

Figure 31: Western blot analysis of protein extracted from C57BL/6 mouse Hh-RPCs before and after FACS based on GFP expression from infection with the HIV1-XIAP/GFP lentivector. 15μg of each protein sample was run on 10% SDS-PAGE and transferred onto PVDF membrane. Exogenous XIAP protein over-expression was detected with an anti-HA antibody. As a positive control, a sample of pure TAT-HA-XIAP was used. For a negative control a sample of protein extracted from uninfected cells was loaded. To demonstrate equal loading, the blot was stripped and re-probed with an anti-β-actin antibody. HA-XIAP runs at approximately 55kDa. TAT-HA-XIAP runs at approximately 60kDa. β-actin runs at approximately 42kDa.

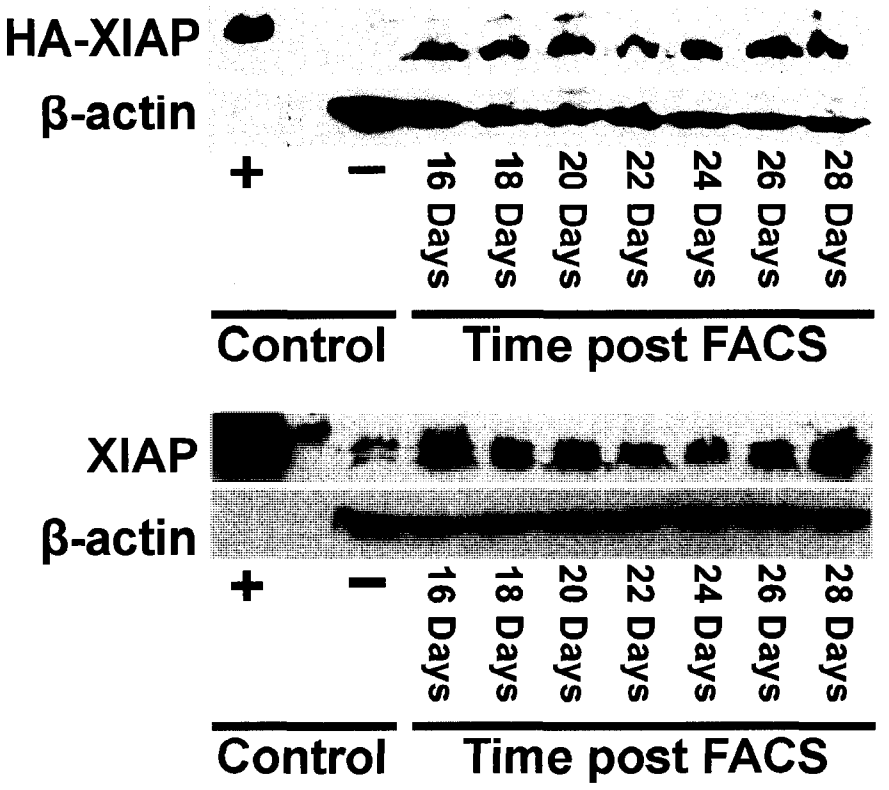

Figure 32: Western blot analysis of protein extracted from C57BL/6 mouse Hh-RPCs between 16 and 28 days after FACS, which was performed based on GFP expression from the HIV1-XIAP/GFP lentivector. The infection was carried out 8 days prior to the sort. 20μg of each protein sample was run on 10% SDS-PAGE and transferred onto PVDF membrane.

A) Exogenous XIAP protein over-expression was detected with an anti-HA antibody.

B) Total XIAP expression (endogenous + exogenous) was detected with an anti-GST-XIAP antibody. In both blots, a sample of pure TAT-HA-XIAP was used as a positive control. For a negative control a sample of protein extracted from uninfected cells was loaded. To demonstrate equal loading, each blot was stripped and re-probed with an anti-β-actin antibody. HA-XIAP runs at approximately 55kDa. TAT-HA-XIAP runs at approximately 60kDa. β-actin runs at approximately 42kDa.

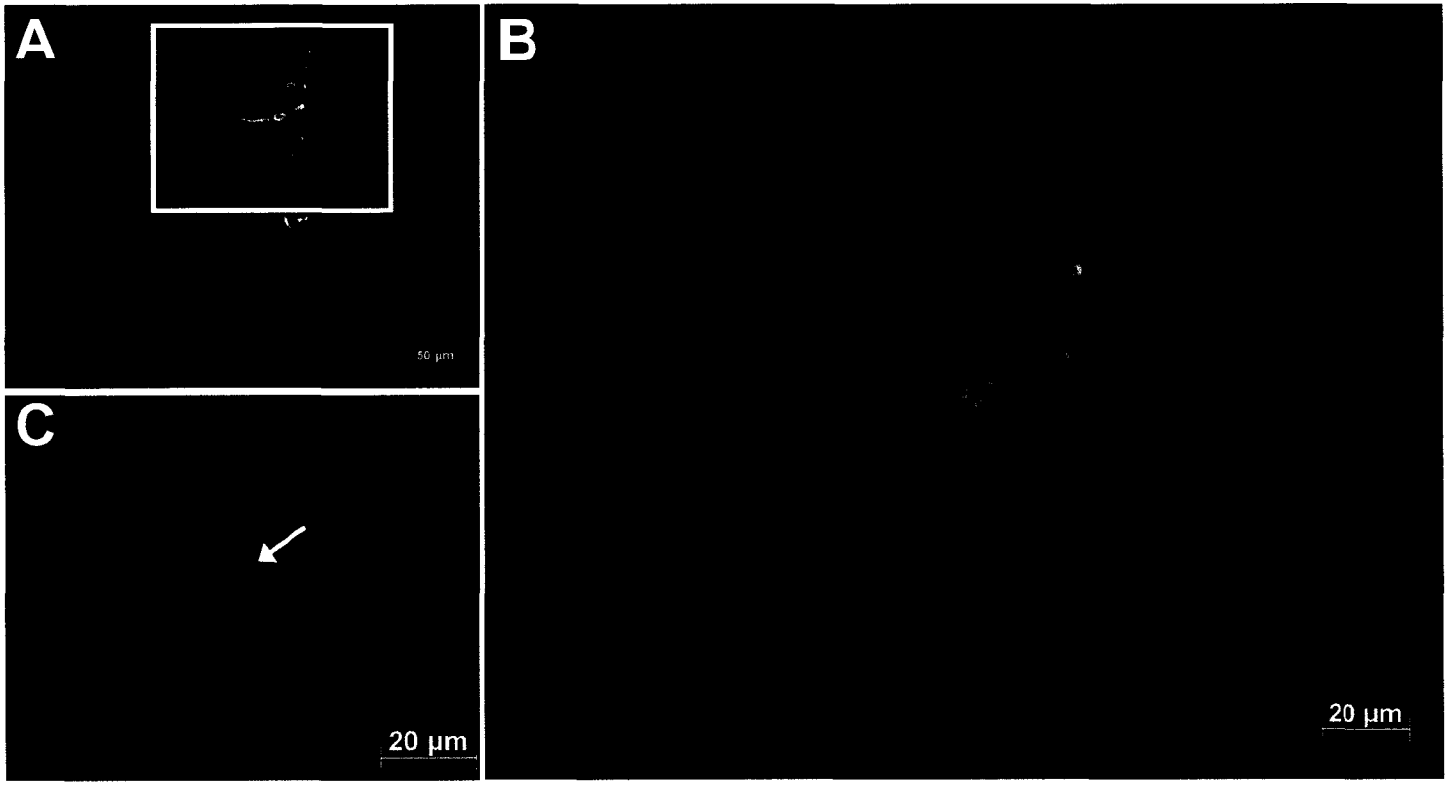

Figure 33: Fluorescence images of HIV1-GFP infected C57BL/6 mouse Hh-RPCs after 8 days of co-culture with P1 C57BL/6 mouse retinal explants. **(A)** Low magnification showing overlay of α-GFP (green), α-Rhodopsin (red) and DAPI (blue) staining. **(B)** Higher magnification of region outlined in panel A showing overlay of α-GFP (green) and α-Rhodopsin (red) staining. **(C)** Higher magnification of DAPI staining. Arrow indicates nucleus which corresponds to integrated Hh-RPC, seen in green in panel B.

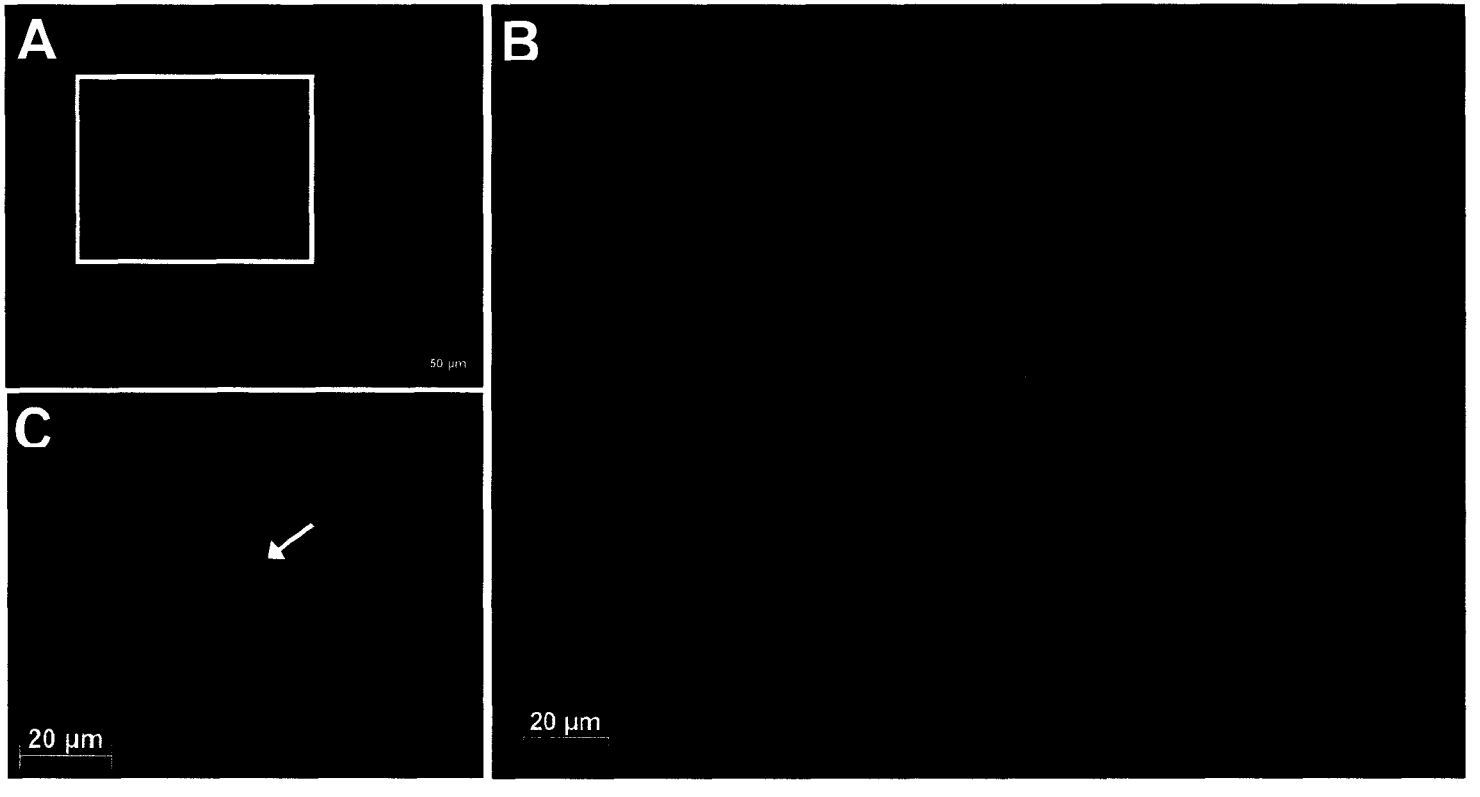

Figure 34: Fluorescence images of HIV1-XIAP/GFP infected C57BL/6 mouse Hh-RPCs after 8 days of co-culture with P1 C57BL/6 mouse retinal explants. **(A)** Low magnification showing overlay of α-GFP (green), α-Rhodopsin (red) and DAPI (blue) staining. **(B)** Higher magnification of region outlined in panel A showing overlay of α-GFP (green) and α-Rhodopsin (red) staining. **(C)** Higher magnification of DAPI staining. Arrow indicates nucleus which corresponds to integrated Hh-RPC, seen in green in panel B.

(Fig. 34). Western blot analysis of protein extracted from HIV1-XIAP/GFP lentivector-infected Hh-RPCs showed that the cells were indeed over- expressing XIAP protein (Fig. 35). Additional experiments are required to optimize the conditions for integration and differentiation of Hh-RPCs.

3.6 TAT-eGFP Assays in Hh-RPCs

3.6.1 Immunohistological Analysis of TAT-eGFP Expression in Hh-RPCs

Hh-RPCs were treated with three different concentrations of TAT-eGFP fusion protein for 1, 24 and 48 hours as well as 3 and 5 days. Phase contrast images of live Hh-RPCs were taken at the end of each time point (Fig. 36). It was evident that even when treated with TAT-eGFP at concentrations as high as 100.0μg/mL, the cells were healthy and retained normal morphology. Cells treated with lower concentrations of TAT-eGFP (50.0 and 10.0μg/mL) did not display any morphological changes either (data not shown).

The number of GFP-positive cells was counted and expressed as a percentage of total counted nuclei to gauge the rate of uptake of the fusion protein by Hh-RPCs (Fig. 37). Within 1 hour of addition of TAT-eGFP, at the highest concentration used, almost 80% of the cells had taken up the fusion protein. After 24 hours, the expression of TAT-eGFP was maximal, reaching 90.05% in the 100.0μg/mL treatment. Starting at 48 hours, the amount of TAT-eGFP expression started to drop off, being almost undetectable at 5 days. There was a statistically-significant increase in GFP-positive cells with increasing concentration of fusion protein used ($P<0.05$) for all time points except 5 days.

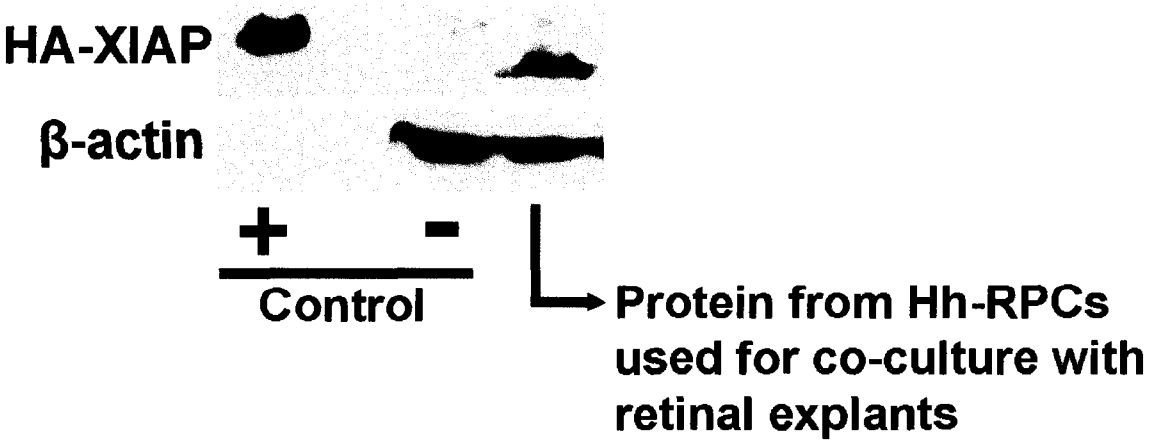

Figure 35: Western blot analysis of protein extracted from HIV1-XIAP/GFP lentivector-infected C57BL/6 mouse Hh-RPCs, which were co-cultured with C57BL/6 mouse retinal explants. 20μg of each protein sample was run on 10% SDS-PAGE and transferred onto PVDF membrane. Exogenous XIAP protein over-expression was detected with an anti-HA antibody. As a positive control, a sample of pure TAT-HA-XIAP was used. A sample of protein extracted from uninfected cells was loaded as a negative control To demonstrate equal loading, the blot was stripped and re-probed with an anti-β-actin antibody. HA-XIAP runs at approximately 55kDa. TAT-HA-XIAP runs at approximately 60kDa. β-actin runs at approximately 42kDa.

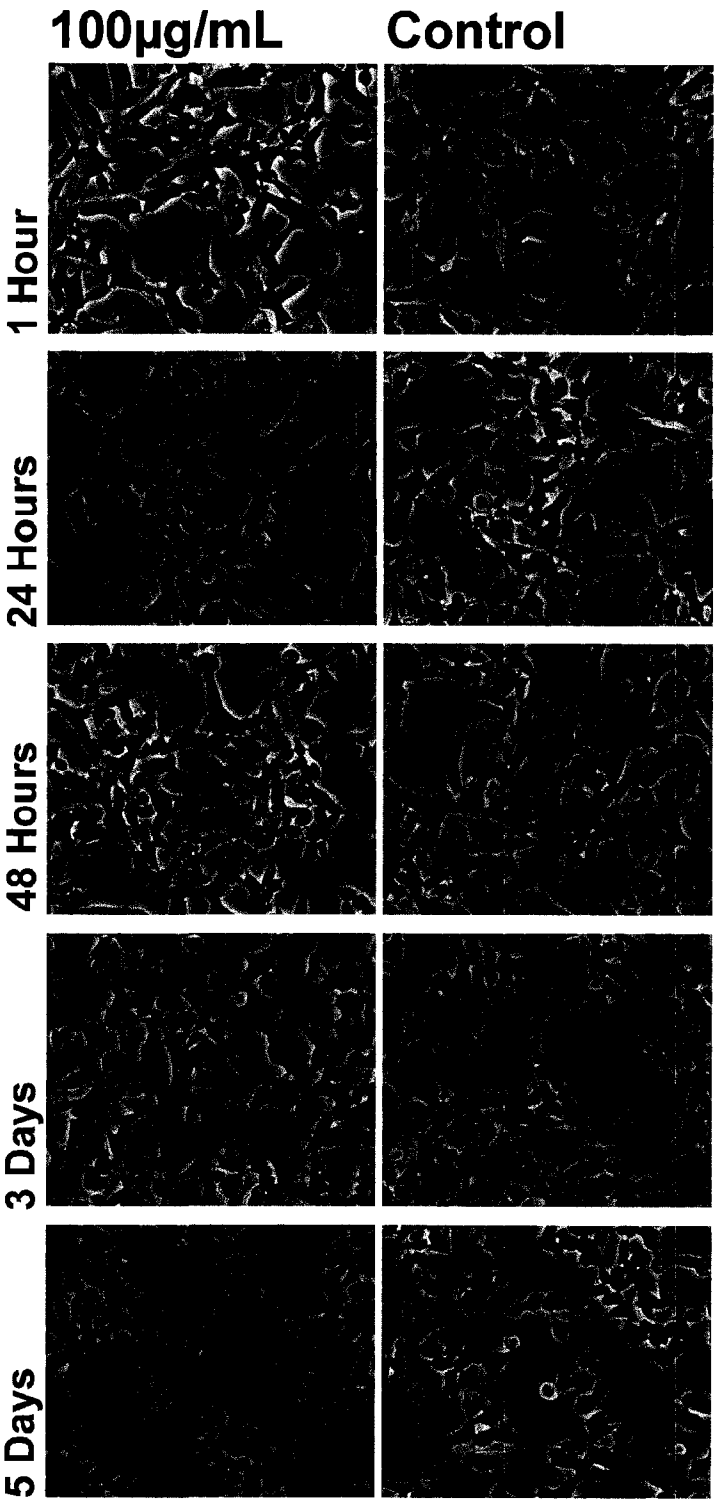

Figure 36: Phase contrast images of C57BL/6 mouse Hh-RPCs treated with 100µg/mL of TAT-eGFP in PBS or PBS alone (Control) for 1, 24 and 48 hours as well as 3 and 5 days. Following the documentation of live cell morphology, the Hh-RPCs were fixed and labeled for GFP as shown in subsequent figures (Fig. 37 to 41). **Bar = 100µm**

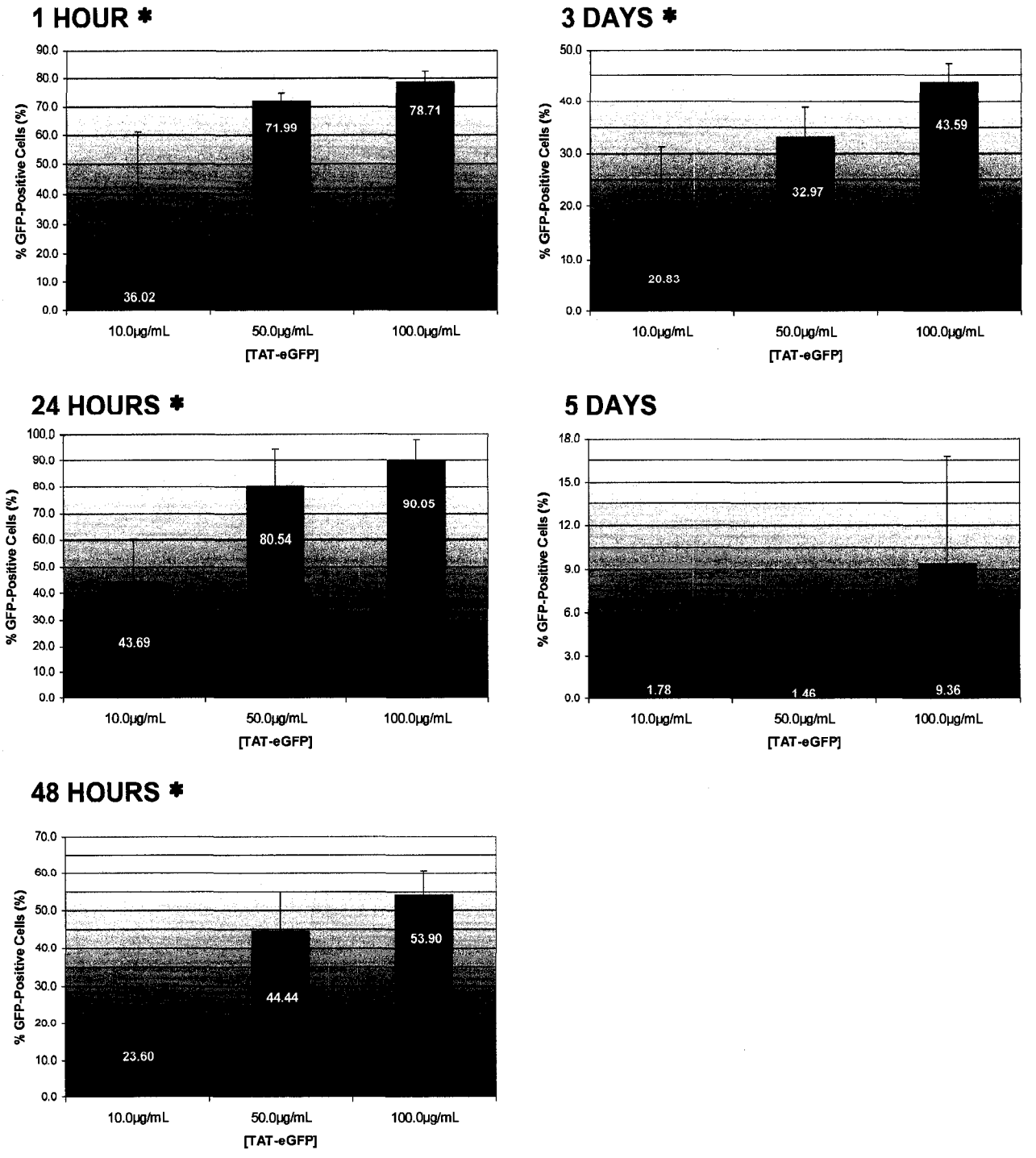

Figure 37: Percentage of GFP-positive cells out of total counted nuclei vs. amount of TAT-fusion protein added for the treatment of C57BL/6 mouse Hh-RPCs with TAT-eGFP for 1, 24 and 48 hours and 3 and 5 days. Values represent the average for three independent experiments; error bars indicate standard deviation.

* Time points which display a significant difference in % GFP-positive cells with respect to TAT-eGFP concentration. ($P<0.05$, $n = 3$, ANOVA).

Immunohistological analysis also demonstrated the cellular localization of TAT-eGFP in the Hh-RPCs (Fig. 38-42). One and 24 hours after addition of TAT-eGFP, it appeared that TAT-eGFP was mainly detected in the cytoplasm of Hh-RPCs. Starting at 48 hours until the last time point surveyed with the assay, the fusion protein appeared to localize almost exclusively in the nucleus of the cells.

3.6.2 Western Blot Analysis of TAT-eGFP Expression in Hh-RPCs

Western blot analysis of protein samples extracted from Hh-RPCs treated with TAT-eGFP showed that there was maximal protein uptake 24 hours after addition of the fusion protein (Fig. 43). There were no detectable differences in the intensity of protein expression between the two concentrations of protein used in the assay. From 48 hours on, TAT-eGFP was not observed in Hh-RPC protein extracts, within the limits of detection of Western blot analysis.

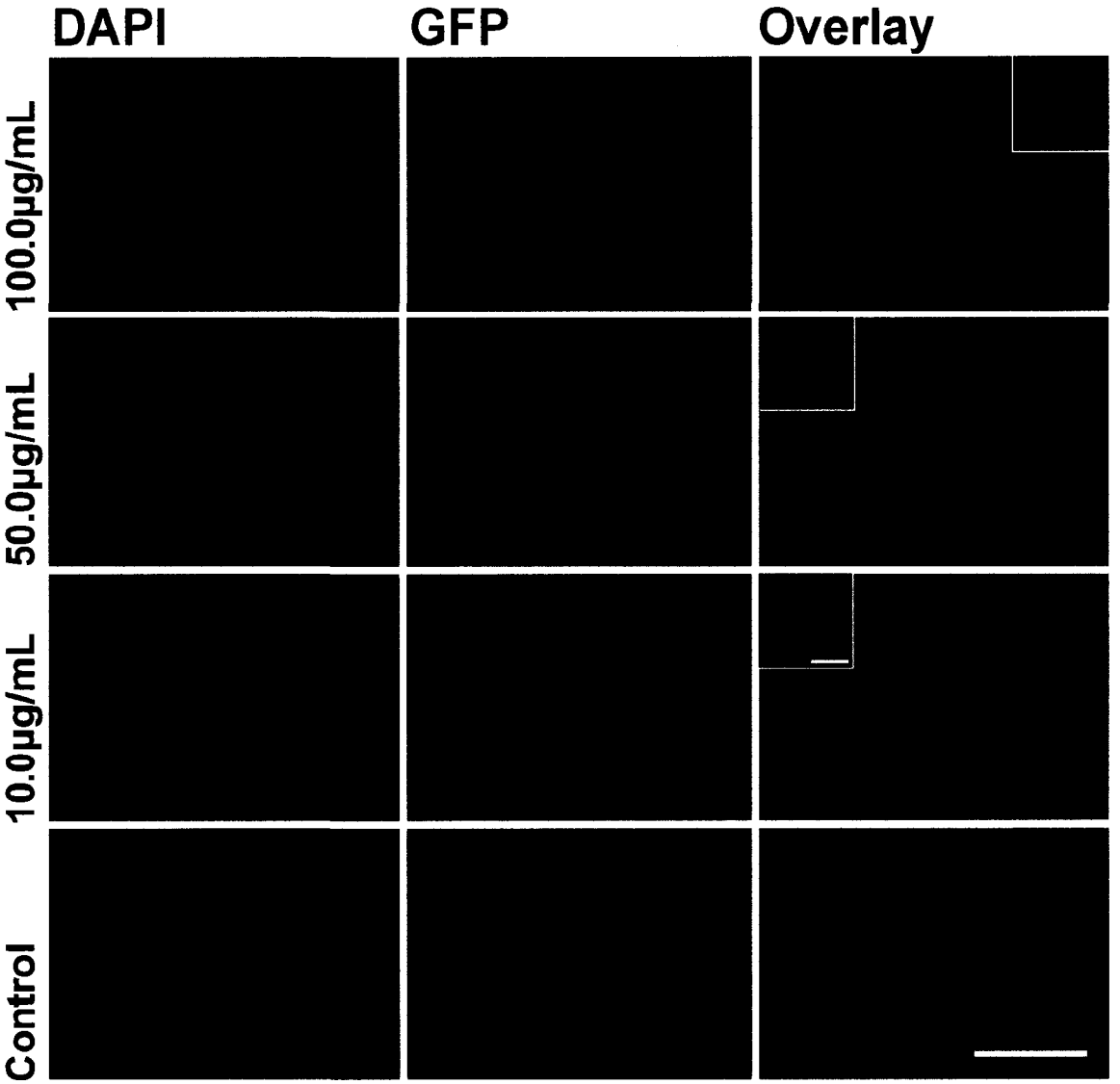

Figure 38: Fluorescence images following immunohistological analysis of C57BL/6 mouse Hh-RPCs treated for 1 hour with various concentrations of TAT-eGFP in PBS or PBS alone (Control). At the end of the time point, the cells were fixed with 4% paraformaldehyde, labeled with anti-GFP antibody (green) and counterstained with DAPI (blue). The number of GFP positive cells was counted and expressed as a percentage of the total counted nuclei. **Bar = 67µm** Inset images depict selected areas of the overlay magnified 3 times to better show cellular localization of TAT-eGFP. **Inset Bar ≈ 7.5µm**

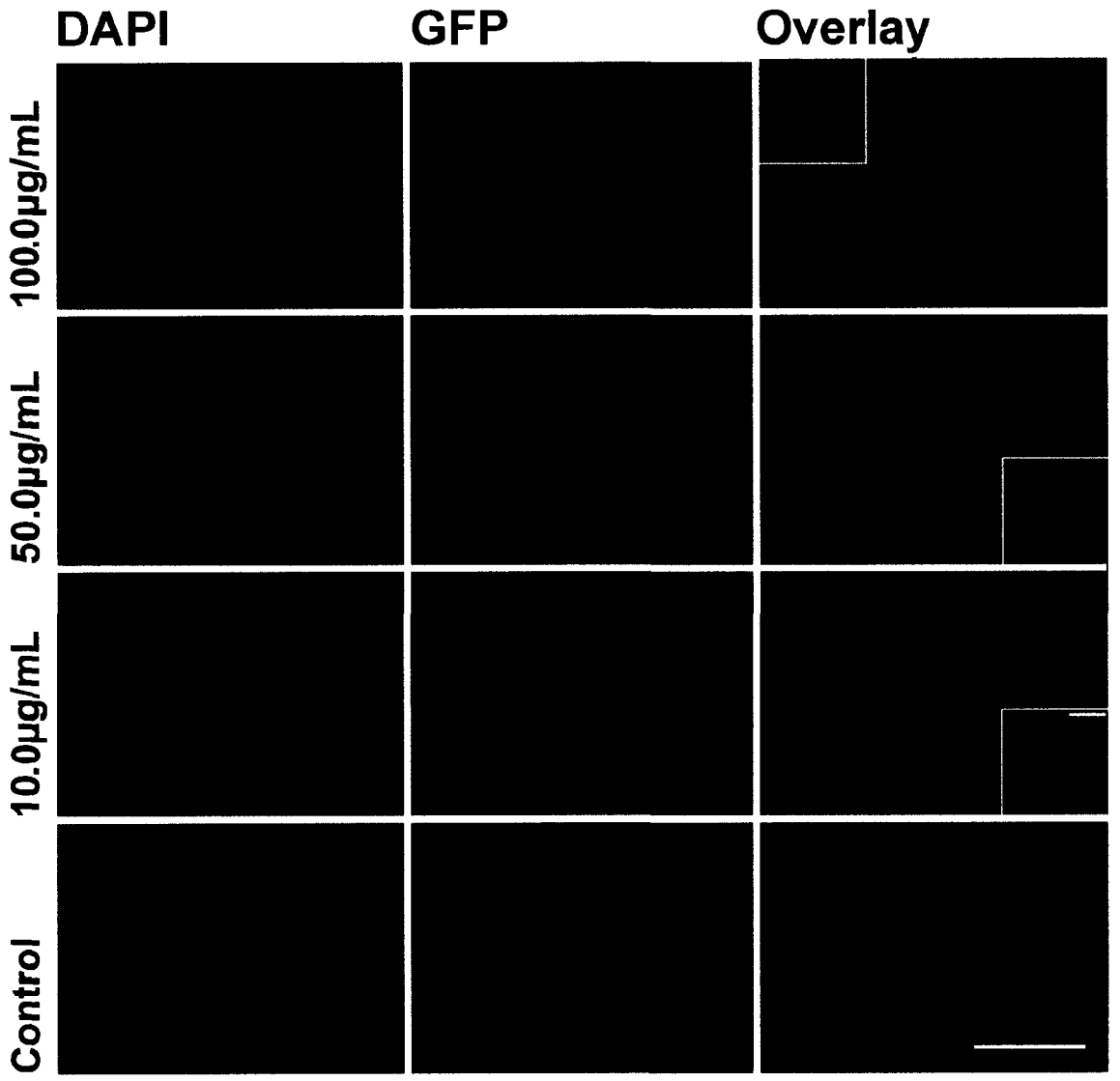

Figure 39: Fluorescence images following immunohistological analysis of C57BL/6 mouse Hh-RPCs treated for 24 hours with various concentrations of TAT-eGFP in PBS or PBS alone (Control). At the end of the time point, cells were processed as in Figure 37. **Bar = 67µm** Inset images depict selected areas of the overlay enlarged 3-fold to better show cellular localization of TAT-eGFP. **Inset Bar ≈ 7.5µm**

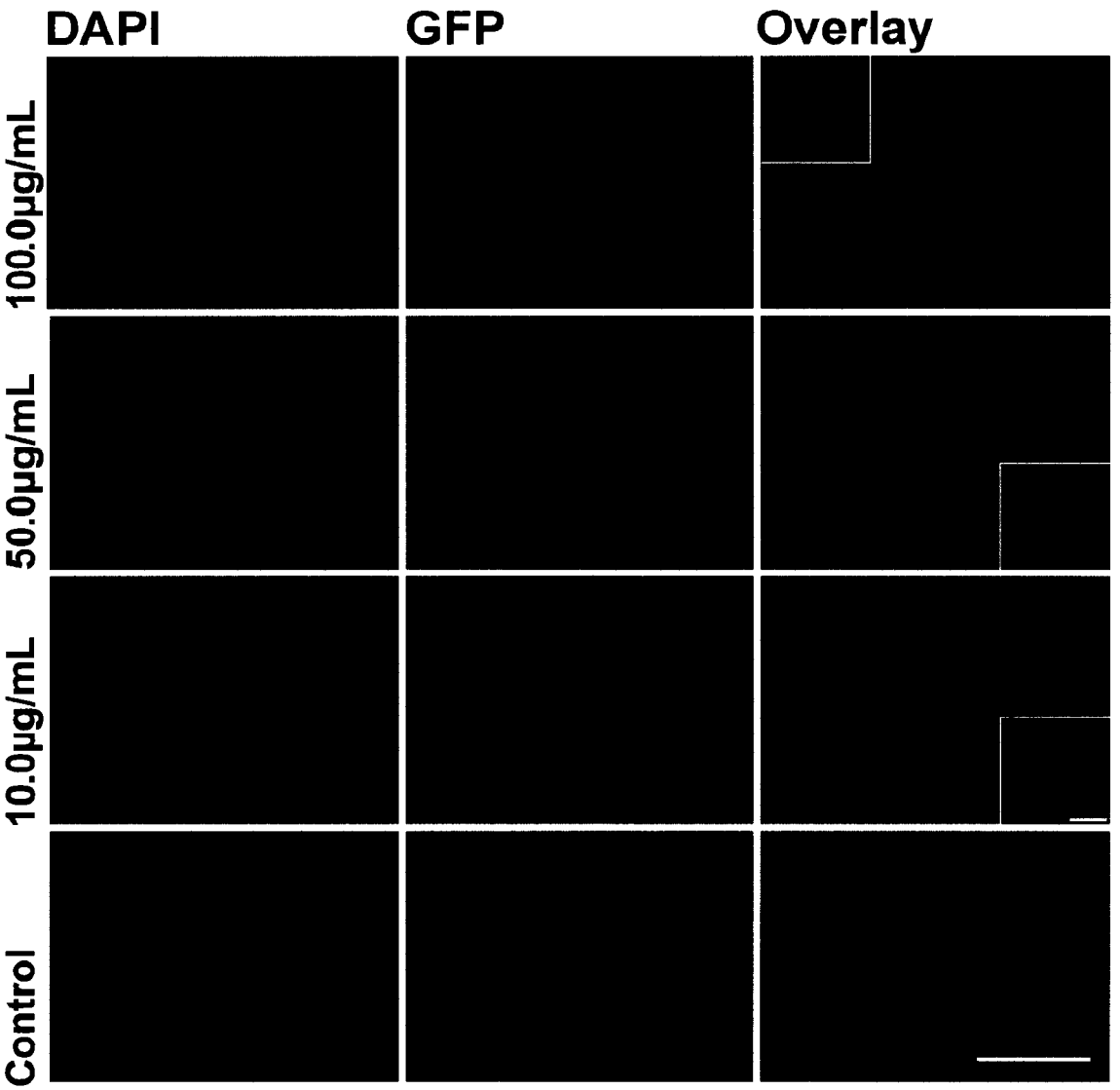

Figure 40: Fluorescence images following immunohistological analysis of C57BL/6 mouse Hh-RPCs treated for 48 hours with various concentrations of TAT-eGFP in PBS or PBS alone (Control). At the end of the time point, cells were processed as in Figure 37. **Bar = 67µm** Inset images depict selected areas of the overlay enlarged 3-fold to better show cellular localization of TAT-eGFP. **Inset Bar ≈ 7.5µm**

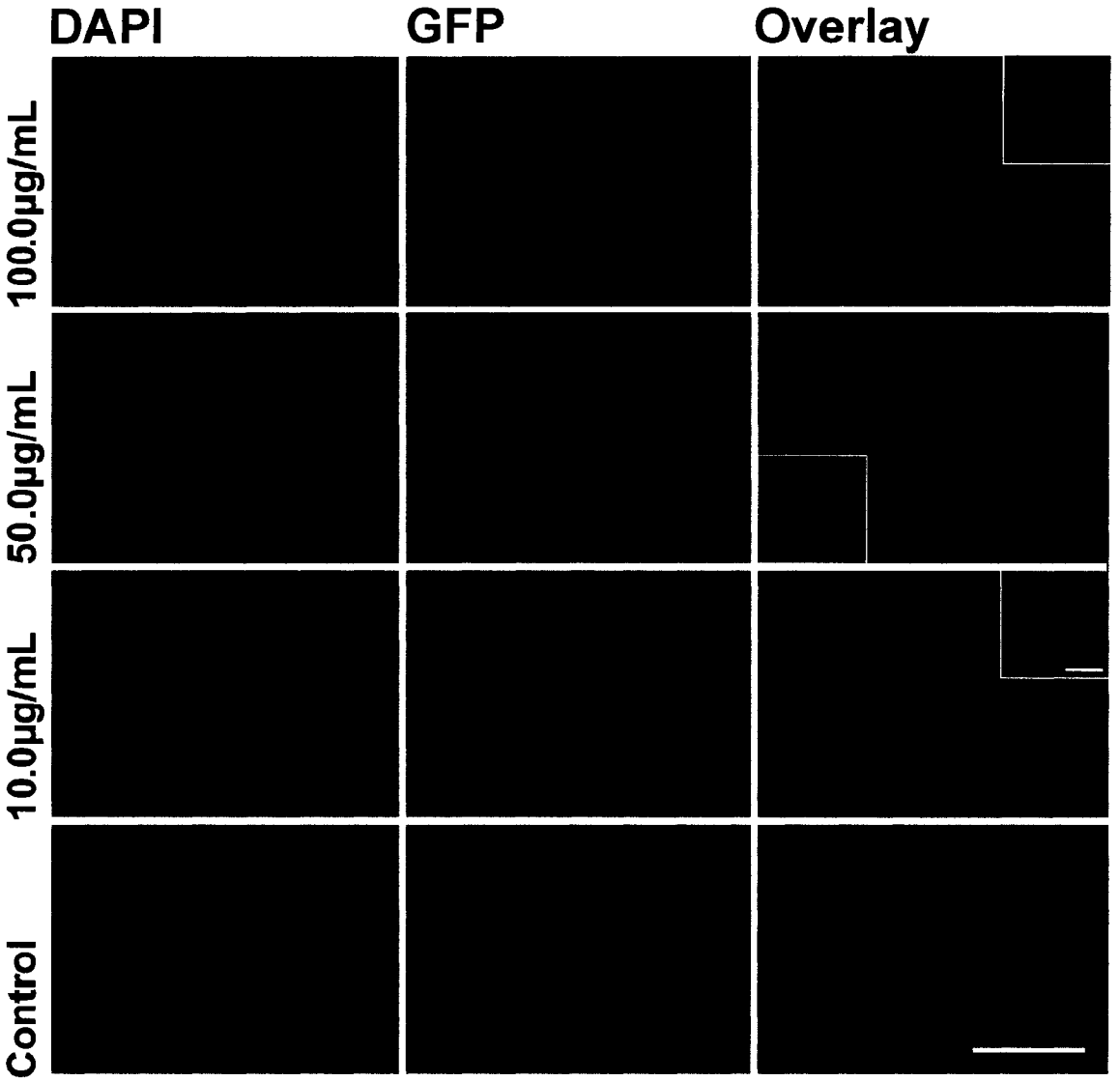

Figure 41: Fluorescence images following immunohistological analysis of C57BL/6 mouse Hh-RPCs treated for 3 days with various concentrations of TAT-eGFP in PBS or PBS alone (Control). At the end of the time point, cells were processed as in Figure 37. **Bar = 67µm** Inset images depict selected areas of the overlay enlarged 3-fold to better show cellular localization of TAT-eGFP. **Inset Bar ≈ 7.5µm**

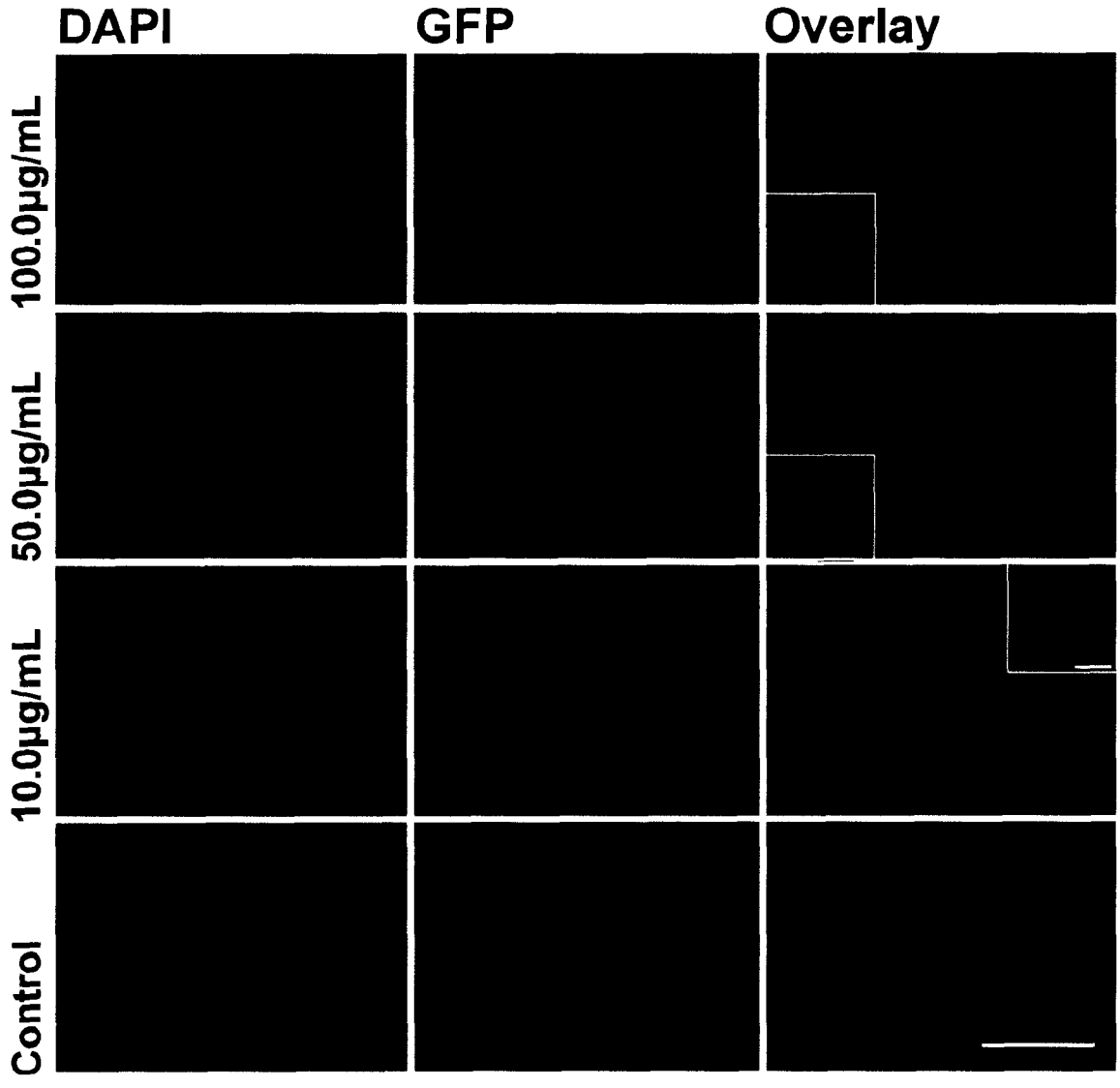

Figure 42: Fluorescence images following immunohistological analysis of C57BL/6 mouse Hh-RPCs treated for 5 days with various concentrations of TAT-eGFP in PBS or PBS alone (Control). At the end of the time point, cells were processed as in Figure 37. **Bar = 67µm** Inset images depict selected areas of the overlay enlarged 3-fold to better show cellular localization of TAT-eGFP. **Inset Bar ≈ 7.5µm**

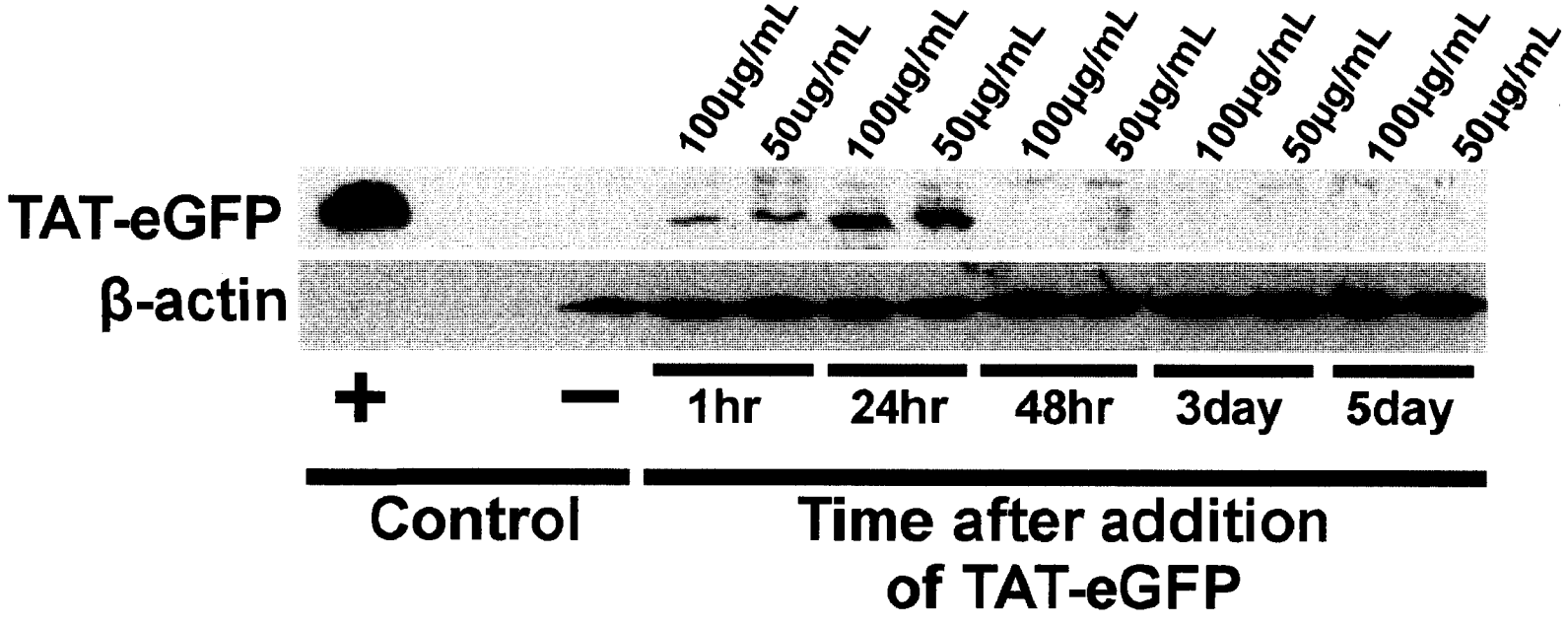

Figure 43: Western blot analysis of protein samples extracted from C57BL/6 mouse Hh-RPCs between 1 hour and 5 days after treatment with 100µg/mL and 50µg/mL of TAT-eGFP fusion protein. 15µg of each protein sample was run on 10% SDS-PAGE and transferred onto PVDF membrane. TAT-eGFP was detected with an anti-GFP antibody. A sample of pure TAT-eGFP was used as a positive control. As a negative control, a sample of protein extracted from untreated cells was loaded. To demonstrate equal loading, each blot was stripped and re-probed with an anti-β-actin antibody. TAT-eGFP runs at approximately 37kDa. β-actin runs at approximately 42kDa.

4. DISCUSSION

Cell replacement therapy presents the potential to reverse the damage caused by RP, instead of preventing its progress, as is the outcome of current treatments. A major obstacle to successful cell replacement therapy is post-transplant apoptotic death of the grafted tissues. XIAP protein could be delivered with a vector to Hh-RPCs prior to transplantation, providing protection against apoptosis. The current results show that it is possible to transduce primary retinal precursor cells with lentiviral vectors and a TAT-fusion protein. The use of these two delivery vectors is particularly exciting because each proved rapid and highly safe in primary retinal progenitor cells. In addition, the two systems vary in the duration of transgene expression. TAT-fusion proteins provide a rapid burst of protein over-expression which subsides within a few days while lentiviral vectors allow for steady levels of transgene expression for at least 36 days after infection. By establishing the parameters for optimal transgene delivery in retinal progenitor cells, this research represents a very important first step towards the development of effective therapies for the treatment of retinal degeneration.

4.1 Lentiviral Infection of Hh-RPCs

The titres of the vectors produced and used for this study were calculated to be approximately 1 x 10^7 TU/mL, which is typical of protocols for the production of lentiviral vectors (Tiscornia, Singer et al. 2006). The highest titres of lentivectors which have been obtained ranged from 1 x 10^8 to 1 x 10^9 TU/mL (Zhang, Xia et al. 2001; Tiscornia, Singer et al. 2006). Compared to some viral vectors currently in use, lentivirus titres are low. AAV vectors can commonly be obtained at titres of 1 x 10^{13} infectious particles/mL (Salvetti, Oreve et al. 1998). In addition to the low titres, only about one

milliliter of a particular viral preparation was produced at a time. Therefore, the amount of lentivirus available was a limiting factor when attempting to optimize the infection of C57BL/6 mouse Hh-RPCs. A fixed MOI of 2x was used for all infections with the HIV1-GFP lentivector. Titres of the HIV1-XIAP/GFP vector were lower than those of HIV1-GFP. So low in fact that even to achieve 2x MOI would have required the addition of such volumes of virus as to rapidly exhaust the supply of vector, therefore an MOI of 1.5x was chosen. The fact that two different MOIs were used during infections eliminated the possibility of comparing infection rates for the two vectors. This, however, was not the aim of the experiment. The goal was to establish the optimal infection conditions for each separate vector to be applied in future experiments.

An obvious solution to the problem of limiting amounts of virus would have been to simply produce more viral prep of higher titres. The protocol employed to produce the vector is highly labour and time intensive, requiring at least 8 days from the initial plating of 293T cells up to the titration of a complete prep. Secondly, the production of lentivector required the successful transfection of 293T cells with three separate plasmids. This led to few 293T cells which received all plasmids and which could produce functional vector, ultimately limiting the titres obtained. The three plasmid transfection, however, was necessary to prevent the formation of replication competent lentivirus via DNA or RNA recombination events. Attempting to scale-up lentiviral production was deemed not feasible due to safety and time constraints and instead an approach to optimize infection conditions via other means was taken.

Instead of varying the vector titre to try and increase infection efficiency, the amount of polybrene used during infection was changed. Varying polybrene

concentration proved to be a viable method for infection optimization, as a statistically significant increase in infection efficiency with increasing polybrene concentration was observed. At the highest concentration of polybrene used, 10.0μg/mL, maximal infection efficiencies of 32.87 and 26.48% were obtained with the HIV1-GFP and HIV1-XIAP/GFP vectors, respectively. There was no statistically significant change in infection efficiency from 24 to 48 hours after infection with either vector, indicating that maximal transgene expression was achieved within the first 24 hours after infection.

The presence of the virus as well as high polybrene concentrations yielded high infection efficiencies, however they also resulted in significant amounts of cell death following infection with both vectors at both time points examined. The cell death following lentiviral infection could have been caused in one of several ways. Polybrene is a proven cytotoxic agent (Ransdell, Haller et al. 1965; Ribelin 1984), therefore, it is plausible that raising its concentration during lentiviral infection protocols caused death of Hh-RPCs. If polybrene was indeed toxic to Hh-RPCs, significant amounts of cell death would have been observed in treatments where it was present even without virus. For both vectors at both time points, the amount of cell death in the Ctrl 10.0PB treatment was not significant when compared to the Ctrl 0.0PB treatments, however it was higher. With an increased number of trials, statistical significance would probably be achieved indicating that polybrene is having cytotoxic effects on Hh-RPCs at higher concentrations.

The observed cell death following lentiviral infection could also have been caused by the presence of the virus in one of two ways. Firstly, a component of the viral preparation could have been toxic to the cells. Secondly, lentiviral vectors, upon

integration into the host genome, could potentially disrupt a gene in the host cell, leading to cell death. HIV1 DNA has been shown to integrate randomly into host DNA (Park 2007); therefore a risk of insertional mutation exists. Insertional mutation, however poses a higher risk of oncogenesis, and not cell death.

During infections with the HIV1-GFP vector, there was a significant increase in cell death observed in the 2x MOI 7.5PB and 2x MOI 10.0PB treatments from 24 to 48 hours after infection (Fig. 16). When looking at the amount of cell death following infection with the HIV1-XIAP/GFP vector, there was no significant difference between the two time points for any of the treatments (Fig. 23). This would suggest that the GFP vector was having an adverse effect on cell survival, which the XIAP vector did not exert. However, when one compares the actual amount of cell death achieved by 48 hours after infection for both vectors, it is clear that the levels are the same. It appears that the levels of cell death are just achieved quicker with the XIAP vector, within 24 hours, thus eliminating statistical significance when comparing the two time points. The low viral titres of the HIV1-XIAP/GFP lentivector necessitated the use of larger volumes of viral preparation when carrying out infections, approximately four times as much as with the HIV1-GFP vector. The fact that cell death occurred more rapidly when larger volumes of viral preparation were used seems to suggest that some component of the preparation is toxic to Hh-RPCs.

The viral preparation could produce cytotoxicity in several ways. The virus was originally collected from 293T cell supernatant, and even though it was purified, perhaps some residual agents remain that are toxic to the cells. Additionally, the virus was contained in a solution of 20% sucrose. The addition of the sucrose could be detrimental

to the cells, or even the simple dilution of the cell media and growth factors could have had adverse effects on Hh-RPC survival.

It appears, therefore, that the presence of the viral preparation and increasing polybrene concentrations lead to increased cell death. These factors also lead to increased infection efficiency. Therefore, the most advantageous option is to adopt a middle ground which balances some cell death with some increase in infection. It was determined that the optimal conditions for infecting C57BL/6 mouse Hh-RPCs were achieved by using 7.5μg/mL of polybrene. At this concentration of polybrene, infection efficiencies of 24% for the HIV1-GPF vector, and almost 20% for the HIV1-XIAP/GFP lentivector were obtained and the amount of cell death observed, although still significant, was decreased compared to treatment groups which received virus and 10.0μg/mL of polybrene.

Total cell numbers following lentiviral infection were also examined. Within each individual experiment the total cell number was expressed as a total cell ratio with respect to the Ctrl 0.0PB treatment. The absolute number of cells is dependent on how many cells were initially seeded and how long the treatment lasted, cells incubated for 48 hours having had additional time in which to divide. Dealing with ratios allowed for comparison of cell numbers between treatments and time points.

Comparison of total cell numbers showed fewer cells in treatments which received the virus. During infection with HIV1-GFP, the 2xMOI 10.0PB treatment showed significantly decreased total cell ratio as compared to Ctrl 0.0PB after 24 hours. Over-expression of proteins from a vector has been suggested to interfere with cell growth and division causing transgenic cells to divide slower (Alberts, Johnson et al.

2002; Lu, Kitazawa et al. 2005). One study with mesenchymal stem cells showed that these cells temporarily arrested in S phase following lentiviral transduction leading to a reduction in cell divisions (Lee, Kohn et al. 2004). Cell cycle slow down seems a likely explanation for the observed results especially considering that by 48 hours after infection, all treatments which contained virus showed a significant decrease in total cell ratio. With increased passage of time, the control cells divided normally, while infected cells lagged behind, increasing the disparity in observed cell number.

When looking at total cell ratios following infection with the HIV1-XIAP/GFP lentivector, at both time points there was a significant decrease observed for all treatments which received virus when compared to the Ctrl 0.0PB group. The fact that there was such a marked difference within a short time span could be attributed to two proteins being encoded by this construct. With cell resources, such as transcription factors and protein translation machinery, being monopolized for the over-expression of two transgenic proteins, it is possible that cell cycling slowed down so dramatically as to create significant changes within just 24 hours after infection (Lee, Kohn et al. 2004).

4.1.1 Optimal Lentiviral Infection Conditions

The sum of experiments performed to elucidate infection conditions with the HIV1-GFP and HIV1-XIAP/GFP lentivectors indicated that maximal infection efficiencies were obtained using 10.0μg/mL of polybrene during infection of C57BL/6 mouse Hh-RPCs. The amount of cytotoxicity due to insertional mutation observed under these conditions, however, was high, and it was deemed that optimal infection conditions require the use of 7.5μg/mL of polybrene. At this concentration of polybrene, fewer infected cells were obtained but cell survival was higher. In addition, as maximal gene

expression from the vector was obtained within 24 hours after infection, the viral prep and polybrene should be removed from the cell media after this time point to avoid any further toxic effects. Finally, when considering the use of a lentivirus as a vector for gene delivery to Hh-RPCs, it must be noted that successful transduction may lead to slower cell division.

4.2 Long-Term Transgene Expression from Lentivirus

Based on fluorescence images showing relatively steady levels of GFP expression, it is known that Hh-RPCs can express lentivirally-delivered genes for at least 13 days after infection (Fig. 24 and 25). However, Western blot analysis of cells infected with HIV1-XIAP/GFP showed a marked decrease in XIAP protein expression (Fig. 26). This decrease could be explained in several ways. First, it could be that the Hh-RPCs silenced gene expression from the virus. Epigenetic silencing of integrated retroviral DNA has been documented to occur via DNA methylation and histone modification (Poleshko, Palagin et al. 2008). It is commonly observed following the transduction of reporter and therapeutic genes using retroviral vectors. The incidence and severity of silencing is influenced by several factors, including: differentiation state of host cell, location of integration of retroviral DNA into host chromosome and composition of virus-encoded gene (Poleshko, Palagin et al. 2008). If silencing of lentiviral vector-delivered genes was indeed occurring in Hh-RPCs, we would also expect there to have been a decrease in GFP-expression. As mentioned above, this decrease in GFP-expressing cells was observed. Second, the decrease observed following Western blot analysis could be a result of total cellular XIAP protein expression being silenced following lentiviral infection. Apoptosis is a hallmark event observed upon infection

with many viral pathogens. For example, Wurzer and colleagues found that influenza A virus propagation was severely impaired in cells where caspase-3 was knocked down (Wurzer, Planz et al. 2003). Therefore, it likely follows that during normal infection with influenza virus, agents which inhibit apoptosis, such as XIAP protein, would be down-regulated within the cell in order to promote viral spreading. This was found to occur during reovirus infection. Apoptosis is an important mechanism of tissue injury during reovirus infection *in vivo*, and inhibition of apoptosis dramatically reduces the severity of disease. Further investigation revealed that during reovirus infection, cellular IAPs, are actively down-regulated (Kominsky, Bickel et al. 2002). The final possibility as to why there was an observed decrease in XIAP protein expression on the Western blot is that the assay was carried out in a heterogeneous population of infected and uninfected cells. If transgene over-expressing cells are cycling slower as suggested above, their proportion in the cell population would have decreased over time, diluting the transgenic protein signal. This would account for an observed GFP signal decrease as well.

Even without any further experiments to elucidate which mechanism is responsible for the transgenic signal decrease, these results show that XIAP protein can be over-expressed in Hh-RPCs for at least 13 days, which would be sufficient time to inject them into a host and to potentially confer protection from post-transplant apoptosis.

4.3 FACS

FACS of primary cells is a well established process (Maric and Barker 2005). The concern in this study was that Hh-RPCs may not survive the procedure as they are highly sensitive to changes in pH and temperature. Two independent experiments showed that Hh-RPCs can successfully undergo FACS. Following the procedure, no

morphological changes were evident and cells continued to be cultured as previously described.

According to the FACS readings, the average amount of GFP-positive cells following infection with HIV1-GFP under optimal conditions, 2x MOI and 7.5μg/mL of polybrene, was 20.2%. This is in accordance with previous findings which put the infection efficiency of HIV1-GFP at 7.5μg/mL of polybrene at approximately 24%. In the HIV1-XIAP/GFP infected group, where infection was carried out at 1.5x MOI and 7.5μg/mL of polybrene, the average amount of GFP-positive cells according to the FACS data was only 9.64%. Based on results presented in Figure 20, at 7.5μg/mL of polybrene, the percent of infected cells should have been closer to 20%.

The threshold for GFP-detection in each sort was set using HIV1-GFP infected Hh-RPCs. In this vector, GFP expression is driven by the EF1-α promoter. In the HIV1-XIAP/GFP construct, GFP expression is weaker because it is driven by the EMCV IRES. The level of expression of genes driven by an IRES varies based on such factors as the exact IRES sequence (Bochkov and Palmenberg 2006), the size of the encoded gene (Houdebine and Attal 1999) and the presence of stressors in the cellular environment (Nevins, Harder et al. 2003; Holcik and Sonenberg 2005; Lewis and Holcik 2005). In general, research shows that gene expression downstream of the IRES occurs at a lower level as compared to genes upstream of it (Kaufman, Davies et al. 1991; Dirks, Wirth et al. 1993; Zhou, Aran et al. 1998; Houdebine and Attal 1999). The infection rate data in Figure 20 was generated from indirect immunohistochemistry for GFP. Signal amplification allowed for detection of even low levels of GFP expression from the HIV1-XIAP/GFP lentivector. FACS, however, did not detect every HIV1-XIAP/GFP infected

cell as thresholds were set using the more robustly GFP-expressing HIV1-GFP vector, resulting in the observed discrepancy.

Overall, the sorting process was not highly efficient, capturing less than 10% of Hh-RPCs. This was the result of a low proportion of cells being GFP-positive following lentiviral infection compounded with cell death occurring during the sort itself. However, this is not an obstacle to the use of FACS on Hh-RPCs because, once recovered, the cells can be expanded indefinitely, yielding whatever numbers of cells that may be required.

Sorting of lentivirus-infected Hh-RPCs greatly enriched the proportion of transgene-expressing cells in the population. Long-term transgene expression was monitored in these highly-purified post-FACS cells. Western blot analysis of protein samples extracted periodically from sorted HIV1-XIAP/GFP infected cells, showed exogenous XIAP protein expression to be steady (Fig. 32.A). Furthermore, probing for total XIAP protein showed that overall levels of expression, exogenous and endogenous, were stable during the surveyed time period (Fig. 32.B). These results indicated that neither the lentiviral genes nor XIAP protein expression were silenced following lentiviral infection of Hh-RPCs for at least 28 days after the sorting (36 days after infection). It appears, therefore, that the observed decrease in XIAP protein expression discussed in section 4.2 can be solely attributed to the proportional decrease in number of slowly-dividing infected cells. Once heterogeneity in the population was eliminated, so was the decrease in transgene expression. Consequently, this indicates that to obtain significant amounts of long-term transgene expression from a lentiviral vector, isolation and concentration of the infected cells is necessary. If left as a heterogeneous population,

the slowly-dividing infected cells will steadily be outnumbered by wild-type cells, diluting the amount of transgene expression over time to undetectable levels.

Probing for total XIAP protein also allowed for the clear demonstration of over-expression of XIAP protein in lentivirally-infected cells, as there was a marked increase in signal in samples from infected cells when compared to the uninfected negative control (Fig. 32.B). Finally, this experiment demonstrated that transgene expression from lentiviral infection is sustained beyond the above stated 13 days for up to 36 days after infection.

4.4 Photoreceptor Differentiation of Hh-RPCs

The concern was raised that inhibiting caspase-3 activity with XIAP protein over-expression could prevent Hh-RPCs from differentiating into photoreceptors. XIAP-protein over-expressing Hh-RPCs were co-cultured with retinal explants to verify this. A few cells which morphologically resembled photoreceptors and co-localized with rhodopsin staining were found following co-culture of the HIV1-XIAP/GFP infected cells (Fig. 34). This suggests that the level of XIAP protein over-expression achieved in Hh-RPCs following lentiviral infection does not inhibit photoreceptor differentiation. Definitive photoreceptor differentiation, however, was not observed following the co-culture of the control, HIV1-GFP infected, cells. Overall there appeared to be several limitations to the assay employed.

Firstly, the amount of Hh-RPCs observed to successfully integrate into the retinal explants was low. Figure 6 demonstrates the level of integration which can be achieved upon co-culture. In the current study the amount of integration was significantly lower perhaps due to limited experience with the techniques. With few cells integrating, the

probability of observing an Hh-RPC, which had specifically differentiated into a photoreceptor, was low. Secondly, it has been demonstrated that late-passage Hh-RPCs do not possess as robust an ability to differentiate into retinal neurons and glia (Wang and Wallace, unpublished). The Hh-RPCs used in the assay had already been in culture for over three months and were perhaps too old to integrate into explants and to differentiate into photoreceptors. Finally, support of the RPE is required for normal neural retina development (Raymond and Jackson 1995) and structure (Fisher, Lewis et al. 2005). In the retinal explant model, the lack of RPE leads to a characteristic whorling of the retinal layers. The whorls made it difficult to judge cellular morphology and positively identify photoreceptors.

In summary, the differentiation potential of Hh-RPCs appears to be unaffected by XIAP protein over-expression from lentivirus. To be able to draw definitive conclusions, the assay must be repeated with younger Hh-RPCs. In addition, if *in vivo* injections, instead of the retinal co-culture assay, were employed to induce photoreceptor differentiation of Hh-RPCs, laminar structure of the neural retina would be preserved and morphology would be easier to discern.

4.5 TAT-eGFP Assays in Hh-RPCs

The use of the TAT PTD allows for upregulation of a target protein. The upregulation is temporary, therefore the expression pattern has to be mapped out to determine how quickly a particular fusion protein is taken up by a cell and how quickly it is degraded. The ultimate goal of this study was to use a TAT fusion protein to deliver XIAP protein to Hh-RPCs. Although a TAT-XIAP construct has been cloned, thus far there have been obstacles to obtaining it in sufficiently large quantities for use in tissue

culture (personal communication from Dr. W.G. Fong). Therefore, the present study sought to map out the expression of a reporter construct, TAT-eGFP, in Hh-RPCs to determine optimal conditions for later use with the XIAP construct.

C57BL/6 mouse Hh-RPCs could withstand treatment with TAT-eGFP fusion protein up to concentrations of 100.0μg/mL and retained normal morphology and growth patterns. Based on the data summarized in Figure 37, it was apparent that a large amount of fusion protein was taken up in as little as 1 hour. Maximal expression was at 24 hours, with 80% of GFP-positive cells at 50.0μg/mL and 90% at 100.0μg/mL of fusion protein. By 48 hours, the amount of TAT-eGFP was already dropping, although approximately half the cells still expressed the fusion protein in the 50.0μg/mL and 100.0μg/mL treatments. Five days after addition of the fusion protein it was barely detectable in Hh-RPCs by immunohistochemistry, except at the 100.0μg/mL dose (Fig. 42). Statistical analysis of the data in Figure 37, showed there was a significant increase in GFP-positive cells with increasing TAT-eGFP concentration for all time points except 5 days. Therefore, TAT-eGFP uptake and expression are concentration dependent for up to 3 days after addition of the fusion protein. Five days post treatment with TAT-eGFP, degradation of the protein was so advanced that concentration-based differences in expression were no longer evident. Overall, these results indicate that the use of the TAT PTD would allow for quick delivery of target proteins to large numbers of Hh-RPCs in as little as 1 hour.

The results of immunohistochemical analysis of TAT-eGFP expression in Hh-RPCs revealed a problem with the TAT PTD used in this study. Forty-eight hours after

the addition of the fusion protein, the majority co-localized with the nucleus. At 3 and 5 days, TAT-eGFP could only be detected in the nucleus.

Immunohistochemistry only proved the presence or absence of TAT-eGFP and its localization inside Hh-RPCs. To quantitatively map out TAT-eGFP expression, Western blots were run on protein extracted from Hh-RPCs treated with TAT-eGFP. Figure 43 shows that the TAT-eGFP signal was much stronger at 24 hours than at 1 hour after addition of the protein. This is in accordance with results which showed that maximal TAT-eGFP expression was achieved 24 hours after addition of the protein. From 48 hours on, however, there was no protein detected. These result prevented the original goal of the experiment, the quantification of TAT-eGFP uptake by Hh-RPCs from 1 hour to 5 days after addition of the fusion protein, from being fulfilled. However, the findings did reveal something useful. CelLyticM Reagent (Sigma), used for all protein extractions in this study, requires the addition of salts to lyse nuclear membranes and to extract nuclear proteins (Sigma-Aldrich 2007). Since salts were not added, all extracts represent only the cytoplasmic fraction of proteins. Therefore, the fact that Western blots of cytoplasmic fractions from TAT-eGFP treated Hh-RPCs showed no signal past 24 hours of treatment, suggests that beyond this time point, the fusion protein was localized in the nucleus of cells.

Previous studies suggest that the TAT PTD has a nuclear-localization signal (NLS) (Vives, Brodin et al. 1997; Ferrari, Pellegrini et al. 2003). Nuclear magnetic resonance studies revealed that TAT PTD possesses an extended coil-structure similar in structure and location to four consecutive Lysine residues found in the C-terminal region of the mouse nucleoplasmin NLS (Fontes, Teh et al. 2000; Friedler, Friedler et al. 2000).

XIAP protein is active in the cytoplasm of the cell, therefore it must be delivered and remain there. The above stated findings, along with the current work involving the TAT-eGFP reporter construct, indicated that using the TAT PTD would not be a feasible method of XIAP protein delivery to Hh-RPCs.

Kim and colleagues have created a cytoplasmic transduction peptide (CTP) (Kim, Jeon et al. 2006). The sequence retains the 5 Arginine residues required for membrane transduction but is altered to eliminate the NLS found in the TAT PTD. The study showed that CTP and its fusion partners exhibited a clear preference for cytoplasmic localization, and also markedly enhanced membrane transduction potential. The effectiveness of CTP was demonstrated *in vitro* and *in vivo* (Kim, Jeon et al. 2006). The generation and testing of CTP fusion proteins is currently underway and constructs will soon be applied to Hh-RPCs.

Despite the fact that the TAT PTD cannot be used to deliver XIAP protein to Hh-RPCs, the current results showed that in general, the use of a PTD allowed for a very effective protein uptake and did not cause cytotoxicity even at high concentrations. With the introduction of CTP constructs, the full potential of fusion proteins will hopefully be harnessed for acute transgene delivery to Hh-RPCs.

4.6 Final Thoughts

The aim of this project was to explore a lentiviral vector and a TAT-fusion protein as potential means of delivering XIAP protein to Hh-RPCs.

The optimal infection conditions for the HIV1-GFP and HIV1-XIAP/GFP lentiviral vectors were determined and employed, in conjunction with FACS, to obtain highly purified lines of GFP-only or XIAP protein and GFP expressing Hh-RPCs. It was

shown that these cells can express the transgenes at steady levels for up to 36 days after infection. These cells are ideally suited to be used in transplantation experiments to verify whether XIAP over-expression confers protection against post-transplant apoptosis.

Using a GFP-reporter construct, it was shown that TAT PTD mediates uptake of the protein to Hh-RPCs in a concentration dependent manner. Uptake was very rapid, within 1 hour after addition of the fusion protein, and maximal at 24 hours. The expression dropped off, being virtually undetectable after 5 days. The current constructs, however, were directed to the nucleus, which is problematic for future applications with XIAP protein. A lot of work is required before being able to use XIAP fusion protein-transduced Hh-RPCs in transplantation experiments. The PTD has to be modified to eliminate the NLS. Large quantities of PTD-XIAP fusion protein have to be obtained and the expression patterns of the new constructs have to be mapped out in Hh-RPCs.

More progress towards obtaining XIAP protein over-expressing Hh-RPCs was made with the lentiviral vector than with the PTD fusion protein. Development of lentivirally-transduced progenitor cells is important and will be very useful for proof-of-principle research studies. For clinical applications, however, the use of a PTD fusion protein would be preferable. Lentiviruses, as already mentioned, integrate randomly into host genome and could cause insertional mutation leading to oncogenesis (Park 2007). In addition, the use of a viral vector could trigger an immune response in the host (Follenzi, Santambrogio et al. 2007). By delivering a protein product directly, these problems are circumvented because integration into the host genome is not required, and the up-regulation is not long-term.

When analyzed, this work is significant as it demonstrated two very different methods of transducing primary retinal progenitor cells. More importantly, this study has been an important step towards transplanting XIAP protein over-expressing Hh-RPCs into models of retinal degeneration. Future work will examine the transplant potential and survival of XIAP protein over-expressing cells in retinal explants and *in vivo* models of retinal disease. The hope is that XIAP protein over-expression will protect the cells against post-transplant apoptosis leaving a larger population of donor cells to repopulate degenerating retinas. Therefore, progress is being made towards developing an efficient cell replacement therapy to treat retinal degenerative disorders.

5. REFERENCES

Acland, G. M., G. D. Aguirre, et al. (2005). "Long-term restoration of rod and cone vision by single dose rAAV-mediated gene transfer to the retina in a canine model of childhood blindness." Mol Ther **12**(6): 1072-82.

Acland, G. M., G. D. Aguirre, et al. (2001). "Gene therapy restores vision in a canine model of childhood blindness." Nat Genet **28**(1): 92-5.

Adams, J. M. and S. Cory (1998). "The Bcl-2 protein family: arbiters of cell survival." Science **281**(5381): 1322-6.

Ahmad, I., L. Tang, et al. (2000). "Identification of neural progenitors in the adult mammalian eye." Biochem Biophys Res Commun **270**(2): 517-21.

Akagi, T., M. Mandai, et al. (2004). "Otx2 homeobox gene induces photoreceptor-specific phenotypes in cells derived from adult iris and ciliary tissue." Invest Ophthalmol Vis Sci **45**(12): 4570-5.

Alberts, B., A. Johnson, et al. (2002). Molecular Biology of the Cell. New York, Garland Science.

Bakhshi, A., J. P. Jensen, et al. (1985). "Cloning the chromosomal breakpoint of t(14;18) human lymphomas: clustering around JH on chromosome 14 and near a transcriptional unit on 18." Cell **41**(3): 899-906.

Bakshi, A., C. A. Keck, et al. (2005). "Caspase-mediated cell death predominates following engraftment of neural progenitor cells into traumatically injured rat brain." Brain Res **1065**(1-2): 8-19.

Becker-Hapak, M., S. S. McAllister, et al. (2001). "TAT-mediated protein transduction into mammalian cells." Methods **24**(3): 247-56.

Berson, E. L. (1993). "Retinitis pigmentosa. The Friedenwald Lecture." Invest Ophthalmol Vis Sci **34**(5): 1659-76.

Berson, E. L., B. Rosner, et al. (1993). "A randomized trial of vitamin A and vitamin E supplementation for retinitis pigmentosa." Arch Ophthalmol **111**(6): 761-72.

Berson, E. L., B. Rosner, et al. (2004). "Further evaluation of docosahexaenoic acid in patients with retinitis pigmentosa receiving vitamin A treatment: subgroup analyses." Arch Ophthalmol **122**(9): 1306-14.

Biarnes, M., M. Montolio, et al. (2002). "Beta-cell death and mass in syngeneically transplanted islets exposed to short- and long-term hyperglycemia." Diabetes **51**(1): 66-72.

Bochkov, Y. A. and A. C. Palmenberg (2006). "Translational efficiency of EMCV IRES in bicistronic vectors is dependent upon IRES sequence and gene location." Biotechniques **41**(3): 283-4, 286, 288 passim.

Boonman, Z. and O. Isacson (1999). "Apoptosis in neuronal development and transplantation: role of caspases and trophic factors." Exp Neurol **156**(1): 1-15.

Buj-Bello, A., F. Fougerousse, et al. (2008). "AAV-mediated intramuscular delivery of myotubularin corrects the myotubular myopathy phenotype in targeted murine muscle and suggests a function in plasma membrane homeostasis." Hum Mol Genet.

Capowski, E. E., B. L. Schneider, et al. (2007). "Lentiviral vector-mediated genetic modification of human neural progenitor cells for ex vivo gene therapy." J Neurosci Methods **163**(2): 338-49.

Chai, J., C. Du, et al. (2000). "Structural and biochemical basis of apoptotic activation by Smac/DIABLO." Nature **406**(6798): 855-62.

Cheng, E. H., M. C. Wei, et al. (2001). "BCL-2, BCL-X(L) sequester BH3 domain-only molecules preventing BAX- and BAK-mediated mitochondrial apoptosis." Mol Cell **8**(3): 705-11.

Cherqui, S., K. M. Kingdon, et al. (2007). "Lentiviral gene delivery of vMIP-II to transplanted endothelial cells and endothelial progenitors is proangiogenic in vivo." Mol Ther **15**(7): 1264-72.

Chipuk, J. E. and D. R. Green (2008). "How do BCL-2 proteins induce mitochondrial outer membrane permeabilization?" Trends Cell Biol **18**(4): 157-64.

Cleary, M. L. and J. Sklar (1985). "Nucleotide sequence of a t(14;18) chromosomal breakpoint in follicular lymphoma and demonstration of a breakpoint-cluster region near a transcriptionally active locus on chromosome 18." Proc Natl Acad Sci U S A **82**(21): 7439-43.

Clelland, C. D., R. A. Barker, et al. (2008). "Cell therapy in Huntington disease." Neurosurg Focus **24**(3-4): E9.

Coles, B. L., B. Angenieux, et al. (2004). "Facile isolation and the characterization of human retinal stem cells." Proc Natl Acad Sci U S A **101**(44): 15772-7.

Daiger, S. P. (2008). RetNet Retinal Information Network.

Danial, N. N. and S. J. Korsmeyer (2004). "Cell death: critical control points." Cell **116**(2): 205-19.

Davis, H. E., M. Rosinski, et al. (2004). "Charged polymers modulate retrovirus transduction via membrane charge neutralization and virus aggregation." Biophys J **86**(2): 1234-42.

Derossi, D., A. H. Joliot, et al. (1994). "The third helix of the Antennapedia homeodomain translocates through biological membranes." J Biol Chem **269**(14): 10444-50.

Dirks, W., M. Wirth, et al. (1993). "Dicistronic transcription units for gene expression in mammalian cells." Gene **128**(2): 247-9.

Eberling, J. L., W. J. Jagust, et al. (2008). "Results from a phase I safety trial of hAADC gene therapy for Parkinson disease." Neurology **70**(21): 1980-3.

Eftekharpour, E., S. Karimi-Abdolrezaee, et al. (2008). "Current status of experimental cell replacement approaches to spinal cord injury." Neurosurg Focus **24**(3-4): E19.

Elliott, G. and P. O'Hare (1997). "Intercellular trafficking and protein delivery by a herpesvirus structural protein." Cell **88**(2): 223-33.

Emamaullee, J. A., R. V. Rajotte, et al. (2005). "XIAP overexpression in human islets prevents early posttransplant apoptosis and reduces the islet mass needed to treat diabetes." Diabetes **54**(9): 2541-8.

Federico, M. (2003). "From lentiviruses to lentivirus vectors." Methods Mol Biol **229**: 3-15.

Fernando, P., S. Brunette, et al. (2005). "Neural stem cell differentiation is dependent upon endogenous caspase 3 activity." Faseb J **19**(12): 1671-3.

Fernando, P., J. F. Kelly, et al. (2002). "Caspase 3 activity is required for skeletal muscle differentiation." Proc Natl Acad Sci U S A **99**(17): 11025-30.

Ferrari, A., V. Pellegrini, et al. (2003). "Caveolae-mediated internalization of extracellular HIV-1 tat fusion proteins visualized in real time." Mol Ther **8**(2): 284-94.

Fisher, S. K., G. P. Lewis, et al. (2005). "Cellular remodeling in mammalian retina: results from studies of experimental retinal detachment." Prog Retin Eye Res **24**(3): 395-431.

Follenzi, A., L. Santambrogio, et al. (2007). "Immune responses to lentiviral vectors." Curr Gene Ther **7**(5): 306-15.

Fontes, M. R., T. Teh, et al. (2000). "Structural basis of recognition of monopartite and bipartite nuclear localization sequences by mammalian importin-alpha." J Mol Biol **297**(5): 1183-94.

Frank-Kamenetsky, M., X. M. Zhang, et al. (2002). "Small-molecule modulators of Hedgehog signaling: identification and characterization of Smoothened agonists and antagonists." J Biol **1**(2): 10.

Frankel, A. D. and C. O. Pabo (1988). "Cellular uptake of the tat protein from human immunodeficiency virus." Cell **55**(6): 1189-93.

Friedler, A., D. Friedler, et al. (2000). "Development of a functional backbone cyclic mimetic of the HIV-1 Tat arginine-rich motif." J Biol Chem **275**(31): 23783-9.

Giordano, F., A. De Marzo, et al. (2007). "Fibroblast growth factor and epidermal growth factor differently affect differentiation of murine retinal stem cells in vitro." Mol Vis **13**: 1842-50.

Green, M. and P. M. Loewenstein (1988). "Autonomous functional domains of chemically synthesized human immunodeficiency virus tat trans-activator protein." Cell **55**(6): 1179-88.

Grieger, J. C. and R. J. Samulski (2005). "Adeno-associated virus as a gene therapy vector: vector development, production and clinical applications." Adv Biochem Eng Biotechnol **99**: 119-45.

Gropp, M. and B. Reubinoff (2006). "Lentiviral vector-mediated gene delivery into human embryonic stem cells." Methods Enzymol **420**: 64-81.

Gross, A., J. M. McDonnell, et al. (1999). "BCL-2 family members and the mitochondria in apoptosis." Genes Dev **13**(15): 1899-911.

Guegan, C., J. Braudeau, et al. (2006). "PTD-XIAP protects against cerebral ischemia by anti-apoptotic and transcriptional regulatory mechanisms." Neurobiol Dis **22**(1): 177-86.

Gump, J. M. and S. F. Dowdy (2007). "TAT transduction: the molecular mechanism and therapeutic prospects." Trends Mol Med **13**(10): 443-8.

Hamel, C. (2006). "Retinitis pigmentosa." Orphanet J Rare Dis **1**: 40.

Hempel, C. M., K. Sugino, et al. (2007). "A manual method for the purification of fluorescently labeled neurons from the mammalian brain." Nat Protoc **2**(11): 2924-9.

Hill, C. E., L. D. Moon, et al. (2006). "Labeled Schwann cell transplantation: cell loss, host Schwann cell replacement, and strategies to enhance survival." Glia **53**(3): 338-43.

Holcik, M., H. Gibson, et al. (2001). "XIAP: apoptotic brake and promising therapeutic target." Apoptosis **6**(4): 253-61.

Holcik, M. and N. Sonenberg (2005). "Translational control in stress and apoptosis." Nat Rev Mol Cell Biol **6**(4): 318-27.

Hong, S., D. Y. Hwang, et al. (2007). "Functional analysis of various promoters in lentiviral vectors at different stages of in vitro differentiation of mouse embryonic stem cells." Mol Ther **15**(9): 1630-9.

Horch, R. E., J. Kopp, et al. (2005). "Tissue engineering of cultured skin substitutes." J Cell Mol Med **9**(3): 592-608.

Houdebine, L. M. and J. Attal (1999). "Internal ribosome entry sites (IRESs): reality and use." Transgenic Res **8**(3): 157-77.

Huang, Y., Y. C. Park, et al. (2001). "Structural basis of caspase inhibition by XIAP: differential roles of the linker versus the BIR domain." Cell **104**(5): 781-90.

Hughes, S. M., F. Moussavi-Harami, et al. (2002). "Viral-mediated gene transfer to mouse primary neural progenitor cells." Mol Ther **5**(1): 16-24.

Iizuka, T., S. Kanzaki, et al. (2008). "Noninvasive in vivo delivery of transgene via adeno-associated virus into supporting cells of the neonatal mouse cochlea." Hum Gene Ther **19**(4): 384-90.

Ikeda, H., F. Osakada, et al. (2005). "Generation of Rx+/Pax6+ neural retinal precursors from embryonic stem cells." Proc Natl Acad Sci U S A **102**(32): 11331-6.

Jensen, A. M. and V. A. Wallace (1997). "Expression of Sonic hedgehog and its putative role as a precursor cell mitogen in the developing mouse retina." Development **124**(2): 363-71.

Kaufman, R. J., M. V. Davies, et al. (1991). "Improved vectors for stable expression of foreign genes in mammalian cells by use of the untranslated leader sequence from EMC virus." Nucleic Acids Res **19**(16): 4485-90.

Kerr, J. F., A. H. Wyllie, et al. (1972). "Apoptosis: a basic biological phenomenon with wide-ranging implications in tissue kinetics." Br J Cancer **26**(4): 239-57.

Kim, D., C. Jeon, et al. (2006). "Cytoplasmic transduction peptide (CTP): new approach for the delivery of biomolecules into cytoplasm in vitro and in vivo." Exp Cell Res **312**(8): 1277-88.

Kolb, H., E. Fernandez, et al. (2008). Webvision: The Organization of the Retina and Visual System, John Moran Eye Center, University of Utah.

Komeima, K., B. S. Rogers, et al. (2007). "Antioxidants slow photoreceptor cell death in mouse models of retinitis pigmentosa." J Cell Physiol **213**(3): 809-15.

Kominsky, D. J., R. J. Bickel, et al. (2002). "Reovirus-induced apoptosis requires mitochondrial release of Smac/DIABLO and involves reduction of cellular inhibitor of apoptosis protein levels." J Virol **76**(22): 11414-24.

Krammer, P. H. (2000). "CD95's deadly mission in the immune system." Nature **407**(6805): 789-95.

Krill, A. E. (1972). "Retinitis pigmentosa: a review." Sight Sav Rev **42**(1): 21-8.

Kumar, M., B. Keller, et al. (2001). "Systematic determination of the packaging limit of lentiviral vectors." Hum Gene Ther **12**(15): 1893-905.

Kutschka, I., T. Kofidis, et al. (2006). "Adenoviral human BCL-2 transgene expression attenuates early donor cell death after cardiomyoblast transplantation into ischemic rat hearts." Circulation **114**(1 Suppl): I174-80.

Lamba, D. A., M. O. Karl, et al. (2006). "Efficient generation of retinal progenitor cells from human embryonic stem cells." Proc Natl Acad Sci U S A **103**(34): 12769-74.

Landazuri, N. and J. M. Le Doux (2004). "Complexation of retroviruses with charged polymers enhances gene transfer by increasing the rate that viruses are delivered to cells." J Gene Med **6**(12): 1304-19.

Lee, C. I., D. B. Kohn, et al. (2004). "Morphological analysis and lentiviral transduction of fetal monkey bone marrow-derived mesenchymal stem cells." Mol Ther **9**(1): 112-23.

Leonard, K. C., D. Petrin, et al. (2007). "XIAP protection of photoreceptors in animal models of retinitis pigmentosa." PLoS ONE **2**(3): e314.

Leri, A., J. Kajstura, et al. (2008). "Myocardial regeneration and stem cell repair." Curr Probl Cardiol **33**(3): 91-153.

Leveillard, T., S. Mohand-Said, et al. (2004). "Identification and characterization of rod-derived cone viability factor." Nat Genet **36**(7): 755-9.

Lewis, J., E. Burstein, et al. (2004). "Uncoupling of the signaling and caspase-inhibitory properties of X-linked inhibitor of apoptosis." J Biol Chem **279**(10): 9023-9.

Lewis, S. M. and M. Holcik (2005). "IRES in distress: translational regulation of the inhibitor of apoptosis proteins XIAP and HIAP2 during cell stress." Cell Death Differ **12**(6): 547-53.

Li, W., N. Ma, et al. (2007). "Bcl-2 engineered MSCs inhibited apoptosis and improved heart function." Stem Cells **25**(8): 2118-27.

Liston, P., W. G. Fong, et al. (2003). "The inhibitors of apoptosis: there is more to life than Bcl2." Oncogene **22**(53): 8568-80.

Lu, F. Z., Y. Kitazawa, et al. (2005). "Long-term gene expression using the lentiviral vector in rat chondrocytes." Clin Orthop Relat Res **439**: 243-52.

Lu, X., L. Humeau, et al. (2004). "Safe two-plasmid production for the first clinical lentivirus vector that achieves >99% transduction in primary cells using a one-step protocol." J Gene Med **6**(9): 963-73.

MacLaren, R. E., R. A. Pearson, et al. (2006). "Retinal repair by transplantation of photoreceptor precursors." Nature **444**(7116): 203-7.

Maegele, M. and U. Schaefer (2008). "Stem cell-based cellular replacement strategies following traumatic brain injury (TBI)." Minim Invasive Ther Allied Technol **17**(2): 119-31.

Maguire, A. M., F. Simonelli, et al. (2008). "Safety and efficacy of gene transfer for Leber's congenital amaurosis." N Engl J Med **358**(21): 2240-8.

Maric, D. and J. L. Barker (2005). "Fluorescence-based sorting of neural stem cells and progenitors." Curr Protoc Neurosci **Chapter 3**: Unit 3 18.

Marigo, V. (2007). "Programmed cell death in retinal degeneration: targeting apoptosis in photoreceptors as potential therapy for retinal degeneration." Cell Cycle **6**(6): 652-5.

Nevins, T. A., Z. M. Harder, et al. (2003). "Distinct regulation of internal ribosome entry site-mediated translation following cellular stress is mediated by apoptotic fragments of eIF4G translation initiation factor family members eIF4GI and p97/DAP5/NAT1." J Biol Chem **278**(6): 3572-9.

Nicholls, J. G., A. R. Martin, et al. (2001). From Neuron To Brain. Sunderland, MA, Sinauer Associates, Inc.

Nicholson, D. W. (1999). "Caspase structure, proteolytic substrates, and function during apoptotic cell death." Cell Death Differ **6**(11): 1028-42.

O'Reilly, M., A. Palfi, et al. (2007). "RNA interference-mediated suppression and replacement of human rhodopsin in vivo." Am J Hum Genet **81**(1): 127-35.

Oltvai, Z. N., C. L. Milliman, et al. (1993). "Bcl-2 heterodimerizes in vivo with a conserved homolog, Bax, that accelerates programmed cell death." Cell **74**(4): 609-19.

Park, F. (2007). "Lentiviral vectors: are they the future of animal transgenesis?" Physiol Genomics **31**(2): 159-73.

Petrin, D., A. Baker, et al. (2003). "XIAP protects photoreceptors from n-methyl-n-nitrosourea-induced retinal degeneration." Adv Exp Med Biol **533**: 385-93.

Phelan, J. K. and D. Bok (2000). "A brief review of retinitis pigmentosa and the identified retinitis pigmentosa genes." Mol Vis **6**: 116-24.

Pierce, E. A. (2001). "Pathways to photoreceptor cell death in inherited retinal degenerations." Bioessays **23**(7): 605-18.

Poleshko, A., I. Palagin, et al. (2008). "Identification of cellular proteins that maintain retroviral epigenetic silencing: evidence for an antiviral response." J Virol **82**(5): 2313-23.

Rajcan-Separovic, E., P. Liston, et al. (1996). "Assignment of human inhibitor of apoptosis protein (IAP) genes xiap, hiap-1, and hiap-2 to chromosomes Xq25 and 11q22-q23 by fluorescence in situ hybridization." Genomics **37**(3): 404-6.

Ransdell, H. T., Jr., J. A. Haller, Jr., et al. (1965). "Renal Toxicity of Polybrene, (Hexadimethrine Bromide)." J Surg Res **5**: 195-9.

Raymond, S. M. and I. J. Jackson (1995). "The retinal pigmented epithelium is required for development and maintenance of the mouse neural retina." Curr Biol **5**(11): 1286-95.

Renwick, J., M. A. Narang, et al. (2006). "XIAP-mediated neuroprotection in retinal ischemia." Gene Ther **13**(4): 339-47.

Ribelin, W. E. (1984). "The effects of drugs and chemicals upon the structure of the adrenal gland." Fundam Appl Toxicol **4**(1): 105-19.

Ricks, D. M., R. Kutner, et al. (2008). "Optimized Lentiviral Transduction of Mouse Bone Marrow-Derived Mesenchymal Stem Cells." Stem Cells Dev.

Ross, M. H., L. J. Romrell, et al. (1995). Histology: A Text and Atlas. Baltimore, MA, Williams and Wilkins.

Salvetti, A., S. Oreve, et al. (1998). "Factors influencing recombinant adeno-associated virus production." Hum Gene Ther **9**(5): 695-706.

Schroder, A. R., P. Shinn, et al. (2002). "HIV-1 integration in the human genome favors active genes and local hotspots." Cell **110**(4): 521-9.

Schwarze, S. R., A. Ho, et al. (1999). "In vivo protein transduction: delivery of a biologically active protein into the mouse." Science **285**(5433): 1569-72.

Seaberg, R. M. and D. van der Kooy (2003). "Stem and progenitor cells: the premature desertion of rigorous definitions." Trends Neurosci **26**(3): 125-31.

Shapiro, A. M., J. R. Lakey, et al. (2000). "Islet transplantation in seven patients with type 1 diabetes mellitus using a glucocorticoid-free immunosuppressive regimen." N Engl J Med **343**(4): 230-8.

Sherman, W. (2007). "Myocyte replacement therapy: skeletal myoblasts." Cell Transplant **16**(9): 971-5.

Shiozaki, E. N., J. Chai, et al. (2003). "Mechanism of XIAP-mediated inhibition of caspase-9." Mol Cell **11**(2): 519-27.

Sigma-Aldrich (2007). CelLyticM C2978 Product Information Bulletin Sigma-Aldrich 1-2.

Smith-Arica, J. R., A. J. Thomson, et al. (2003). "Infection efficiency of human and mouse embryonic stem cells using adenoviral and adeno-associated viral vectors." Cloning Stem Cells **5**(1): 51-62.

Srivastava, A. (2005). "Hematopoietic stem cell transduction by recombinant adeno-associated virus vectors: problems and solutions." Hum Gene Ther **16**(7): 792-8.

Stachler, M. D. and J. S. Bartlett (2006). "Mosaic vectors comprised of modified AAV1 capsid proteins for efficient vector purification and targeting to vascular endothelial cells." Gene Ther **13**(11): 926-31.

Strasser, A., A. W. Harris, et al. (1995). "Bcl-2 and Fas/APO-1 regulate distinct pathways to lymphocyte apoptosis." Embo J **14**(24): 6136-47.

Surace, E. M., A. Auricchio, et al. (2003). "Delivery of adeno-associated virus vectors to the fetal retina: impact of viral capsid proteins on retinal neuronal progenitor transduction." J Virol **77**(14): 7957-63.

Szymanska, I. (2006). Screening of adeno-associated virus serotypes in search of the optimal vector for gene delivery to adult retinal stem cells., University of Ottawa. **B.Sc.:** 1-37.

Szymczyk, K. H., T. A. Freeman, et al. (2006). "Active caspase-3 is required for osteoclast differentiation." J Cell Physiol **209**(3): 836-44.

Thornberry, N. A. and Y. Lazebnik (1998). "Caspases: enemies within." Science **281**(5381): 1312-6.

Thornberry, N. A., T. A. Rano, et al. (1997). "A combinatorial approach defines specificities of members of the caspase family and granzyme B. Functional relationships established for key mediators of apoptosis." J Biol Chem **272**(29): 17907-11.

Tiscornia, G., O. Singer, et al. (2006). "Production and purification of lentiviral vectors." Nat Protoc **1**(1): 241-5.

Tortora, G. J. and S. R. Grabowski (2003). Principles of Anatomy & Physiology. Hoboken, NJ, John Wiley & Sons, Inc.

Tropepe, V., B. L. Coles, et al. (2000). "Retinal stem cells in the adult mammalian eye." Science **287**(5460): 2032-6.

Tsujimoto, Y., J. Cossman, et al. (1985). "Involvement of the bcl-2 gene in human follicular lymphoma." Science **228**(4706): 1440-3.

Vingolo, E. M., M. Rocco, et al. (2008). "Slowing the degenerative process, long lasting effect of hyperbaric oxygen therapy in retinitis pigmentosa." Graefes Arch Clin Exp Ophthalmol **246**(1): 93-8.

Vives, E., P. Brodin, et al. (1997). "A truncated HIV-1 Tat protein basic domain rapidly translocates through the plasma membrane and accumulates in the cell nucleus." J Biol Chem **272**(25): 16010-7.

Wadia, J. S. and S. F. Dowdy (2002). "Protein transduction technology." Curr Opin Biotechnol **13**(1): 52-6.

Wang, M., T. T. Lam, et al. (1997). "Expression of a mutant opsin gene increases the susceptibility of the retina to light damage." Vis Neurosci **14**(1): 55-62.

Wang, Y., G. D. Dakubo, et al. (2005). "Retinal ganglion cell-derived sonic hedgehog locally controls proliferation and the timing of RGC development in the embryonic mouse retina." Development **132**(22): 5103-13.

Wernig, M., J. P. Zhao, et al. (2008). "Neurons derived from reprogrammed fibroblasts functionally integrate into the fetal brain and improve symptoms of rats with Parkinson's disease." Proc Natl Acad Sci U S A **105**(15): 5856-61.

Wurzer, W. J., O. Planz, et al. (2003). "Caspase 3 activation is essential for efficient influenza virus propagation." Embo J **22**(11): 2717-28.

Xu, H., D. D. Sta Iglesia, et al. (2007). "Characteristics of progenitor cells derived from adult ciliary body in mouse, rat, and human eyes." Invest Ophthalmol Vis Sci **48**(4): 1674-82.

Zeiss, C. J., J. Neal, et al. (2004). "Caspase-3 in postnatal retinal development and degeneration." Invest Ophthalmol Vis Sci **45**(3): 964-70.

Zhang, B., H. Q. Xia, et al. (2001). "A highly efficient and consistent method for harvesting large volumes of high-titre lentiviral vectors." Gene Ther **8**(22): 1745-51.

Zhao, J. and A. M. Lever (2007). "Lentivirus-mediated gene expression." Methods Mol Biol **366**: 343-55.

Zhao, X., J. Liu, et al. (2002). "Differentiation of embryonic stem cells into retinal neurons." Biochem Biophys Res Commun **297**(2): 177-84.

Zhou, Y., J. Aran, et al. (1998). "Co-expression of human adenosine deaminase and multidrug resistance using a bicistronic retroviral vector." Hum Gene Ther **9**(3): 287-93.

APPENDIX 1

Sample Calculations

A1.1 Lentiviral Titre

Field of View #	Number of GFP-Positive Cells/Field of View	
	10^{-2} Dilution	10^{-3} Dilution
1	27	4
2	23	7
3	25	3
4	19	2
5	19	3
TOTAL	113	19

* GFP-positive cell = 1 transduction unit (TU)

1 field of view = 1 image
Image is 19.056 inches x 14.222 inches
3.02 inches in image = 100μm
∴ 1 inch = 33.11μm
∴ Image = 19.056 inches(33.11μm/inch) x 14.222 inches(33.11μm/inch)
= 631μm x 431μm
= (0.0631cm x 0.0471cm)
= 2.97×10^{-3} cm^2

5 fields of view have a total area of $5(2.97 \times 10^{-3}\ cm^2) = 1.49 \times 10^{-2}\ cm^2$
1 well of a 24-well plate has total area of 1.90 cm^2

At 10^{-2} Dilution:
Total of 113 GFP-positive cells (TU) in 5 fields of view.
∴ Number of TU in 1 well of 24-well plate:

$$\frac{113}{1.49 \times 10^{-2}\ cm^2} = \frac{x}{1.90\ cm^2}$$

x = 14410 TU in 1 well of 24-well plate.

There are 14410 TU diluted at 10^{-2} (100-fold) in 250μL of media.
∴ Number of TU in 1mL of undiluted viral preparation:

$$= \frac{14410\ TU \times 100\ \text{dilution factor}}{0.250mL}$$

$= 5.76 \times 10^6$ TU/mL

At 10^{-3} Dilution:
Total of 19 GFP-positive cells (TU) in 5 fields of view.
∴ Number of TU in 1 well of 24-well plate:

$$\frac{19}{1.49 \times 10^{-2}\ cm^2} = \frac{x}{1.90\ cm^2}$$

x = 2423 TU in 1 well of 24-well plate.

There are 2423 TU diluted at 10^{-3} (1000-fold) in 250μL of media.
∴ Number of TU in 1mL of undiluted viral preparation:

$$= \frac{2423\ TU \times 1000\ \text{dilution factor}}{0.250mL}$$

$= 9.69 \times 10^6$ TU/mL

FINAL TITRE (Mean of titre calculated at 10^{-2} and 10^{-3} dilution)
$= (5.76 \times 10^6\ TU/mL + 9.69 \times 10^6\ TU/mL)/2$
$= 7.72 \times 10^6$ TU/mL

A1.2 Lentiviral Infection Efficiency

In one field of view:

Number of GFP-Positive Cells = 326
Number of GFP-Negative Cells = 1132
Total Counted Nuclei = 1458

Infection Efficiency = $\frac{\text{Number of GFP-Positive Cells}}{\text{Total Counted Nuclei}} \times 100\%$

$= \frac{326}{1458} \times 100\%$

= 22.4%

A1.3 Percentage Dead Cells following Lentivira Infection

In one count:

Number of Dead (Blue) Cells = 19
Number of Live (Clear) Cells = 162
Number of Cells $\text{Total}_{(\text{Blue + Clear})}$ = 181

Percentage Dead Cells = $\frac{\text{Number of Dead (Blue) Cells}}{\text{Number of Cells Total}_{(\text{Blue + Clear})}} \times 100\%$

$= \frac{19}{181} \times 100\%$

= 10.50%

A1.4 Total Cell Ratio following Lentiviral Infection

Treatment	Mean Counted Total Cell Number
2x MOI 5.0PB	168000
2x MOI 7.5PB	146500
2x MOI 10.0PB	138500
Ctrl 10.0PB	185500
Ctrl 0.0PB	191000

Total Cell Ratio = $\frac{\text{Mean Counted Total Cell Number in Particular Treatment}}{\text{Mean Counted Total Cell Number in 0.0}\mu\text{g/mL Polybrene Control}}$

The total cell ratio in the 2x MOI 5.0PB treatment is:

Total Cell Ratio 2x MOI 5.0PB = $\frac{\text{Mean Counted Total Cell Number 2x MOI 5.0PB}}{\text{Mean Counted Total Cell Number Ctrl 0.0PB}}$

$= \frac{168000}{191000}$

= 0.880

The total cell ratio in the Ctrl 0.0PB treatment is:

Total Cell Ratio Ctrl 0.0PB = $\frac{\text{Mean Counted Total Cell Number Ctrl 0.0PB}}{\text{Mean Counted Total Cell Number Ctrl 0.0PB}}$

$= \frac{191000}{191000}$

= 1.000

A1.5 Percentage GFP-Positive Cells in TAT-eGFP Assay

In one field of view:

Number of GFP-Positive Cells = 68
Number of GFP-Negative Cells = 57
Total Counted Nuclei = 125

$$\textbf{\% GFP-Positive Cells} = \frac{\text{Number of GFP-Positive Cells}}{\text{Total Counted Nuclei}} \times 100\%$$

$$= \frac{68}{125} \times 100\%$$

$$= \mathbf{54.4\%}$$

APPENDIX 2

Basic Protocols

A2.1 TAT-Fusion Protein His Tag Purification

1. Innoculate 5mL of LB-Kanamycin with stock bacteria in glycerol.
2. Grow overnight at 37°C.
3. Inoculate overnight culture into 500mL LB + 0.5mM IPTG. Grow for ≥5 hours at 37°C with agitation.
4. Spin to recover pellet. Resuspend pellet in 20mL PBS to wash. Spin again to recover.
5. **Optional:** Discard supernatant and store pellet at -20°C for use at later time.
6. Resuspend pellet in 20mL Buffer Z.
7. Sonicate 3 times with 15s pulses. Avoid foaming. Allocate 50μL of suspension for SDS-PAGE.
8. Spin at 16,000g (~11,000rpm) for 10min at 4°C.
9. Keep supernatant and adjust to 20mM imidazole. Allocate 50μL of supernatant for SDS-PAGE.
10. Resuspend portion of pellet in 50μL of water and allocate small sample for SDS-PAGE.
11. Equilibrate column (Quiagen Ni-NTA, 8mL bed volume) in Buffer Z + 20mM imidazole.
12. Load supernatant onto column, drip through. Allocate 50μL of flow through for SDS-PAGE.
13. **Optional:** Load flow-through again. Allocate 50μL of second flow through for SDS-PAGE.
14. Wash with 10 bed volumes Buffer Z + 20mM imidazole.
15. Elute with 1 bed volume Buffer Z plus 500mM imidazole. Allocate 50μL of eluate or SDS-PAGE.
16. **Optional:** Elute in steps with 100, 250, 500mM and 1M imidazole in Buffer Z (recommended especially when testing new columns). Allocate 50μL of each eluate for SDS-PAGE. Will have to run gel and perform Coomassie staining to determine which fraction contains majority of protein.
17. **Optional:** Elution fractions can be kept at 4°C overnight for de-salting at later time.
18. When finished, wash column with 10 volumes 1M, then 10 bed volumes 20mM imidazole in Buffer Z prior to next use. Store column at 4°C.

Buffer Z
8M urea
100mM NaCl
20mM Hepes
(pH 8)

A2.2 Retinal Explant Generation and Culture

Before the experiment:

→ Make sure to have membranes ready.

1. Autoclave filter paper.
2. Inside laminar flow hood immerse individual membranes in 70% EtOH.
3. Lay out membranes on filter paper.
4. Spray with 70% EtOH and allow to dry.
5. When dry store under sterile conditions.

→ Make sure to have all necessary aliquots ready and that media is available.

Protocol:

* Entire experiment is conducted in dissecting hood.

1. Place pups (P0 or P1) in clean 100mm dish and spray with 70% EtOH.
2. Cut off head with scissors.
3. Place one pair of tweezers in the neural tube to hold the head.
4. With second pair of tweezers peel of skin and remove the eyes.
5. Place eyes in clean 60mm dish in CO_2-independent medium (GIBCO # 18045-088).
6. Under dissecting microscope, use two pairs of tweezers to rip open the eye cup starting hole left from optic nerve.
7. Separate retina + lens from RPE and transfer RPE to waste plate.
8. In a clean 100mm plate place a membrane (Diameter: 13mm, Pore Size: 0.8μm, Whatman #110409) shiny side down using separate pair of clean tweezers.
9. Transfer one retina + lens using a pasteur pipette onto the membrane. (Take only a small amount of solution to facilitate the manipulation.) Make sure the lens is facing up.
10. Using one pair of tweezers hold the retina down and remove the lens using another pair of tweezers. (Remove the lens using flat side of tweezers and not the point as to not rip the retina.) Discard the lens.
11. Since the retina is cup shaped, it has to be cut in four places along the periphery. (The retina is fragile and can be cut with the tweezers). Leave the middle connected.
12. Spread out the retina along the membrane using the tweezers. (As long as retina + lens were initially arranged with lens up, the photoreceptor side is now facing down and the ganglion cells are facing up).
13. Once the retina is spread out on the membrane, remove excess solution using two pairs of forceps.
14. Transfer the membrane containing the retina into one well of a 24-well plate containing 0.5mL CO_2-independent medium.
15. In a laminar flow hood, change the medium by pipetting away old medium and replacing 0.5mL with fresh retinal explant culture medium (RECM).
16. Incubate at 37°C with 8% CO_2.
17. Refresh medium every 3-4 days.

Solutions:

Retinal Explant Culture Medium

DMEM	10mL	(GIBCO #10569-010)
F12	10mL	(Sigma #N6658)
Sato's	200μL	(See below)
5mg/mL Insulin	40μL	(Sigma #I6634)
12mg/mL N-acetyl-L-cysteine	100μL	(Sigma #A9165)
10mg/mL Gentamicin	20μL	(GIBCO #15710-064)

Sato's

Apo-transferrin	10mg/mL	(Sigma #T1147)
BSA	10mg/mL	(Sigma #A4161)
Progesterone	6μg/mL	(Sigma #P8783)
* Prepare in 100% EtOH first.		
Putrescine	1.6mg/mL	(Sigma #P7505)
Sodium Selenite	4μg/mL	(Sigma #S5261)
* Make 4mg/mL solution in 0.1NaOH first.		

* Prepare Sato's solution in CO_2-independent Medium (GIBCO #18045-088). Make 210μL aliquots and store at -20°C for later use.

A2.3 Indirect Immunohitochemistry on Fixed Cells

1. After fixing cells, aspirate PBS from wells and do one quick wash with 1mL fresh PBS/well.
2. Aspirate PBS.
3. Block each well with 200μL blocking solution (1% BSA and 5% appropriate serum in PBS) for 15-30min at room temperature.
4. Add 200μL of 1° antibody diluted in blocking solution + 0.3% Triton-X 100.
5. Seal plate with parafilm and incubate overnight at 4°C.
6. Wash with blocking solution 3 times for 2min.
7. Dry by aspiration.
8. Add 200µL 2° antibody diluted in PBS for 60min at room temperature.
9. Wash with PBS 3 times for 2min.
10. Add 200μL of DAPI diluted 1:10,000 in PBS and incubate for 3min.
11. Wash with PBS 2 times for 3min.
12. Aspirate media and add 200μL anti-fade/well.
13. Seal plate with parafilm and store long-term at +4°C.

A2.4 Direct Immunohitochemistry on Fixed Cells

1. After fixing cells, aspirate PBS from wells and do one quick wash with 1mL fresh PBS/well.
2. Remove PBS.
3. Incubate with blocking solution (5% FBS in PBS) for 30 min at room temperature.
4. Incubate with antibody in blocking solution + 0.3% Triton-X overnight at +4°C.
5. Wash twice with blocking solution for 5 min.
6. Rinse once with PBS.
7. Incubate with 1:10,000 DAPI solution in PBS for 3 min.
8. Wash twice with PBS for 3 min.
9. Overaly with antifade, seal plate with Parafilm.
10. Store at +4°C long-term.

A2.5 Indirect Immunohistochemistry on Cryosections

1. Remove chosen slides from -20°C storage and let sit at room temperature for 30min.
2. Dip slides in ddH_2O.
3. Lie slides flat on a piece of paper towel and leave for 2min.
4. Dip slides in 4%PFA for 5min.
5. Dip slides in TBS to wash and then do 2 fresh washes in TBS for 5min.
6. Block each slide with 200µL blocking solution (1% BSA and 5% appropriate serum in PBS). Cover with parafilm and incubate in humidified chamber for 15-30min at room temperature.
7. Add 1° antibody diluted in blocking solution + 0.3% Triton-X 100. Cover with parafilm and incubate overnight in humidified chamber at +4°C.
8. Wash 3 times by dipping in fresh TBS for 2min each.
9. Add 2° antibody diluted in TBS and incubate for 60min at room temperature in humidified chamber.
10. Wash 3 times by dipping in fresh TBS for 2min each.
11. Add 200µL of DAPI diluted 1:10,000 in TBS. Incubate for 3min in humidified chamber at room temperature.
12. Wash 2 times by dipping in fresh TBS for 3min each.
13. Prepare coverslips ready with antifade.
14. Remove excess TBS from slide by blotting son Kimwipe and place coverslip over sections.
15. Seal coverslip onto slide with nail polish.
16. Store long-term at +4°C.

APPENDIX 3

Raw Data

A3.1 Infection Efficiency Data for HIV1-GFP Infection of Hh-RPCs

A3.1.1 24 Hours

HIV1-GFP 24Hrs Experiment #1

Trx	[PB] (μg/mL)	Field of View	# GFP-Positive Cells	# GFP-Negative Cells	# Cells Total	Infection Efficiency (% GFP-Positive Cells)
2x MOI	5.0μg/mL	1	93	700	793	11.7
		2	93	647	740	12.6
		3	112	734	847	13.2
		4	105	794	899	11.7
		5	85	618	703	12.1
		MEAN ± Standard Deviation				12.26 ± 0.64
2x MOI	7.5μg/mL	1	177	642	819	21.6
		2	197	619	813	24.1
		3	178	576	754	23.6
		4	152	555	707	21.5
		5	171	547	718	23.8
		MEAN ± Standard Deviation				22.92 ± 1.26
2x MOI	10.0μg/mL	1	262	457	719	36.4
		2	256	556	812	31.5
		3	260	574	834	31.2
		4	251	468	719	34.2
		5	251	488	739	34.0
		MEAN ± Standard Deviation				33.60 ± 2.23

HIV1-GFP 24Hrs Experiment #2

Trx	[PB] (μg/mL)	Field of View	# GFP-Positive Cells	# GFP-Negative Cells	# Cells Total	Infection Efficiency (% GFP-Positive Cells)
2x MOI	5.0μg/mL	1	87	371	458	19.0
		2	84	379	463	18.1
		3	72	345	417	17.3
		4	74	341	415	17.8
		5	66	287	353	18.7
		MEAN ± Standard Deviation				18.18 ± 0.68
2x MOI	7.5μg/mL	1	105	330	435	24.1
		2	118	355	473	24.9
		3	122	387	509	24.0
		4	128	398	526	24.3
		5	160	460	620	25.8
		MEAN ± Standard Deviation				24.62 ± 0.75
2x MOI	10.0μg/mL	1	128	232	360	35.6
		2	109	212	321	34.0
		3	120	249	369	32.5
		4	174	327	501	34.7
		5	92	232	524	28.4
		MEAN ± Standard Deviation				33.04 ± 2.83

HIV1-GFP 24Hrs Experiment #3

Trx	[PB] (μg/mL)	Field of View	# GFP-Positive Cells	# GFP-Negative Cells	# Cells Total	Infection Efficiency (% GFP-Positive Cells)
2x MOI	5.0μg/mL	1	85	478	563	15.1
		2	111	580	691	16.1
		3	106	514	620	17.1
		4	61	426	487	12.5
		5	124	535	659	18.8
		MEAN ± Standard Deviation				15.92 ± 2.31
2x MOI	7.5μg/mL	1	181	560	741	24.4
		2	204	595	799	25.5
		3	191	648	839	22.8
		4	210	574	784	26.8
		5	241	631	872	27.6
		MEAN ± Standard Deviation				25.42 ± 1.91
2x MOI	10.0μg/mL	1	206	448	654	31.5
		2	225	421	646	34.8
		3	208	400	608	34.2
		4	229	487	716	32.0
		5	201	515	716	28.1
		MEAN ± Standard Deviation				32.12 ± 2.65

Summary:

Experiment #	Mean Infection Efficiency at 2x MOI 5.0μg/mL Polybrene (%)	Mean Infection Efficiency at 2x MOI 7.5μg/mL Polybrene (%)	Mean Infection Efficiency at 2x MOI 10.0μg/mL Polybrene (%)
1	12.26	22.92	33.46
2	18.18	24.62	33.04
3	15.92	25.42	32.12

Single Factor ANOVA:

Summary:

Groups	*Count*	*Sum*	*Average*	*Variance*
5.0PB	3	46.36	15.45333	8.924933
7.5PB	3	72.96	24.32	1.63
10.0PB	3	98.62	32.87333	0.469733

ANOVA:

Source of Variation	*SS*	*df*	*MS*	*F*	*P-value*	*F crit*
Between Groups	455.2337	2	227.6168	61.93843	9.86E-05	5.143253
Within Groups	22.04933	6	3.674889			
Total	477.283	8				

A3.1.2 48 Hours

HIV1-GFP 48Hrs Experiment #1

Trx	[PB] (μg/mL)	Field of View	# GFP-Positive Cells	# GFP-Negative Cells	# Cells Total	Infection Efficiency (% GFP-Positive Cells)
2x MOI	5.0μg/mL	1	70	346	416	16.8
		2	85	384	469	18.1
		3	94	429	523	18.0
		4	101	419	520	19.4
		5	81	425	506	16.0
		MEAN ± Standard Deviation				17.66 ± 1.31
2x MOI	7.5μg/mL	1	91	351	442	20.6
		2	116	440	556	26.4
		3	145	352	497	29.2
		4	104	366	470	22.1
		5	87	286	373	23.3
		MEAN ± Standard Deviation				24.32 ± 3.46
2x MOI	10.0μg/mL	1	109	217	326	33.4
		2	108	209	317	34.1
		3	117	200	317	36.9
		4	104	184	288	36.1
		5	105	224	329	31.9
		MEAN ± Standard Deviation				34.48 ± 2.03

HIV1-GFP 48Hrs Experiment #2

Trx	[PB] (μg/mL)	Field of View	# GFP-Positive Cells	# GFP-Negative Cells	# Cells Total	Infection Efficiency (% GFP-Positive Cells)
2x MOI	5.0μg/mL	1	199	914	1113	17.9
		2	208	781	989	21.0
		3	167	719	886	18.8
		4	183	707	890	20.6
		5	189	615	754	18.4
		MEAN ± Standard Deviation				19.34 ± 1.38
2x MOI	7.5μg/mL	1	238	813	1051	22.6
		2	263	823	1086	24.2
		3	249	781	1030	24.2
		4	260	854	1114	23.3
		5	210	862	1072	19.6
		MEAN ± Standard Deviation				22.78 ± 1.90
2x MOI	10.0μg/mL	1	316	787	1103	28.6
		2	249	766	1015	24.5
		3	269	723	992	27.1
		4	255	730	985	25.9
		5	286	650	936	30.6
		MEAN ± Standard Deviation				27.34 ± 2.38

HIV1-GFP 48Hrs Experiment #3						
Trx	**[PB] (μg/mL)**	**Field of View**	**# GFP-Positive Cells**	**# GFP-Negative Cells**	**# Cells Total**	**Infection Efficiency (% GFP-Positive Cells)**
2x MOI	5.0μg/mL	1	204	940	1144	17.8
		2	223	1007	1230	18.1
		3	215	961	1176	18.3
		4	188	880	1068	17.6
		5	193	906	1099	17.6
		MEAN ± Standard Deviation				17.88 ± 0.31
2x MOI	7.5μg/mL	1	282	838	1120	25.2
		2	291	951	1242	23.4
		3	249	804	1053	23.6
		4	224	730	954	23.5
		5	253	801	1054	24.0
		MEAN ± Standard Deviation				23.94 ± 0.74
2x MOI	10.0μg/mL	1	256	681	937	27.3
		2	335	796	1131	29.6
		3	334	740	1072	31.2
		4	372	761	1133	32.8
		5	319	687	1006	31.7
		MEAN ± Standard Deviation				30.52 ± 2.14

Summary:

Experiment #	Mean Infection Efficiency at 2x MOI 5.0μg/mL Polybrene (%)	Mean Infection Efficiency at 2x MOI 7.5μg/mL Polybrene (%)	Mean Infection Efficiency at 2x MOI 10.0μg/mL Polybrene (%)
1	17.88	23.94	30.52
2	17.66	24.32	34.48
3	19.34	22.78	27.34

Single Factor ANOVA:

Summary:

Groups	*Count*	*Sum*	*Average*	*Variance*
5.0PB	3	54.88	18.29333	0.833733
7.5PB	3	71.04	23.68	0.6436
10.0PB	3	92.34	30.78	12.7956

ANOVA:

Source of Variation	*SS*	*df*	*MS*	*F*	*P-value*	*F crit*
Between Groups	235.343	2	117.6715	24.73315	0.001266	5.143253
Within Groups	28.54587	6	4.757644			
Total	263.8889	8				

A3.1.3 Comparison of 24hr to 48hr Infection Efficiency

Two-Tailed Student's T-Test:

Experiment #	Mean Infection Efficiency 24 Hours after Infection (%)	Mean Infection Efficiency 48 Hours after Infection (%)	P-Value
5.0μg/mL Polybrene			
1	12.26	17.88	0.236581
2	18.18	17.66	
3	15.92	19.34	
7.5μg/mL Polybrene			
1	22.92	23.94	0.510135
2	24.62	24.32	
3	25.42	22.78	
10.0μg/mL Polybrene			
1	33.46	30.52	0.418194
2	33.04	34.48	
3	32.12	27.34	

A3. 2 Infection Efficiency Data for HIV1-XIAP/GFP Infection of Hh-RPCs

A3.2.1 24 Hours

HIV1-XIAP/GFP 24Hrs Experiment #1

Trx	[PB] (μg/mL)	Field of View	# GFP-Positive Cells	# GFP-Negative Cells	# Cells Total	Infection Efficiency (% GFP-Positive Cells)
1.5x MOI	5.0μg/mL	1	116	602	718	16.2
		2	121	620	741	16.3
		3	109	612	721	15.1
		4	129	610	739	17.5
		5	110	668	778	14.1
		MEAN ± Standard Deviation				15.84 ± 1.29
1.5x MOI	7.5μg/mL	1	189	809	998	18.9
		2	201	679	880	22.8
		3	187	572	759	24.6
		4	186	642	828	22.5
		5	167	563	730	22.9
		MEAN ± Standard Deviation				22.34 ± 2.09
1.5x MOI	10.0μg/mL	1	239	488	727	32.9
		2	285	525	810	35.2
		3	259	576	835	31.0
		4	243	513	756	32.1
		5	247	501	748	33.0
		MEAN ± Standard Deviation				32.84 ± 1.54

HIV1-XIAP/GFP 24Hrs Experiment #2

Trx	[PB] (μg/mL)	Field of View	# GFP-Positive Cells	# GFP-Negative Cells	# Cells Total	Infection Efficiency (% GFP-Positive Cells)
1.5x MOI	5.0μg/mL	1	214	996	1180	18.1
		2	167	994	1161	14.4
		3	179	1002	1181	15.2
		4	207	1091	1298	15.9
		5	156	1080	1236	12.6
		MEAN ± Standard Deviation				15.23 ± 2.02
1.5x MOI	7.5μg/mL	1	224	988	1212	18.5
		2	177	863	1040	17.0
		3	225	862	1087	20.7
		4	230	743	973	23.6
		5	226	987	1213	18.6
		MEAN ± Standard Deviation				19.68 ± 2.56
1.5x MOI	10.0μg/mL	1	283	726	1019	27.7
		2	247	776	1023	24.1
		3	239	797	1036	23.1
		4	344	757	1101	31.2
		5	262	835	1097	23.9
		MEAN ± Standard Deviation				26.00 ± 3.40

HIV1-XIAP/GFP 24Hrs Experiment #3

Trx	[PB] (μg/mL)	Field of View	# GFP-Positive Cells	# GFP-Negative Cells	# Cells Total	Infection Efficiency (% GFP-Positive Cells)
1.5x MOI	5.0μg/mL	1	204	1179	1383	14.8
		2	135	1010	1145	11.8
		3	217	1167	1384	15.7
		4	175	1248	1423	12.3
		5	203	1194	1397	14.5
		MEAN ± Standard Deviation				13.82 ± 1.68
1.5x MOI	7.5μg/mL	1	222	1133	1355	16.4
		2	260	1247	1507	17.3
		3	198	1000	1198	16.5
		4	211	1093	1304	16.2
		5	206	1012	1218	16.9
		MEAN ± Standard Deviation				16.66 ± 0.44
1.5x MOI	10.0μg/mL	1	232	915	1147	20.2
		2	285	1125	1410	20.2
		3	308	1051	1359	22.7
		4	197	797	994	19.8
		5	279	1110	1389	20.1
		MEAN ± Standard Deviation				20.60 ± 1.19

Summary:

Experiment #	Mean Infection Efficiency at 1.5x MOI 5.0μg/mL Polybrene (%)	Mean Infection Efficiency at 1.5x MOI 7.5μg/mL Polybrene (%)	Mean Infection Efficiency at 1.5x MOI 10.0μg/mL Polybrene (%)
1	15.24	19.68	26
2	15.84	22.34	32.84
3	13.82	16.66	20.6

Single Factor ANOVA:

Summary:

Groups	*Count*	*Sum*	*Average*	*Variance*
5.0PB	3	44.9	14.96667	1.076133
7.5PB	3	58.68	19.56	8.0764
10.0PB	3	79.44	26.48	37.6272

ANOVA:

Source of Variation	*SS*	*df*	*MS*	*F*	*P-value*	*F crit*
Between Groups	201.542	2	100.771	6.462477	0.031868	5.143249
Within Groups	93.55947	6	15.59324			
Total	295.1014	8				

A3.2.2 48 Hours

HIV1-XIAP/GFP 48Hrs Experiment #1

Trx	[PB] (μg/mL)	Field of View	# GFP-Positive Cells	# GFP-Negative Cells	# Cells Total	Infection Efficiency (% GFP-Positive Cells)
1.5x MOI	5.0μg/mL	1	281	1235	1516	18.5
		2	214	1022	1236	17.3
		3	165	848	1013	16.3
		4	202	1109	1311	15.4
		5	211	1039	1250	16.9
		MEAN ± Standard Deviation				16.88 ± 1.15
1.5x MOI	7.5μg/mL	1	297	1136	1410	19.4
		2	284	911	1174	22.4
		3	251	1124	1421	20.9
		4	284	1053	1337	21.2
		5	251	991	1242	20.2
		MEAN ± Standard Deviation				20.82 ± 1.12
1.5x MOI	10.0μg/mL	1	282	1011	1293	21.9
		2	272	898	1170	23.2
		3	330	1085	1415	23.3
		4	270	896	1166	23.2
		5	268	967	1235	21.7
		MEAN ± Standard Deviation				22.6 ± 0.79

HIV1-XIAP/GFP 48Hrs Experiment #2

Trx	[PB] (μg/mL)	Field of View	# GFP-Positive Cells	# GFP-Negative Cells	# Cells Total	Infection Efficiency (% GFP-Positive Cells)
1.5x MOI	5.0μg/mL	1	210	1044	1254	16.7
		2	224	1183	1407	15.9
		3	224	1028	1252	17.9
		4	219	1079	1293	16.9
		5	210	1003	1213	17.3
		MEAN ± Standard Deviation				16.94 ± 0.74
1.5x MOI	7.5μg/mL	1	239	905	1144	20.9
		2	175	748	1013	17.3
		3	138	650	788	17.5
		4	208	773	981	21.2
		5	186	876	1062	17.5
		MEAN ± Standard Deviation				18.88 ± 1.99
1.5x MOI	10.0μg/mL	1	267	903	1170	22.8
		2	305	717	1022	29.8
		3	297	745	1042	28.5
		4	296	968	1264	23.4
		5	298	821	1119	26.6
		MEAN ± Standard Deviation				26.22 ± 3.08

HIV1-XIAP/GFP 48Hrs Experiment #3

Trx	[PB] (μg/mL)	Field of View	# GFP-Positive Cells	# GFP-Negative Cells	# Cells Total	Infection Efficiency (% GFP-Positive Cells)
1.5x MOI	5.0μg/mL	1	60	374	434	13.8
		2	79	419	498	15.9
		3	71	391	462	15.4
		4	101	467	568	17.8
		5	89	516	605	14.7
		MEAN ± Standard Deviation				15.52 ± 1.52
1.5x MOI	7.5μg/mL	1	87	392	479	18.2
		2	109	366	475	22.9
		3	83	404	487	17.0
		4	91	363	454	22.0
		5	84	342	426	19.7
		MEAN ± Standard Deviation				19.56 ± 2.22
1.5x MOI	10.0μg/mL	1	104	406	510	20.4
		2	119	391	510	23.3
		3	126	530	656	19.2
		4	133	424	557	23.9
		5	132	485	617	24.1
		MEAN ± Standard Deviation				21.64 ± 1.96

Summary:

Experiment #	Mean Infection Efficiency at 1.5x MOI 5.0μg/mL Polybrene (%)	Mean Infection Efficiency at 1.5x MOI 7.5μg/mL Polybrene (%)	Mean Infection Efficiency at 1.5x MOI 10.0μg/mL Polybrene (%)
1	16.94	18.88	26.22
2	16.88	20.82	22.66
3	15.52	19.56	21.64

Single Factor ANOVA:

Summary:

Groups	*Count*	*Sum*	*Average*	*Variance*
5.0PB	3	49.34	16.44667	0.644933
7.5PB	3	59.26	19.75333	0.968933
10.0PB	3	70.52	23.50667	5.781733

ANOVA:

Source of Variation	*SS*	*df*	*MS*	*F*	*P-value*	*F crit*
Between Groups	74.86516	2	37.43258	15.1844	0.00449	5.143253
Within Groups	14.7912	6	2.4652			
Total	89.65636	8				

A3.2.3 Comparison of 24hr to 48hr Infection Efficiency

Two-Tailed Student's T-Test:

Experiment #	**Mean Infection Efficiency 24 Hours after Infection (%)**	**Mean Infection Efficiency 48 Hours after Infection (%)**	**P-Value**
5.0μg/mL Polybrene			
1	15.24	16.94	0.126836
2	15.84	16.88	
3	13.82	15.52	
7.5μg/mL Polybrene			
1	19.68	18.88	0.919746
2	22.34	20.82	
3	16.66	19.56	
10.0μg/mL Polybrene			
1	26.00	26.22	0.499321
2	32.84	22.66	
3	20.60	21.64	

A3.3 Live Count Data for HIV1-GFP Infection of Hh-RPCs

A3.3.1 24 Hours

HIV1-GFP Experiment #1

Trx	[PB] (μg/mL)	Count	# Blue (Dead) Cells	# Clear (Live) Cells	# Cells Total	% Dead Cells	# Cells TOT/ # Cells 0.0PB Ctrl
2x MOI	5.0μg/mL Polybrene	1	8	66	74	10.81	
		2	8	56	64	12.50	
		3	9	67	76	11.84	
		4	9	64	73	12.33	
		MEAN			71.75	11.87	0.661
2x MOI	7.5μg/mL Polybrene	1	9	60	69	13.04	
		2	8	66	74	10.81	
		3	9	71	80	11.25	
		4	11	65	76	14.47	
		MEAN			74.75	12.39	0.689
2x MOI	10μg/mL Polybrene	1	14	64	78	17.95	
		2	13	68	81	16.05	
		3	15	68	93	18.07	
		4	16	74	90	17.78	
		MEAN			83.0	17.46	0.765
Ctrl	10μg/mL Polybrene	1	2	90	92	2.17	
		2	3	93	96	3.12	
		3	7	97	104	6.73	
		4	5	92	97	5.15	
		MEAN			97.25	4.30	0.896
Ctrl	0.0μg/mL Polybrene	1	6	105	111	5.41	
		2	5	103	108	4.63	
		3	3	102	105	2.76	
		4	4	106	110	3.64	
		MEAN			108.5	4.13	1.000

HIV1-GFP Experiment #2

Trx	[PB] (μg/mL)	Count	# Blue (Dead) Cells	# Clear (Live) Cells	# Cells Total	% Dead Cells	# Cells TOT/ # Cells 0.0PB Ctrl
2x MOI	5.0μg/mL Polybrene	1	10	71	81	12.35	
		2	9	75	84	10.71	
		3	4	74	78	5.13	
		4	6	80	86	6.98	
		MEAN			82.25	8.79	0.761
2x MOI	7.5μg/mL Polybrene	1	9	74	83	10.84	
		2	9	90	99	9.09	
		3	7	86	93	7.53	
		4	6	92	98	6.12	
		MEAN			93.25	8.40	0.863
2x MOI	10μg/mL Polybrene	1	14	75	89	15.73	
		2	12	69	81	14.81	
		3	13	68	81	16.05	
		4	11	71	82	13.41	
		MEAN			83.25	15.00	0.771
Ctrl	10μg/mL Polybrene	1	8	97	105	7.62	
		2	8	94	102	7.83	
		3	10	102	112	8.93	
		4	8	94	102	7.84	
		MEAN			105.25	8.06	0.975
Ctrl	0.0μg/mL Polybrene	1	4	111	115	3.45	
		2	7	105	112	6.25	
		3	1	99	100	1.00	
		4	3	102	105	2.86	
		MEAN			108.0	3.40	1.000

HIV1-GFP Experiment #3							
Trx	[PB] (μg/mL)	Count	# Blue (Dead) Cells	# Clear (Live) Cells	# Cells Total	% Dead Cells	# Cells TOT/ # Cells 0.0PB Ctrl
2x MOI	5.0μg/mL Polybrene	1	7	92	99	7.07	
		2	8	98	106	7.55	
		3	7	83	90	7.78	
		4	10	102	112	8.93	
		MEAN			101.75	7.83	0.906
2x MOI	7.5μg/mL Polybrene	1	11	80	91	12.09	
		2	12	89	101	11.88	
		3	11	84	95	11.58	
		4	9	90	99	9.09	
		MEAN			96.5	11.16	0.860
2x MOI	10μg/mL Polybrene	1	14	79	93	15.05	
		2	17	80	97	17.52	
		3	14	83	97	14.43	
		4	15	81	96	15.62	
		MEAN			95.75	15.66	0.853
Ctrl	10μg/mL Polybrene	1	12	103	115	10.43	
		2	11	97	108	10.19	
		3	10	97	107	9.35	
		4	13	100	113	11.50	
		MEAN			110.75	10.37	0.987
Ctrl	0.0μg/mL Polybrene	1	7	105	112	6.25	
		2	10	107	117	8.55	
		3	8	99	107	7.48	
		4	9	104	113	7.96	
		MEAN			112.25	7.56	1.000

Student's Two-Tailed T-Test (Comparing Percentage of Dead Cells):

Category 1		Category 2		P-Value
2x MOI 5.0PB		**Ctrl 0.0PB**		
1	11.87	1	4.13	0.065179
2	8.79	2	3.40	
3	7.83	3	7.56	
2x MOI 7.5PB		**Ctrl 0.0PB**		
1	12.39	1	4.13	0.032441
2	8.40	2	3.40	
3	11.16	3	7.56	
2x MOI 10.0PB		**Ctrl 0.0PB**		
1	17.46	1	4.13	0.004061
2	15.00	2	3.40	
3	15.66	3	7.56	
Ctrl 10.0PB		**Ctrl 0.0PB**		
1	4.30	1	4.13	0.314292
2	8.06	2	3.40	
3	10.37	3	7.56	

Student's Two-Tailed T-Test (Comparing Total Cell Ratio):

Category 1		Category 2		P-Value
2x MOI 5.0PB		**Ctrl 0.0PB**		
1	0.661	1	1.000	0.087746
2	0.761	2	1.000	
3	0.906	3	1.000	
2x MOI 7.5PB		**Ctrl 0.0PB**		
1	0.689	1	1.000	0.076355
2	0.863	2	1.000	
3	0.860	3	1.000	
2x MOI 10.0PB		**Ctrl 0.0PB**		
1	0.765	1	1.000	0.020381
2	0.771	2	1.000	
3	0.856	3	1.000	
Ctrl 10.0PB		**Ctrl 0.0PB**		
1	0.765	1	1.000	0.239128
2	0.771	2	1.000	
3	0.856	3	1.000	

A3.3.2 48 Hours

HIV1-GFP Experiment #1

Trx	[PB] (μg/mL)	Count	# Blue (Dead) Cells	# Clear (Live) Cells	# Cells Total	% Dead Cells	# Cells TOT/ # Cells 0.0PB Ctrl
2x MOI	5.0μg/mL Polybrene	1	18	68	86	20.93	
		2	12	69	81	14.81	
		3	13	70	83	15.66	
		4	13	73	86	15.12	
		MEAN			84.0	16.63	0.880
2x MOI	7.5μg/mL Polybrene	1	16	55	71	22.54	
		2	17	60	77	22.08	
		3	15	55	70	21.43	
		4	16	59	75	21.33	
		MEAN			73.25	21.84	0.767
2x MOI	10μg/mL Polybrene	1	16	57	73	21.92	
		2	17	53	71	24.29	
		3	18	51	69	26.09	
		4	15	50	65	23.08	
		MEAN			69.25	23.84	0.725
Ctrl	10μg/mL Polybrene	1	10	79	89	11.24	
		2	15	81	96	15.62	
		3	13	80	93	13.99	
		4	9	84	93	9.68	
		MEAN			92.75	12.63	0.971
Ctrl	0.0μg/mL Polybrene	1	9	81	90	10.0	
		2	10	86	96	10.42	
		3	8	92	100	8.0	
		4	6	90	96	6.25	
		MEAN			95.5	8.67	1.000

HIV1-GFP Experiment #2

Trx	[PB] (μg/mL)	Count	# Blue (Dead) Cells	# Clear (Live) Cells	# Cells Total	% Dead Cells	# Cells TOT/ # Cells 0.0PB Ctrl
2x MOI	5.0μg/mL Polybrene	1	25	127	152	16.45	
		2	23	136	159	14.47	
		3	25	132	158	15.92	
		4	27	161	188	14.36	
		MEAN			164.0	15.30	0.865
2x MOI	7.5μg/mL Polybrene	1	29	113	142	20.42	
		2	24	114	138	17.39	
		3	28	123	151	18.54	
		4	24	130	154	15.58	
		MEAN			146.25	17.99	0.772
2x MOI	10μg/mL Polybrene	1	34	121	155	21.94	
		2	28	112	140	20.00	
		3	32	102	134	23.88	
		4	30	106	136	22.06	
		MEAN			141.25	21.97	0.745
Ctrl	10μg/mL Polybrene	1	17	166	183	9.29	
		2	22	163	185	11.89	
		3	21	168	189	11.11	
		4	24	159	183	13.11	
		MEAN			185.0	11.35	0.976
Ctrl	0.0μg/mL Polybrene	1	15	174	189	7.94	
		2	15	176	191	7.85	
		3	17	165	182	9.34	
		4	18	178	196	9.18	
		MEAN			189.5	8.58	1.000

HIV1-GFP Experiment #3

Trx	[PB] (μg/mL)	Count	# Blue (Dead) Cells	# Clear (Live) Cells	# Cells Total	% Dead Cells	# Cells TOT/ # Cells 0.0PB Ctrl
2x MOI	5.0μg/mL Polybrene	1	15	152	167	8.98	
		2	20	139	159	12.58	
		3	14	149	163	8.59	
		4	17	156	173	9.83	
		MEAN			165.5	9.99	0.840
2x MOI	7.5μg/mL Polybrene	1	22	132	154	14.29	
		2	24	144	168	14.29	
		3	27	144	171	15.79	
		4	24	132	156	15.38	
		MEAN			162.25	14.94	0.824
2x MOI	10μg/mL Polybrene	1	34	118	152	22.37	
		2	33	115	148	22.30	
		3	32	119	151	21.19	
		4	37	129	166	22.29	
		MEAN			154.25	22.04	0.783
Ctrl	10μg/mL Polybrene	1	17	188	205	8.29	
		2	14	178	192	7.29	
		3	22	171	193	11.40	
		4	19	173	192	9.90	
		MEAN			195.5	9.22	0.992
Ctrl	0.0μg/mL Polybrene	1	11	186	197	5.58	
		2	15	179	194	7.73	
		3	20	198	218	9.17	
		4	17	162	179	8.50	
		MEAN			197.0	8.00	1.000

Student's Two-Tailed T-Test (Comparing Percentage of Dead Cells):

Category 1		Category 2		P-Value
2x MOI 5.0PB		**Ctrl 0.0PB**		
1	16.63	1	8.67	0.109413
2	15.3	2	8.53	
3	9.99	3	8.00	
2x MOI 7.5PB		**Ctrl 0.0PB**		
1	21.84	1	8.67	0.037446
2	17.99	2	8.53	
3	14.94	3	8.00	
2x MOI 10.0PB		**Ctrl 0.0PB**		
1	23.84	1	8.67	0.000723
2	21.97	2	8.53	
3	22.04	3	8.00	
Ctrl 10.0PB		**Ctrl 0.0PB**		
1	12.63	1	8.67	0.110027
2	11.35	2	8.53	
3	9.22	3	8.00	

Student's Two-Tailed T-Test (Comparing Total Cell Ratio):

Category 1		Category 2		P-Value
2x MOI 5.0PB		**Ctrl 0.0PB**		
1	0.880	1	1.000	0.007038
2	0.865	2	1.000	
3	0.840	3	1.000	
2x MOI 7.5PB		**Ctrl 0.0PB**		
1	0.767	1	1.000	0.007286
2	0.772	2	1.000	
3	0.824	3	1.000	
2x MOI 10.0PB		**Ctrl 0.0PB**		
1	0.725	1	1.000	0.004634
2	0.745	2	1.000	
3	0.783	3	1.000	
Ctrl 10.0PB		**Ctrl 0.0PB**		
1	0.971	1	1.000	0.084851
2	0.976	2	1.000	
3	0.992	3	1.000	

A3.3.3 Comparison of 24hr to 48hr Percentage of Cell Death

Two-Tailed Student's T-Test:

Experiment #	Mean Percentage of Cell Death 24 Hours after Infection (%)	Mean Percentage of Cell Death 48 Hours after Infection (%)	P-Value
2x MOI 5.0PB			
1	11.87	16.63	
2	8.79	15.30	0.147033
3	7.83	9.99	
2x MOI 7.5PB			
1	12.39	21.84	
2	8.40	17.99	0.041425
3	11.16	14.94	
2x MOI 10.0PB			
1	17.46	23.84	
2	15.00	21.97	0.002637
3	15.66	22.04	
Ctrl 10.0PB			
1	4.30	12.63	
2	8.06	11.35	0.179588
3	10.37	9.22	
Ctrl 0.0PB			
1	4.13	8.67	
2	3.40	8.53	0.116004
3	7.56	8.00	

A3.3.4 Comparison of 24hr to 48hr Total Cell Ratio

Two-Tailed Student's T-Test:

Experiment #	Mean Percentage of Cell Death 24 Hours after Infection (%)	Mean Percentage of Cell Death 48 Hours after Infection (%)	P-Value
2x MOI 5.0PB			
1	0.661	0.880	
2	0.761	0.865	0.35126
3	0.906	0.840	
2x MOI 7.5PB			
1	0.689	0.767	
2	0.863	0.772	0.808153
3	0.860	0.824	
2x MOI 10.0PB			
1	0.765	0.725	
2	0.771	0.745	0.260282
3	0.856	0.783	
Ctrl 10.0PB			
1	0.896	0.971	
2	0.975	0.976	0.445676
3	0.987	0.992	
Ctrl 0.0PB			
1	1.000	1.000	
2	1.000	1.000	N/A
3	1.000	1.000	

A3.4 Live Count Data for HIV1-XIAP/GFP Infection of Hh-RPCs

A3.4.1 24 Hours

HIV1-XIAP/GFP Experiment #1

Trx	[PB] (μg/mL)	Count	# Blue (Dead) Cells	# Clear (Live) Cells	# Cells Total	% Dead Cells	# Cells TOT/ # Cells 0.0PB Ctrl
1.5x MOI	5.0μg/mL Polybrene	1	23	137	160	14.38	
		2	25	179	204	12.25	
		3	36	140	176	20.45	
		4	30	144	174	17.24	
		MEAN			178.5	16.08	0.800
1.5x MOI	7.5μg/mL Polybrene	1	33	138	171	19.30	
		2	33	126	159	20.75	
		3	40	136	176	22.73	
		4	35	125	160	21.8	
		MEAN			166.5	21.16	0.746
1.5x MOI	10μg/mL Polybrene	1	38	121	159	23.90	
		2	40	120	160	25.00	
		3	42	137	179	23.46	
		4	43	123	166	25.90	
		MEAN			166.0	24.57	0.744
Ctrl	10μg/mL Polybrene	1	16	165	181	8.87	
		2	18	175	193	9.33	
		3	27	171	206	13.11	
		4	26	169	187	13.90	
		MEAN			191.75	11.29	0.859
Ctrl	0.0μg/mL Polybrene	1	20	187	207	9.66	
		2	18	204	222	8.11	
		3	28	199	227	12.33	
		4	22	215	237	9.28	
		MEAN			223.25	9.85	1.000

HIV1-XIAP/GFP Experiment #2

Trx	[PB] (μg/mL)	Count	# Blue (Dead) Cells	# Clear (Live) Cells	# Cells Total	% Dead Cells	# Cells TOT/ # Cells 0.0PB Ctrl
1.5x MOI	5.0μg/mL Polybrene	1	22	138	160	13.75	
		2	16	156	172	9.30	
		3	20	144	164	12.20	
		4	20	169	189	10.58	
		MEAN			171.25	11.46	0.883
1.5x MOI	7.5μg/mL Polybrene	1	24	131	155	15.48	
		2	25	128	153	16.34	
		3	23	117	140	16.43	
		4	31	131	162	19.14	
		MEAN			152.5	16.85	0.786
1.5x MOI	10μg/mL Polybrene	1	25	114	139	17.99	
		2	24	126	150	16.00	
		3	26	109	135	19.26	
		4	23	112	135	17.04	
		MEAN			139.25	17.57	0.720
Ctrl	10μg/mL Polybrene	1	12	152	164	7.32	
		2	12	174	186	6.45	
		3	20	164	184	10.87	
		4	16	166	182	8.79	
		MEAN			179.0	8.36	0.923
Ctrl	0.0μg/mL Polybrene	1	14	175	19	7.41	
		2	16	181	197	8.12	
		3	17	168	185	9.19	
		4	17	188	205	8.29	
		MEAN			194.0	8.25	1.000

HIV1-XIAP/GFP Experiment #3							
Trx	[PB] (μg/mL)	Count	# Blue (Dead) Cells	# Clear (Live) Cells	# Cells Total	% Dead Cells	# Cells TOT/ # Cells 0.0PB Ctrl
1.5x MOI	5.0μg/mL Polybrene	1	12	176	188	6.38	
		2	14	165	179	7.82	
		3	16	153	169	9347	
		4	18	170	188	9.57	
		MEAN			181.0	8.31	0.864
1.5x MOI	7.5μg/mL Polybrene	1	22	141	163	13.50	
		2	18	154	172	1.47	
		3	25	147	172	14.53	
		4	24	142	166	14.46	
		MEAN			168.25	13.24	0.803
1.5x MOI	10μg/mL Polybrene	1	19	150	169	11.24	
		2	27	131	158	17.09	
		3	29	147	176	16.48	
		4	35	130	165	21.21	
		MEAN			167.0	16.51	0.797
Ctrl	10μg/mL Polybrene	1	14	156	170	8.24	
		2	14	153	167	8.38	
		3	26	168	194	13.40	
		4	16	157	173	9.25	
		MEAN			176.0	9.82	0.840
Ctrl	0.0μg/mL Polybrene	1	13	184	197	6.60	
		2	19	206	225	8.44	
		3	25	180	205	12.20	
		4	14	197	211	6.64	
		MEAN			209.5	8.47	1.000

Student's Two-Tailed T-Test (Comparing Percentage of Dead Cells):

Category 1		Category 2		P-Value
1.5x MOI 5.0PB		**Ctrl 0.0PB**		
1	11.46	1	8.25	0.302456
2	16.08	2	9.85	
3	8.31	3	8.47	
1.5x MOI 7.5PB		**Ctrl 0.0PB**		
1	16.85	1	8.25	0.063405
2	21.16	2	9.85	
3	13.24	3	8.47	
1.5x MOI 10.0PB		**Ctrl 0.0PB**		
1	17.57	1	8.25	0.046924
2	24.57	2	9.85	
3	16.51	3	8.47	
Ctrl 10.0PB		**Ctrl 0.0PB**		
1	8.36	1	8.25	0.392834
2	11.29	2	9.85	
3	9.82	3	8.47	

Student's Two-Tailed T-Test (Comparing Total Cell Ratio):

Category 1		Category 2		P-Value
1.5x MOI 5.0PB		**Ctrl 0.0PB**		
1	0.882	1	1.000	0.025984
2	0.800	2	1.000	
3	0.864	3	1.000	
1.5x MOI 7.5PB		**Ctrl 0.0PB**		
1	0.786	1	1.000	0.005759
2	0.746	2	1.000	
3	0.803	3	1.000	
1.5x MOI 10.0PB		**Ctrl 0.0PB**		
1	0.720	1	1.000	0.00842
2	0.744	2	1.000	
3	0.797	3	1.000	
Ctrl 10.0PB		**Ctrl 0.0PB**		
1	0.923	1	1.000	0.037485
2	0.859	2	1.000	
3	0.840	3	1.000	

A3.4.2 48 Hours

HIV1-XIAP/GFP Experiment #1

Trx	[PB] (μg/mL)	Count	# Blue (Dead) Cells	# Clear (Live) Cells	# Cells Total	% Dead Cells	# Cells TOT/ # Cells 0.0PB Ctrl
1.5x MOI	5.0μg/mL Polybrene	1	19	162	181	10.50	
		2	24	154	178	13.48	
		3	26	159	185	14.05	
		4	27	165	192	14.06	
		MEAN			184.0	13.02	0.767
1.5x MOI	7.5μg/mL Polybrene	1	26	157	183	14.21	
		2	38	138	176	21.59	
		3	36	140	176	20.45	
		4	28	162	190	14.74	
		MEAN			181.25	17.75	0.756
1.5x MOI	10μg/mL Polybrene	1	31	126	157	19.75	
		2	39	119	158	24.68	
		3	33	139	172	19.19	
		4	42	140	182	23.08	
		MEAN			167.25	21.57	0.698
Ctrl	10μg/mL Polybrene	1	13	199	212	6.13	
		2	37	210	247	14.98	
		3	30	190	220	13.64	
		4	30	201	231	12.99	
		MEAN			227.5	11.93	0.949
Ctrl	0.0μg/mL Polybrene	1	21	204	225	9.33	
		2	19	210	229	8.30	
		3	20	228	248	8.06	
		4	26	231	257	10.12	
		MEAN			29.75	8.98	1.000

HIV1-XIAP/GFP Experiment #2

Trx	[PB] (μg/mL)	Count	# Blue (Dead) Cells	# Clear (Live) Cells	# Cells Total	% Dead Cells	# Cells TOT/ # Cells 0.0PB Ctrl
1.5x MOI	5.0μg/mL Polybrene	1	12	142	154	7.79	
		2	16	134	150	10.67	
		3	22	132	154	14.29	
		4	18	141	159	11.32	
		MEAN			154.25	11.02	0.849
1.5x MOI	7.5μg/mL Polybrene	1	23	119	142	16.20	
		2	21	139	160	13.13	
		3	25	112	137	18.25	
		4	27	119	146	18.49	
		MEAN			146.25	16.52	0.805
1.5x MOI	10μg/mL Polybrene	1	27	111	138	19.57	
		2	27	114	141	19.15	
		3	28	120	148	18.92	
		4	26	116	142	18.31	
		MEAN			142.25	18.99	0.783
Ctrl	10μg/mL Polybrene	1	16	157	172	9.25	
		2	16	150	166	9.65	
		3	14	164	178	7.87	
		4	14	154	168	8.33	
		MEAN			171.25	8.77	0.942
Ctrl	0.0μg/mL Polybrene	1	13	171	184	7.07	
		2	18	152	170	10.59	
		3	14	170	184	7.61	
		4	17	172	189	8.99	
		MEAN			181.75	8.56	1.000

HIV1-XIAP/GFP Experiment #3

Trx	[PB] (μg/mL)	Count	# Blue (Dead) Cells	# Clear (Live) Cells	# Cells Total	% Dead Cells	# Cells TOT/ # Cells 0.0PB Ctrl
1.5x MOI	5.0μg/mL Polybrene	1	19	132	151	12.58	
		2	23	132	155	14.84	
		3	25	136	161	15.53	
		4	24	125	149	16.11	
		MEAN			154.0	14.76	0.837
1.5x MOI	7.5μg/mL Polybrene	1	30	110	140	21.43	
		2	23	118	141	16.31	
		3	34	131	165	20.61	
		4	30	124	154	19.48	
		MEAN			150.0	19.46	0.815
1.5x MOI	10μg/mL Polybrene	1	33	120	153	21.57	
		2	33	112	145	22.76	
		3	32	98	130	24.62	
		4	39	113	152	25.66	
		MEAN			145.0	23.65	0.788
Ctrl	10μg/mL Polybrene	1	23	152	175	13.14	
		2	25	156	181	13.81	
		3	25	146	171	14.62	
		4	33	161	194	17.01	
		MEAN			180.25	14.65	0.980
Ctrl	0.0μg/mL Polybrene	1	19	155	174	10.92	
		2	21	175	196	10.71	
		3	29	164	193	15.03	
		4	21	152	173	12.14	
		MEAN			184.0	12.20	1.000

Student's Two-Tailed T-Test (Comparing Percentage of Dead Cells):

Category 1		Category 2		P-Value
1.5x MOI 5.0PB		**Ctrl 0.0PB**		
1	13.03	1	8.98	0.128122
2	11.02	2	8.56	
3	14.76	3	12.20	
1.5x MOI 7.5PB		**Ctrl 0.0PB**		
1	17.75	1	8.98	0.006381
2	16.52	2	8.56	
3	19.46	3	12.20	
1.5x MOI 10.0PB		**Ctrl 0.0PB**		
1	21.67	1	8.98	0.003156
2	18.99	2	8.56	
3	23.65	3	12.20	
Ctrl 10.0PB		**Ctrl 0.0PB**		
1	11.93	1	8.98	0.420155
2	8.77	2	8.56	
3	14.65	3	12.20	

Student's Two-Tailed T-Test (Comparing Total Cell Ratio):

Category 1		Category 2		P-Value
1.5x MOI 5.0PB		**Ctrl 0.0PB**		
1	0.767	1	1.000	0.019103
2	0.849	2	1.000	
3	0.837	3	1.000	
1.5x MOI 7.5PB		**Ctrl 0.0PB**		
1	0.756	1	1.000	0.007594
2	0.805	2	1.000	
3	0.815	3	1.000	
1.5x MOI 10.0PB		**Ctrl 0.0PB**		
1	0.698	1	1.000	0.014061
2	0.783	2	1.000	
3	0.788	3	1.000	
Ctrl 10.0PB		**Ctrl 0.0PB**		
1	0.949	1	1.000	0.066467
2	0.942	2	1.000	
3	0.980	3	1.000	

A3.4.3 Comparison of 24hr to 48hr Percentage of Cell Death

Two-Tailed Student's T-Test:

Experiment #	Mean Percentage of Cell Death 24 Hours after Infection (%)	Mean Percentage of Cell Death 48 Hours after Infection (%)	P-Value
1.5x MOI 5.0PB			
1	11.46	13.03	
2	16.08	11.02	0.720749
3	8.31	14.76	
1.5x MOI 7.5PB			
1	16.85	17.75	
2	21.16	16.52	0.761014
3	13.24	19.46	
1.5x MOI 10.0PB			
1	17.57	21.67	
2	24.57	18.99	0.55665
3	16.51	23.65	
Ctrl 10.0PB			
1	8.36	11.93	
2	11.29	8.77	0.379231
3	9.82	14.65	
Ctrl 0.0PB			
1	8.25	8.98	
2	9.85	8.56	0.466791
3	8.47	12.20	

A3.4.4 Comparison of 24hr to 48hr Total Cell Ratio

Two-Tailed Student's T-Test:

Experiment #	Mean Percentage of Cell Death 24 Hours after Infection (%)	Mean Percentage of Cell Death 48 Hours after Infection (%)	P-Value
1.5x MOI 5.0PB			
1	0.883	0.767	
2	0.800	0.849	0.431279
3	0.864	0.837	
1.5x MOI 7.5PB			
1	0.786	0.756	
2	0.746	0.805	0.611838
3	0.803	0.815	
1.5x MOI 10.0PB			
1	0.720	0.698	
2	0.744	0.783	0.946225
3	0.797	0.788	
Ctrl 10.0PB			
1	0.923	0.949	
2	0.859	0.942	0.062308
3	0.840	0.980	
Ctrl 0.0PB			
1	1.000	1.000	
2	1.000	1.000	N/A
3	1.000	1.000	

A3.5 Transduction Efficiency for TAT-eGFP in Hh-RPCs

A3.5.1 TAT-eGFP 1 Hour

TAT-eGFP 1 Hour Experiment #1

[TAT-eGFP]	Field of View	# GFP-Positive Cells	# GFP-Negative Cells	# Cells Total	% GFP-Positive Cells (%)
100.0μg/mL	1	147	52	199	7.9
	2	136	38	174	78.2
	3	115	40	155	74.2
	4	117	34	151	77.5
	5	121	37	158	76.6
	MEAN ± Standard Deviation				76.08 ± 1.94
50.0μg/mL	1	88	44	132	66.7
	2	93	43	136	68.4
	3	122	56	178	68.5
	4	106	35	141	75.2
	5	89	45	134	66.4
	MEAN ± Standard Deviation				69.04 ± 3.57
10.0μg/mL	1	1	154	171	9.9
	2	26	184	210	12.4
	3	21	154	175	12.0
	4	22	149	171	12.9
	5	12	96	108	11.1
	MEAN ± Standard Deviation				11.66 ± 1.18

TAT-eGFP 1 Hour Experiment #2

[TAT-eGFP]	Field of View	# GFP-Positive Cells	# GFP-Negative Cells	# Cells Total	% GFP-Positive Cells (%)
100.0μg/mL	1	107	17	124	86.3
	2	135	27	162	83.3
	3	120	26	146	82.2
	4	116	26	142	81.7
	5	143	33	176	81.2
	MEAN ± Standard Deviation				87.94 ± 2.03
50.0μg/mL	1	90	27	117	76.9
	2	122	42	164	74.4
	3	92	46	138	66.7
	4	111	27	138	80.4
	5	94	29	123	76.4
	MEAN ± Standard Deviation				74.96 ± 5.10
10.0μg/mL	1	52	85	137	38.0
	2	41	100	141	29.1
	3	42	75	117	35.9
	4	53	100	152	34.9
	5	45	76	121	37.2
	MEAN ± Standard Deviation				35.02 ± 3.52

TAT-eGFP 1 Hour Experiment #3					
[TAT-eGFP]	**Field of View**	**# GFP-Positive Cells**	**# GFP-Negative Cells**	**# Cells Total**	**% GFP-Positive Cells (%)**
10.0μg/mL	1	143	41	184	77.7
	2	195	71	266	73.3
	3	128	47	175	73.1
	4	145	40	185	78.4
	5	112	23	135	83.0
	MEAN ± Standard Deviation				77.10 ± 4.10
50.0μg/mL	1	138	77	215	64.2
	2	124	48	172	72.1
	3	156	51	207	75.4
	4	129	50	179	72.1
	5	140	44	184	76.1
	MEAN ± Standard Deviation				71.98 ± 4.72
100.0μg/mL	1	153	115	268	57.1
	2	138	86	226	61.1
	3	14	76	200	62.0
	4	105	53	158	66.5
	5	121	80	201	60.2
	MEAN ± Standard Deviation				61.38 ± 3.41

Single Factor ANOVA:

Summary:

Groups	*Count*	*Sum*	*Average*	*Variance*
10.0μg/mL	3	108.06	36.02	618.7696
50.0μg/mL	3	215.98	71.99333	8.761733
100.0μg/mL	3	236.12	78.70667	13.70093

ANOVA:

Source of Variation	*SS*	*df*	*MS*	*F*	*P-value*	*F crit*
Between Groups	3161.301	2	1580.651	7.395061	0.024037	5.143253
Within Groups	1282.465	6	213.7441			
Total	4443.766	8				

A3.5.2 TAT-eGFP 24 Hours

TAT-eGFP 24 Hours Experiment #1

[TAT-eGFP]	Field of View	# GFP-Positive Cells	# GFP-Negative Cells	# Cells Total	% GFP-Positive Cells (%)
100.0μg/mL	1	103	0	103	100.0
	2	69	1	70	98.6
	3	61	0	61	100.0
	4	134	7	141	95.0
	5	116	9	125	92.8
	MEAN ± Standard Deviation				97.28 ± 3.23
50.0μg/mL	1	124	15	139	89.2
	2	112	10	122	91.8
	3	159	18	177	89.8
	4	124	10	134	92.5
	5	121	12	19*9	91.0
	MEAN ± Standard Deviation				90.86 ± 1.37
10.0μg/mL	1	52	83	135	38.5
	2	50	89	139	36.0
	3	45	97	142	31.7
	4	43	109	162	32.7
	5	43	112	165	32.1
	MEAN ± Standard Deviation				34.20 ± 2.94

TAT-eGFP 24 Hours Experiment #2

[TAT-eGFP]	Field of View	# GFP-Positive Cells	# GFP-Negative Cells	# Cells Total	% GFP-Positive Cells (%)
100.0μg/mL	1	272	18	290	93.8
	2	268	24	292	91.8
	3	284	31	315	90.2
	4	272	29	301	90.4
	5	337	22	359	93.9
	MEAN ± Standard Deviation				92.02 ± 1.78
50.0μg/mL	1	276	39	315	87.7
	2	300	44	344	87.2
	3	286	42	328	87.2
	4	294	51	345	85.2
	5	276	57	333	82.9
	MEAN ± Standard Deviation				86.04 ± 2.00
10.0μg/mL	1	236	88	324	72.8
	2	185	115	300	61.7
	3	202	144	346	58.4
	4	185	127	312	59.3
	5	267	173	340	60.9
	MEAN ± Standard Deviation				62.62 ± 1.78

TAT-eGFP 24 Hours Experiment #3					
[TAT-eGFP]	**Field of View**	**# GFP-Positive Cells**	**# GFP-Negative Cells**	**# Cells Total**	**% GFP-Positive Cells (%)**
100.0μg/mL	1	268	81	349	76.8
	2	327	82	409	80.0
	3	307	64	371	32.7
	4	350	62	412	85.0
	5	228	58	286	79.7
	MEAN ± Standard Deviation				80.84 ± 3.13
50.0μg/mL	1	151	86	237	63.7
	2	165	85	250	66.0
	3	174	89	263	66.2
	4	206	95	301	68.4
	5	150	103	253	59.3
	MEAN ± Standard Deviation				64.72 ± 3.46
10.0μg/mL	1	77	179	256	30.1
	2	101	180	281	25.9
	3	112	177	289	38.8
	4	83	166	249	33.3
	5	92	185	277	33.2
	MEAN ± Standard Deviation				34.26 ± 3.27

Single Factor ANOVA:

Summary:

Groups	*Count*	*Sum*	*Average*	*Variance*
10.0μg/mL	3	131.08	43.69333	268.6649
50.0μg/mL	3	241.62	80.54	193.5124
100.0μg/mL	3	270.14	90.04667	70.48893

ANOVA:

Source of Variation	*SS*	*df*	*MS*	*F*	*P-value*	*F crit*
Between Groups	3596.685	2	1798.343	10.12834	0.011933	5.143253
Within Groups	1065.333	6	177.5554			
Total	4662.018	8				

A3.5.3 TAT-eGFP 48 Hours

TAT-eGFP 48 Hours Experiment #1

[TAT-eGFP]	Field of View	# GFP-Positive Cells	# GFP-Negative Cells	# Cells Total	% GFP-Positive Cells (%)
100.0μg/mL	1	70	83	153	45.8
	2	83	94	177	46.9
	3	87	59	146	59.6
	4	89	113	192	41.1
	5	63	106	169	37.3
	MEAN ± Standard Deviation				46.20 ± 8.40
50.0μg/mL	1	42	125	167	25.1
	2	43	77	120	35.8
	3	72	98	170	42.4
	4	68	92	160	42.5
	5	59	81	140	42.1
	MEAN ± Standard Deviation				37.58 ± 7.53
10.0μg/mL	1	25	174	199	12.6
	2	36	143	179	20.1
	3	38	122	160	23.8
	4	41	206	247	16.6
	5	21	180	201	10.5
	MEAN ± Standard Deviation				16.72 ± 5.41

TAT-eGFP 48 Hours Experiment #2

[TAT-eGFP]	Field of View	# GFP-Positive Cells	# GFP-Negative Cells	# Cells Total	% GFP-Positive Cells (%)
100.0μg/mL	1	68	57	125	54.4
	2	67	59	126	53.2
	3	78	65	143	54.5
	4	89	55	144	61.8
	5	84	63	147	57.1
	MEAN ± Standard Deviation				56.26 ± 3.44
50.0μg/mL	1	80	110	190	42.1
	2	85	130	215	39.5
	3	82	161	243	33.7
	4	90	147	237	38.0
	5	97	132	229	42.4
	MEAN ± Standard Deviation				39.14 ± 3.55
10.0μg/mL	1	30	69	99	30.3
	2	23	66	89	25.8
	3	26	92	88	29.5
	4	21	66	87	24.1
	5	28	80	108	25.9
	MEAN ± Standard Deviation				27.12 ± 2.65

TAT-eGFP 48 Hours Experiment #3					
[TAT-eGFP]	**Field of View**	**# GFP-Positive Cells**	**# GFP-Negative Cells**	**# Cells Total**	**% GFP-Positive Cells (%)**
100.0μg/mL	1	45	54	99	45.5
	2	46	27	73	63.0
	3	39	25	64	60.9
	4	48	38	86	55.8
	5	40	16	56	71.4
	MEAN ± Standard Deviation				58.32 ± 9.56
50.0μg/mL	1	74	84	158	46.8
	2	94	83	177	53.1
	3	97	62	159	61.0
	4	81	59	140	57.9
	5	97	54	151	64.2
	MEAN ± Standard Deviation				56.60 ± 6.84
10.0μg/mL	1	45	88	133	33.8
	2	34	84	118	28.8
	3	46	179	225	20.4
	4	50	192	242	20.7
	5	68	151	219	31.1
	MEAN ± Standard Deviation				26.96 ± 6.11

Single Factor ANOVA:

Summary:

Groups	*Count*	*Sum*	*Average*	*Variance*
10.0μg/mL	3	70.8	23.6	35.5072
50.0μg/mL	3	133.32	44.44	111.5076
100.0μg/mL	3	159.78	53.26	43.7836

ANOVA:

Source of Variation	*SS*	*df*	*MS*	*F*	*P-value*	*F crit*
Between Groups	1391.814	2	695.9068	10.94202	0.009963	5.143253
Within Groups	381.5968	6	63.59947			
Total	1773.41	8				

A3.5.4 TAT-eGFP 3 Days

TAT-eGFP 3 Days Experiment #1

[TAT-eGFP]	Field of View	# GFP-Positive Cells	# GFP-Negative Cells	# Cells Total	% GFP-Positive Cells (%)
100.0μg/mL	1	71	83	154	46.1
	2	50	64	114	43.9
	3	52	69	121	43.0
	4	58	86	144	40.3
	5	61	98	159	38.4
	MEAN ± Standard Deviation				42.34 ± 3.03
50.0μg/mL	1	33	64	97	34.0
	2	44	62	106	41.5
	3	25	83	108	23.1
	4	35	55	90	38.9
	5	34	104	138	24.6
	MEAN ± Standard Deviation				32.42 ± 8.29
10.0μg/mL	1	25	106	131	19.1
	2	24	104	128	18.1
	3	37	126	163	22.7
	4	30	123	153	19.6
	5	25	153	178	14.0
	MEAN ± Standard Deviation				18.84 ± 3.12

TAT-eGFP 3 Days Experiment #2

[TAT-eGFP]	Field of View	# GFP-Positive Cells	# GFP-Negative Cells	# Cells Total	% GFP-Positive Cells (%)
100.0μg/mL	1	38	53	91	41.8
	2	45	58	103	43.7
	3	43	46	89	48.3
	4	47	63	110	42.7
	5	51	132	183	27.9
	MEAN ± Standard Deviation				40.88 ± 7.68
50.0μg/mL	1	44	98	143	31.0
	2	34	102	136	25.0
	3	36	80	116	31.0
	4	35	117	152	23.0
	5	41	111	152	27.0
	MEAN ± Standard Deviation				27.40 ± 3.58
10.0μg/mL	1	13	247	260	5.0
	2	10	146	156	6.4
	3	22	100	122	18.0
	4	19	72	91	20.9
	5	10	119	129	7.8
	MEAN ± Standard Deviation				11.62 ± 7.29

TAT-eGFP 3 Days Experiment #3					
[TAT-eGFP]	**Field of View**	**# GFP-Positive Cells**	**# GFP-Negative Cells**	**# Cells Total**	**% GFP-Positive Cells (%)**
100.0μg/mL	1	31	86	117	26.5
	2	43	39	82	52.4
	3	44	43	87	50.6
	4	43	40	83	51.8
	5	31	24	55	56.4
	MEAN ± Standard Deviation				47.54 ± 11.96
50.0μg/mL	1	40	56	96	41.7
	2	48	56	104	46.2
	3	35	61	96	36.5
	4	30	56	86	34.9
	5	25	44	69	36.2
	MEAN ± Standard Deviation				39.10 ± 4.74
10.0μg/mL	1	13	50	63	20.6
	2	28	50	78	35.9
	3	19	59	78	24.4
	4	32	46	78	41.0
	5	29	47	76	38.2
	MEAN ± Standard Deviation				32.02 ± 8.98

Single Factor ANOVA:

Summary:

Groups	*Count*	*Sum*	*Average*	*Variance*
10.0μg/mL	3	62.48	20.82667	107.0001
50.0μg/mL	3	98.92	32.97333	34.45213
100.0μg/mL	3	130.76	43.58667	12.25453

ANOVA:

Source of Variation	*SS*	*df*	*MS*	*F*	*P-value*	*F crit*
Between Groups	778.202	2	389.101	7.594348	0.022706	5.143253
Within Groups	307.4136	6	51.2356			
Total	1085.616	8				

A3.5.5 TAT-eGFP 5 Days

TAT-eGFP 5 Days Experiment #1

[TAT-eGFP]	Field of View	# GFP-Positive Cells	# GFP-Negative Cells	# Cells Total	% GFP-Positive Cells (%)
100.0μg/mL	1	34	239	273	12.5
	2	18	250	268	7.2
	3	43	247	290	14.8
	4	46	214	260	17.7
	5	43	287	330	13.0
	MEAN ± Standard Deviation				13.04 ± 3.85
50.0μg/mL	1	1	327	328	0.3
	2	0	298	298	0.0
	3	0	315	312	0.0
	4	0	277	277	0.0
	5	0	251	251	0.0
	MEAN ± Standard Deviation				0.06 ± 0.13
10.0μg/mL	1	0	249	249	0.0
	2	0	231	231	0.0
	3	0	324	324	0.0
	4	0	302	302	0.0
	5	0	279	279	0.0
	MEAN ± Standard Deviation				0.0 ± 0.0

TAT-eGFP 5 Days Experiment #2

[TAT-eGFP]	Field of View	# GFP-Positive Cells	# GFP-Negative Cells	# Cells Total	% GFP-Positive Cells (%)
100.0μg/mL	1	3	343	346	0.87
	2	5	348	353	1.42
	3	2	373	375	0.53
	4	2	289	391	0.51
	5	3	370	373	0.80
	MEAN ± Standard Deviation				0.83 ± 0.37
50.0μg/mL	1	0	359	359	0.0
	2	2	271	273	0.73
	3	0	381	381	0.0
	4	0	302	302	0.0
	5	0	299	299	0.0
	MEAN ± Standard Deviation				0.15 ± 0.33
10.0μg/mL	1	0	277	377	0.0
	2	0	321	321	0.0
	3	0	244	344	0.0
	4	0	280	280	0.0
	5	0	342	342	0.0
	MEAN ± Standard Deviation				0.0 ± 0.0

TAT-eGFP 5 Days Experiment #3					
[TAT-eGFP]	**Field of View**	**# GFP-Positive Cells**	**# GFP-Negative Cells**	**# Cells Total**	**% GFP-Positive Cells (%)**
100.0μg/mL	1	10	73	83	12.0
	2	7	125	132	5.3
	3	39	87	126	31.0
	4	12	80	92	13.0
	5	13	120	133	9.8
	MEAN ± Standard Deviation				14.21 ± 9.84
50.0μg/mL	1	3	84	87	3.4
	2	3	103	106	2.8
	3	10	92	102	9.8
	4	1	94	95	1.1
	5	4	104	108	3.7
	MEAN ± Standard Deviation				4.16 ± 3.31
10.0μg/mL	1	5	121	126	4.0
	2	11	140	151	7.3
	3	7	96	103	6.8
	4	2	87	89	2.2
	5	6	88	94	6.4
	MEAN ± Standard Deviation				5.34 ± 2.17

Single Factor ANOVA:

Summary:

Groups	*Count*	*Sum*	*Average*	*Variance*
10.0μg/mL	3	28.08	9.36	54.9129
50.0μg/mL	3	4.37	1.456667	5.483033
100.0μg/mL	3	5.34	1.78	9.5052

ANOVA:

Source of Variation	*SS*	*df*	*MS*	*F*	*P-value*	*F crit*
Between Groups	120.0236	2	60.01181	2.575572	0.155774	5.143253
Within Groups	139.8023	6	23.30038			
Total	259.8259	8				